1 ION CHEMISTRY IN ATMOSPHERIC AND ASTROPHYSICAL PLASMAS

A. Dalgarno
Harvard-Smithsonian Center for Astrophysics, 60 Garden Street, Cambridge, MA 02138, USA

and

J. L. Fox
Institute for Terrestrial and Planetary Atmospheres, State University of New York, Stony Brook, NY 11794, USA

CONTENTS

Unimolecular and Bimolecular Reaction Dynamics
Edited by C. Y. Ng, T. Baer and I. Powis

1.1 INTRODUCTION

There are many differences and also remarkable similarities between the ion chemistry and physics of planetary ionospheres and the ion chemistry and physics of astronomical environments beyond the solar system.

In the early Universe, an expanded cooling gas of hydrogen and helium was embedded in the cosmic background radiation field and ionized by it. As the Universe cooled by adiabatic expansion, recombination occurred and molecular formation was driven by catalytic reactions involving the relict electrons and protons. Similar chemical processes are effective in the ionized zones of gaseous and planetary nebulae and in stellar winds where the ionization is due to radiation from the central stars, in the envelopes of supernovae where the ionization is initiated by the deposition of γ-rays, in dissociative shocks where the ionization arises from electron impacts in a hot gas and in quasar broad-line region clouds where the quasar is responsible for the ionization. At high altitudes in the atmospheres of the Jovian planets, the main constituents are hydrogen and helium and the ion chemistry and physics is determined by the same processes, the source of the ionization being solar ultraviolet radiation and cosmic rays.

After the collapse of the first distinct astronomical entities to emerge from the uniform flow, heavy elements were created by nuclear burning in the cores of the collapsed objects and distributed throughout the Universe by winds and explosions. The chemistry and physics became more complicated. Over 90 distinct molecular species have been identified in interstellar clouds where they are ionized globally by cosmic ray impacts and locally by radiation and shocks associated with star formation and evolution. Complex molecules have also been found in circumstellar shells of evolved stars. At intermediate and low altitudes in the Jovian atmospheres, the ion chemistry is complicated by the increasing abundance of heavy elements such as carbon, and an extensive array of complex molecules has been predicted. Reactions involving heavy elements dominate the structure of the ionospheres of the terrestrial planets and the satellites Titan and Triton.

1.2 HYDROGEN AND HELIUM PLASMAS

We begin with a discussion of the chemistry and physics of various astrophysical and planetary plasmas in which the major gas components are hydrogen and helium. After establishing the elements of the hydrogen–helium plasma chemistry, we will consider the complexities that arise with the introduction of heavier elements.

1.2.1 ASTROPHYSICAL ENVIRONMENTS

Much of the Universe consists of plasmas dominated by hydrogen and helium. We compare the chemistry and physics of several such plasmas.

1.2.1.1 Early Universe

The formation of the first molecules in the Universe was a result of chemical reactions in which electrons and protons acted as catalysts. According to the standard cosmology, space occupied by the Universe expanded adiabatically. At $t = 10^{-4}$ s, the temperature was 10^{12} K. The Universe then cooled rapidly as it expanded, reaching a temperature of 10^9 K after 100 s. At 10^9 K, protons and neutrons had formed and a brief period of nucleosynthesis occurred during which a substantial abundance of helium was produced together with trace amounts of deuterium and ^{7}Li. The matter was embedded in a radiation field characterized by the same temperature as the matter. The radiation field contained energetic photons and photoionization ensured that all the atoms were fully stripped.

As the expansion continued, the supply of energetic photons diminished as the temperature continued to decrease. After some tens of thousands of years, Li^{3+} and He^{2+} captured electrons by radiative recombination

$$Li^{3+} + e \longrightarrow Li^{2+} + h\nu \quad (1)$$

$$He^{2+} + e \longrightarrow He^{+} + h\nu \quad (2)$$

while the reverse processes of photoionization

$$h\nu + Li^{2+} \longrightarrow Li^{3+} + e \quad (3)$$

$$h\nu + He^{+} \longrightarrow He^{2+} + e \quad (4)$$

were ineffective. The initial recombinations were soon followed by

$$Li^{2+} + e \longrightarrow Li^{+} + h\nu \quad (5)$$

$$He^{+} + e \longrightarrow He + h\nu \quad (6)$$

and Li^+ and He could survive photoionization by the radiation field because of their high ionization potentials of respectively 75.62 and 24.56 eV.

With the formation of neutral helium, the first molecular ions He_2^+ and $LiHe^+$ came into existence through the processes of radiative association

$$He^+ + He \longrightarrow He_2^+ + h\nu \tag{7}$$

$$Li^+ + He \longrightarrow LiHe^+ + h\nu \tag{8}$$

In the radiative association of He^+ and He, during their approach along the $^2\Sigma_g$ potential energy curve, a photon may be emitted in an electronic transition to bound vibrational levels of the ground $^2\Sigma_u^+$ state of He_2^+. The rate coefficient of reaction (7) has been calculated (Stancil *et al.* 1993). The radiative association of Li^+ and He is a much less probable event because the radiative transition involved is a spontaneous emission from the vibrational continuum of the ground $^1\Sigma$ state into the discrete vibrational levels.

The molecular ion He_2^+ has a dissociation energy of 2.47 eV (Ackermann and Hogreve, 1991) and an effective threshold for ground state photodissociation near 115 nm. The vibrational level populations are in thermal equilibrium at the cosmic background temperature and the ions are quickly removed by photodissociation (Gaur *et al.*, 1988)

$$He_2^+ + h\nu \longrightarrow He^+ + He \tag{9}$$

by the background radiation field. They are also removed by dissociative recombination

$$He_2^+ + e \longrightarrow He + He \tag{10}$$

and by charge transfer

$$He_2^+ + H \longrightarrow He + He + H^+ \tag{11}$$

The rate coefficients of reaction (10) and (11) are uncertain.

The ion $LiHe^+$ is removed by photodissociation into the excited electronic $^1\Sigma$ and $^1\Pi$ states

$$LiHe^+ + h\nu \longrightarrow Li^+ + He \tag{12}$$

and by dissociative recombination

$$LiHe^+ + e \longrightarrow Li + He \tag{13}$$

The rate coefficient of reaction (13) is unknown. It may be slow compared to most such processes. In any event, photodestruction severely limits the abundances of He_2^+ and $LiHe^+$ that can be achieved and the ions play an insignificant role in the early chemistry.

The presence of neutral helium leads also to the formation of HeH^+ by

radiative association

$$H^+ + He \longrightarrow HeH^+ + h\nu \tag{14}$$

in a process analogous to reaction (8). The rate coefficient is small with a value at 10000 K of 1.3×10^{-20} cm^3 s^{-1} (Roberge and Dalgarno, 1992). Once formed, HeH^+ is only slowly destroyed. Photodissociation by absorption into the vibrational continuum of the ground state is negligible (Roberge and Dalgarno, 1992) and photodissociation by absorption into the excited $A^1\Sigma$ state has a high threshold near 19 eV. Dissociative recombination

$$HeH^+ + e \longrightarrow He + H \tag{15}$$

which proceeds with a rate coefficient measured by Yousif and Mitchell (1989) to be $1 \times 10^{-8}(300/T)^{1/2}$ cm^3 s^{-1}, and

$$HeH^+ + H \longrightarrow H_2{}^+ + He \tag{16}$$

which proceeds with a rate coefficient of $(9.1 \pm 2.5)10^{-10}$ cm^3 s^{-1} (Karpas *et al.*, 1979), are the main destruction mechanisms.

The processes involving helium and lithium ions were preliminary events to the main activity which began when the temperature had decreased to about 4000 K and photoionization of atomic hydrogen

$$H + h\nu \longrightarrow H^+ + e \tag{17}$$

had ceased to be effective. Then hydrogen was rapidly neutralized by radiative recombination

$$H^+ + e \longrightarrow H + h\nu \tag{18}$$

The Universe entered the recombination era which was also the dawn of chemistry, giving rise to the formation of the first neutral molecule H_2. The particle density at this time of 10^5 years was about 10^3 cm^{-3}.

Direct formation of molecular hydrogen by radiative association of ground state hydrogen atoms is highly forbidden because it involves a triplet–singlet transition from the $b^3\Sigma_u{}^+$ state of H_2 to the $X^1\Sigma_g{}^+$ state. The suggestion has often been made that the excited state population may be sufficient such that

$$H(2s) + H \longrightarrow H_2 + h\nu \tag{19}$$

$$H(2p) + H \longrightarrow H_2 + h\nu \tag{20}$$

which involve allowed transitions, make significant contributions to the formation of H_2. Latter and Black (1991) have made estimates of the rate coefficients. The process (20) can be viewed alternatively as a Raman scattering of Lyman alpha radiation from the vibrational continuum of the ground electronic state, terminating in vibrational levels of the ground state. Raman scattering, as a mechanism for forming H_2, was investigated by Federman and Frommhold (1982).

More important is the process of associative ionization

$$H(n = 2) + H \longrightarrow H_2^+ + e \tag{21}$$

Urbain *et al.* (1991) have presented the cross sections for H(2s). The possible influence of associative ionization has not yet been included in any model of the early Universe, but it has been incorporated in the envelope chemistry of Supernova 1987a (Miller *et al.*, 1992; Yan *et al.*, 1994).

With hydrogen not entirely neutral, H_2^+ molecular ions could be formed by radiative association

$$H^+ + H \longrightarrow H_2^+ + h\nu \tag{22}$$

and negative hydrogen ions H^- could be formed by radiative attachment

$$H + e \longrightarrow H^- + h\nu \tag{23}$$

The reverse reactions of photodissociation

$$H_2^+ + h\nu \longrightarrow H^+ + H \tag{24}$$

and photodetachment

$$H^- + h\nu \longrightarrow H + e \tag{25}$$

delayed but could not prevent the formation of hydrogen molecules by charge transfer

$$H_2^+ + H \longrightarrow H_2 + H^+ \tag{26}$$

and associative detachment

$$H^- + H \longrightarrow H_2 + e \tag{27}$$

In these sequences, the protons and the electrons act as catalysts for the formation of H_2.

Mutual neutralization processes

$$H_2^+ + H^- \longrightarrow H + H + H \tag{28}$$

$$H^+ + H^- \longrightarrow H + H \tag{29}$$

$$He^+ + H^- \longrightarrow He + H \tag{30}$$

play a minor role in limiting the abundance of H_2.

Molecular hydrogen can be destroyed by (Chupka *et al.*, 1968; Glass-Maujean, 1989; Dalgarno, 1993a)

$$H(n = 2) + H_2 \longrightarrow H_3^+ + e \tag{31}$$

It is reformed in part by dissociative recombination

$$H_3^+ + e \longrightarrow H_2 + H \tag{32}$$

but

$$H_3^+ + e \longrightarrow H + H + H \tag{33}$$

may also be a significant channel. The rate coefficient of dissociative recombination of H_3^+ is a crucial parameter in chemical models of interstellar clouds, supernova envelopes and planetary ionospheres. It has experienced a checkered history. The most recent experiments (Yousif *et al.*, 1991; Canosa *et al.*, 1992; Larsson *et al.*, 1993) appear to establish a rate coefficient of order $10^{-7}(300/T)^{1/2}$ cm^3 s^{-1} but the actual mechanism responsible for the fast rate has yet to be established (Bates, 1992; Bates *et al.*, 1993).

An additional source of H_2^+ is reaction (16), but the reverse process

$$H_2^+ + He \longrightarrow HeH^+ + H \tag{34}$$

which is exothermic for vibrational levels of H_2^+ with $v \geq 3$ also occurs.

Some chemistry took place involving the trace constituents deuterium and lithium. Lithium remained mostly ionized because of the scarcity of electrons left over after hydrogen recombination. Some formation of LiH^+ occurred through (Lepp and Dalgarno, 1987)

$$Li^+ + H \longrightarrow LiH^+ + h\nu \tag{35}$$

and, more important, formation of HD through

$$D^+ + H_2 \longrightarrow H^+ + HD \tag{36}$$

The reaction (36) is the major source of HD in interstellar clouds (Dalgarno *et al.*, 1973a). Its rate coefficient was measured by Ferguson (1986).

Figure 1 shows the results of a calculation by Latter (1989) of the fractional abundances of the various forms of hydrogen and helium as a function of the redshift z. The relict ionization fraction after recombination is 1.8×10^{-4}.

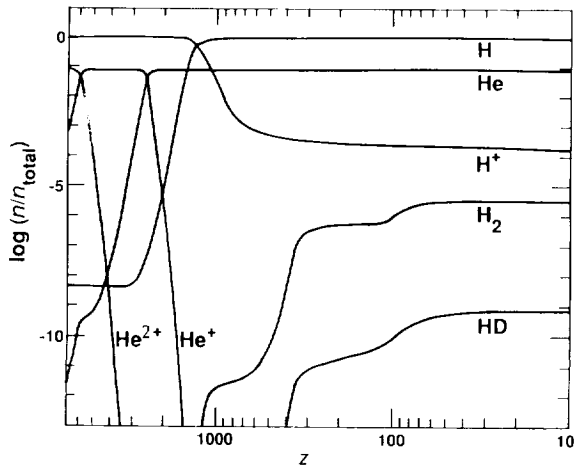

Figure 1.1 The fractional abundance of the various ions of hydrogen and helium as a fraction of red shift. (From Latter, 1989)

1.2.1.2 Gaseous nebulae and stellar winds

In gaseous nebulae and planetary nebulae, a warm ionized zone is created by the action of the central stars. The main components of the gas are hydrogen and helium. With increasing distance from the ionizing sources, geometrical dilution and optical depth effects reduce the ionizing flux and the gas becomes largely neutral. Some ionization persists from the photoionization of minor constituents C, S and Si. The formation of molecular hydrogen occurs through the reaction sequences (22) to (27) (Black, 1978). Of greater interest is the formation of the molecular ion HeH^+ because it may be detectable through its infrared vibrational emission. In gaseous nebulae, its formation is enhanced by the radiative association He^+ and H

$$He^+ + H \longrightarrow HeH^+ + h\nu \tag{37}$$

which has a rate coefficient of about 10^{-15} cm^3 s^{-1} (Zygelman and Dalgarno, 1990). Reaction (37) is not effective in the early Universe because of the small overlap of ionized helium and neutral hydrogen. Figure 1.2 is an illustration of the distributions of H^-, H_2^+, H_2 and HeH^+ in a nebula of density $n(H) = 10^4$ cm^{-3} and $n(He) = 10^3$ cm^{-3} as functions of distance from a central star with a hydrogen ionizing flux of 10^{48} s^{-1} and a blackbody temperature of

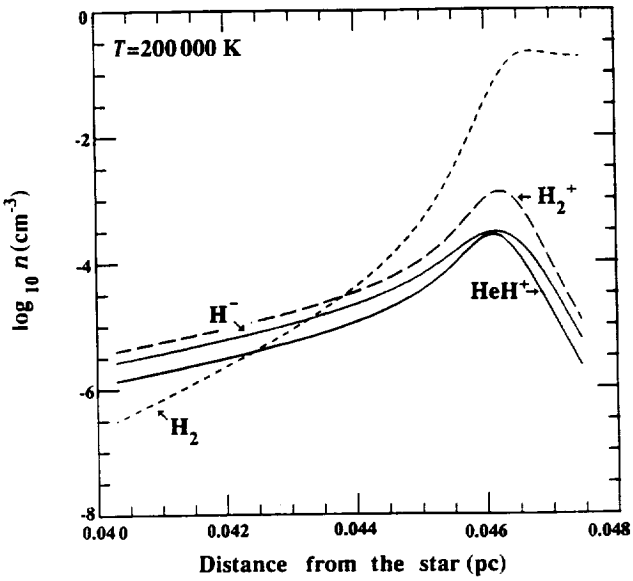

Figure 1.2 The abundances of H_2, H^-, H_2^+ and HeH^+ in a model spherical nebula with a density of 10^4 cm^{-3} corresponding to a central star with an effective temperature of 200 000 K as a function of radial distance. (From Cecchi-Pestillini and Dalgarno, 1993)

200000 K (Cecchi-Pestillini and Dalgarno, 1993). A search for HeH^+ in the planetary nebula NGC 7027 (Moorhead *et al.*, 1988) was unsuccessful. Model calculations (Cecchi-Pestillini and Dalgarno, 1993) suggest that the emission may be close to the observational upper limit.

High-velocity winds are generated by newly formed protostars. The winds may be partly neutral (Natta *et al.*, 1988) and molecular synthesis may be driven by reactions of the ionized and neutral components in a chemistry closely analogous to that occurring in the early Universe (Rawlings *et al.*, 1988; Glassgold, 1991). The gas is heated by ultraviolet photons from the protostar. In addition to the H^+ and H^- sequences, three-body recombination

$$H + H + H \longrightarrow H_2 + H \tag{38}$$

contributes to the formation of molecular hydrogen in the higher density winds. Reaction (38) was important also in the evolution of the first collapsing objects in which cooling due to molecular hydrogen controlled the fragmentation mass spectrum (Stahler *et al.*, 1986).

1.2.1.3 Supernova 1987a

The envelope of Supernova 1987a is composed mostly of hydrogen and helium with a minor component of heavy elements appropriate to the interstellar medium of the Large Magellanic Cloud galaxy. The gas is heated and ionized by events initiated by the absorption of γ-rays emitted in the decay of ^{60}Co. The ion chemistry is modified by an important additional sequence for the formation of H_2 in which the radiative association of He^+ and H in reaction (37) is followed by reactions (16) and (26).

The He^+ ions can be removed by reaction with H_2. It appears that despite the substantial exoergicity, He^+ reacts very slowly with H_2 in the lowest $v = 0$ and $v = 1$ vibrational levels but very rapidly for H_2 in vibrational levels greater than or equal to $v = 2$ (Jones *et al.*, 1986). The corresponding rate coefficient is $1 \times 10^{-9} \exp(-12000/T)\ cm^3\ s^{-1}$. The reaction is probably (Jones *et al.*, 1986)

$$He^+ + H_2(v \geq 2) \longrightarrow He + H + H^+ \tag{39}$$

Reactions (21) and (31) involving excited hydrogen atoms are significant sources of H_2^+ and H_3^+ in the envelope.

The chemistry of the supernova envelope is of special interest because of the possible identification of emission features at 3.41 and 3.53 μm as transitions between rotation–vibrational levels of H_3^+ (Miller *et al.*, 1992). Figure 1.3 illustrates the match obtained between the observational data (Meikle *et al.*, 1989) and a thermal emission spectrum at a temperature of 2050 K and an expansion velocity of 3200 km s^{-1} (Miller *et al.*, 1992). The identification was stimulated by the positive identification of H_3^+ emission in the spectra of Jovian

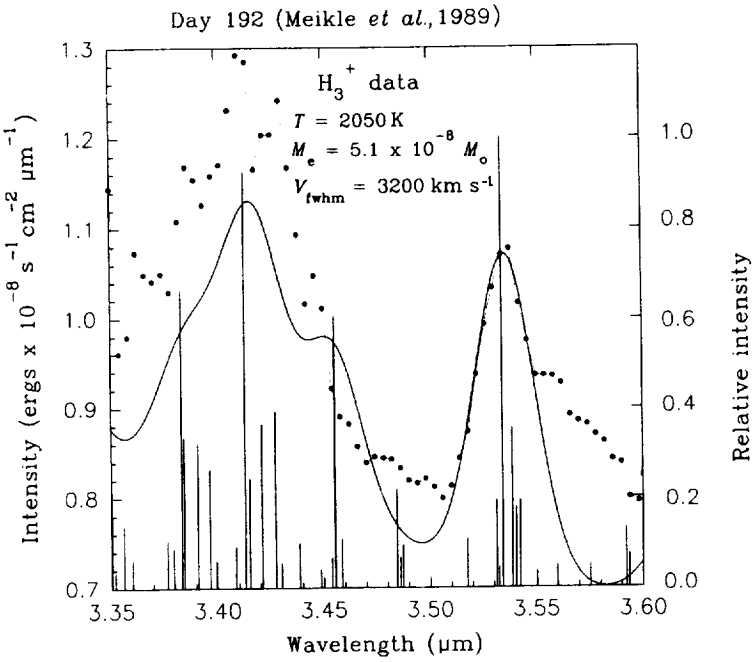

Figure 1.3 The points are observational data on the infrared emission spectrum of supernova 1987a. The solid line is a theoretical curve showing the thermal emission spectrum at 2050 K and an expansion velocity of 3200 km s^{-1} for H_3^+. (From Miller *et al.*, 1992)

auroras (Trafton *et al.*, 1989; Drossart *et al.*, 1989, 1993; Kim *et al.*, 1990; Maillard *et al.*, 1990; Miller *et al.*, 1990; Oka and Getalle, 1990; Geballe *et al.*, 1993; Trafton *et al.*, 1993).

1.2.1.4 Quasar broad-line regions

Broad emission lines in allowed transitions observed toward quasars appear to originate in small dense high-velocity clouds. They are ionized by the ultraviolet and X-radiation from the quasar, and the formation of molecular hydrogen in the broad-line region clouds proceeds by the same reactions that occur in the supernova (Kallman *et al.*, 1987; Crosas and Weisheit, 1993).

1.2.1.5 Dissociative shocks

Fast shocks result from protostellar outflows, stellar winds and supernova explosions in the interstellar gas. If the shock velocity exceeds 50 km s^{-1}, all

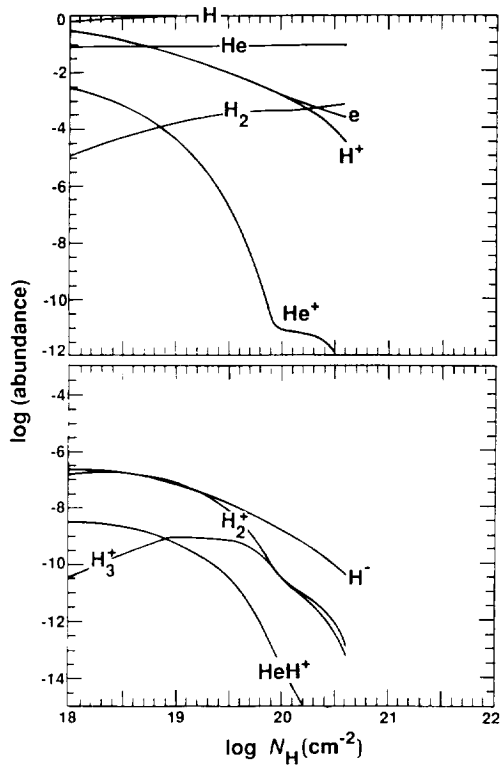

Figure 1.4 The abundance of various ions of hydrogen and helium in gas of density 10^5 cm^{-3} subjected to a shock of velocity 80 km s^{-1} as a function of column density of hydrogen behind the shock. (From Neufeld and Dalgarno, 1989)

the molecules are destroyed in the heated gas and ionization is produced by electron impacts. The ionized gas then recombines and cools and, as it does, it releases ultraviolet photons. This precursor radiation modifies the chemistry behind and ahead of the shock (Hollenbach and McKee, 1989; Neufeld and Dalgarno, 1989). The cooling gas eventually recombines and molecular hydrogen is formed by reactions (22) and (26) and (23) and (27). The formation of molecular hydrogen occurs whilst the gas is still warm and it initiates chemistry in which the hydroxyl radical occupies a central role. If dust grains survive the shock, the abundance of molecular hydrogen may be enhanced by formation on the grain surfaces. Figure 1.4 illustrates the density profiles of the shocked gas as a function of the column density of shocked material (Neufeld and Dalgarno, 1989).

1.2.2 PLANETARY ENVIRONMENTS

Most of the ionization in a planetary atmosphere occurs in a region called the thermosphere. The thermosphere is so named for the temperature structure of the terrestrial upper atmosphere, which increases rapidly from a local minimum (the mesopause) of 160–190 K near 85 km to a large and constant value (the exospheric temperature) of 700–2000 K, depending upon solar activity. This increase in temperature is caused by absorption of solar extreme and far ultraviolet radiation, while the tendency to approach a constant value results from the increase in conductivity that accompanies the exponentially decreasing number densities. In the terrestrial atmosphere, the base of the thermosphere occurs at a pressure of a few μbar. In the atmospheres of other planets, similar thermal structure is encountered, but the limiting temperature is not always large. Exospheric temperatures of 180–200 K have been reported for low solar activity on Mars (Nier and McElroy, 1977). On the nightside of Venus, the temperature actually decreases above the mesopause, from about 160 K to an exospheric temperature of about 100 K (Seiff *et al.*, 1985).

The same ultraviolet radiation that leads to thermospheric heating also produces ionization, and in this process energetic photoelectrons are ejected that cause further ionization.

The chemical structure of the upper atmosphere is determined to a great extent by the location of the homopause (or turbopause), which is usually found in the lower thermosphere of a planet. Below the homopause, the major constituents are assumed to be thoroughly mixed by convection and/or turbulence. Above the homopause, diffusion becomes the dominant transport mechanism, and the constituents separate out under the force of gravity. The mixing ratios of heavier species therefore decrease and those of lighter constituents increase with altitude. This simple distribution does not apply to minor species whose densities are photochemically determined, such as atomic oxygen in the terrestrial lower thermosphere.

1.2.2.1 Outer planets

Unlike the terrestrial planets, the outer planets have retained their primordial atmospheres, the composition of which is similar to that of the sun. The dominant atmospheric species is H_2, with a few percent He by number. There are also small quantities of methane and higher hydrocarbons present in the thermospheres of the major planets, but, because hydrocarbons are heavy, their densities decrease rapidly above the homopause. Photodissociation of H_2 and diffusive separation lead to increasing densities of hydrogen atoms above the homopause. At sufficient heights, atomic hydrogen is predicted to become the dominant constituent. Model atmospheres for the Jovian and Saturnian thermospheres are shown in Figures 1.5 and 1.6 (Smith *et al.*, 1983a; Kim, 1991).

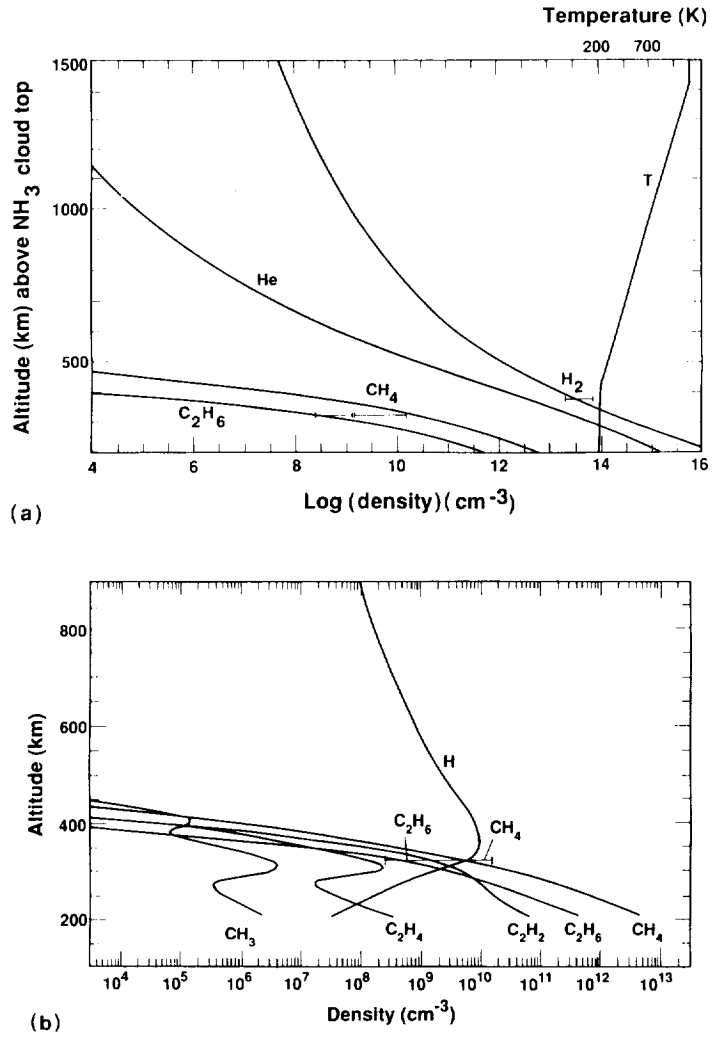

Figure 1.5 (a) A model of the Jovian thermosphere. The altitude scale refers to height above the ammonia cloud tops (near 0.6 bar). The H_2 density and temperature profiles were taken from Atreya *et al.* (1981). The horizontal bars indicate the densities of H_2, CH_4 and C_2H_6 inferred from Voyager stellar occultation data. The other density profiles are computed without photochemistry. (b) Computed density profiles of hydrocarbons and hydrogen atoms. The values shown were computed with coupled hydrocarbon and ion chemistry. (Adapted from Kim, 1991)

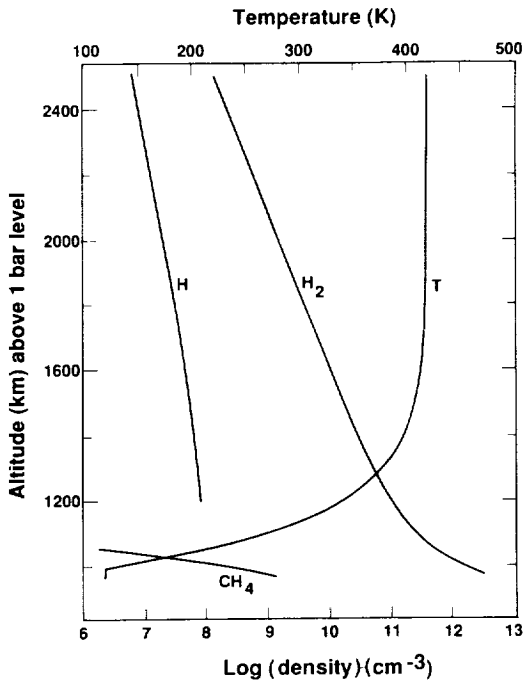

Figure 1.6 Model for the thermosphere of Saturn derived from the Voyager 2 solar and stellar occultation data. The altitude is referred to the 1 bar level. It should be noted that from the same data Festou and Atreya (1982) derived an exospheric temperature about twice that shown here. (Adapted from Smith *et al.*, 1983)

They are consistent with the neutral density structure of these atmospheres inferred from the Voyager ultraviolet stellar occultation experiment (Smith *et al.*, 1983a; Kim, 1991).

Altitude profiles of the production rate of ions in the Jovian ionosphere are shown in Figure 1.7(a). Above 500 km, photoionization of H_2

$$H_2 + h\nu \longrightarrow H_2^+ + e \tag{40}$$

is the major ion production process. Below 500 km, photoelectron impact ionization

$$e + H_2 \longrightarrow e + H_2^+ + e \tag{41}$$

assumes a greater importance, because of the steepening of the incident spectrum as the radiation penetrates into the atmosphere. This radiation hardening leads to energetic photoelectrons. Although H_2 is the major atmospheric constituent between 350 and 450 km, photoionization of atomic hydrogen is the most efficient source of ionization because the photons that are

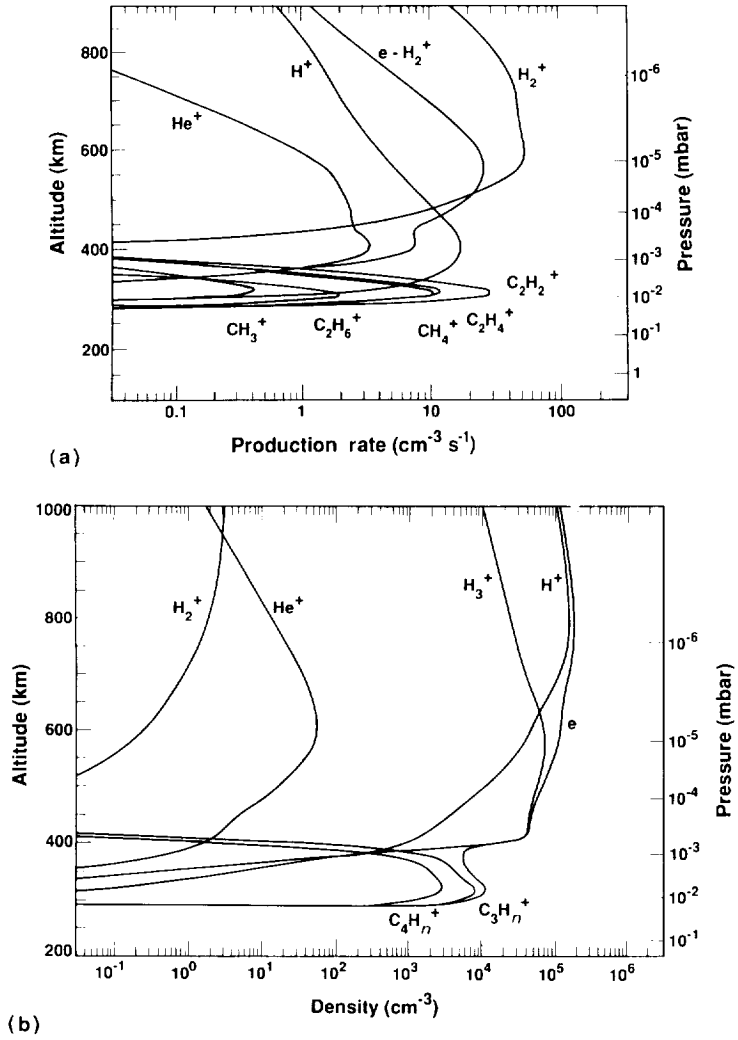

Figure 1.7 (a) Computed production rate profiles of ions in the Jovian ionosphere for solar maximum conditions and a solar zenith angle of 22.5 °. The hydrocarbon ions are labeled in order of increasing peak production rate. The curve labeled e-H_2^+ is the production rate of H_2^+ from electron impact ionization of H_2. (b) Computed ion density profiles for a local time of noon for a latitude of 22.5 °C. A magnetic dip angle of 45 ° is assumed. Altitude is referred to the ammonia cloud tops. (Adapted from Kim, 1991)

energetic enough to ionize molecular hydrogen are absorbed at higher altitudes. Photons with wavelengths between the ionization threshold of $H_2(v = 0)$ at 80.4 nm and the ionization threshold of H at 91.2 nm penetrate down and ionize H in the photoionization process (17).

Although H_2^+ is the major ion produced over a large altitude range of the Jovian ionosphere, it is quickly transformed to H_3^+ in the fast ion–molecule reaction

$$H_2^+ + H_2 \longrightarrow H_3^+ + H \tag{42}$$

In steady state, the density of H_2^+ is accordingly very small.

Protons are produced in direct ionization of hydrogen atoms and in dissociative ionization of hydrogen molecules. Radiative recombination (18) is slow with a rate coefficient of $4 \times 10^{-12}(250/T_e)^{0.7}$ cm^3 s^{-1}, where T_e is the electron temperature (Bates and Dalgarno, 1962). The protons may diffuse downwards and be removed at high densities by the three-body recombination (Miller *et al.*, 1968)

$$H^+ + H_2 + H_2 \longrightarrow H_3^+ + H_2 \tag{43}$$

producing H_3^+. The charge transfer of H^+ to H_2 in the ground vibrational state is endothermic by 1.8 eV, but it becomes exothermic for vibrational levels $v \geq 4$. Then (McElroy, 1973a)

$$H^+ + H_2(v \geq 4) \longrightarrow H + H_2^+ \tag{44}$$

may be an efficient mechanism for removing ionization that could help in resolving the discrepancy between the electron densities inferred from the radio occultation experiments on the Pioneer 10 and 11 and Voyager 1 and 2 spacecraft and the theoretical models (Chen, 1981; McConnell *et al.*, 1982; Waite *et al.*, 1983; Atreya, 1986; Cravens, 1987; Majeed *et al.*, 1991). The measured electron density peaks are an order of magnitude higher and occur at an altitude 600 km above the theoretical predictions made neglecting vibrationally excited H_2.

The electron densities in Figure 1.7(b) were calculated assuming a vibrational temperature of 1500 K over the entire altitude range. Charge transfer to vibrationally excited H_2 is not effective under all conditions and ion transport along field lines driven by meridional winds or electric fields has been invoked (Atreya, 1986; Majeed and McConnell, 1991).

Similar problems have been encountered in models of the ionosphere of Saturn. A possible resolution will be discussed in Section 1.3.2.

The process (44) may contribute to the removal of protons in photon-dominated regions of the interstellar medium, but it is there counter-balanced by the photoionization of vibrationally excited H_2 (Black and van Dishoeck, 1987)

$$H_2(v \geq 4) + h\nu \longrightarrow H_2^+ + e \tag{45}$$

The H_3^+ molecule is produced by reactions (42) and (43) and removed at high altitudes by the dissociative recombination reactions (32) and (33). Emission from H_3^+ in the infrared has been observed in auroras on Jupiter (Trafton *et al.*, 1989; Drossart *et al.*, 1989, 1993; Kim *et al.*, 1990; Maillard *et al.*, 1990; Miller *et al.*, 1990; Oka and Geballe, 1990), Uranus (Trafton *et al.*, 1993) and Saturn (Geballe *et al.*, 1993). Figure 1.8 is an illustration of the spectrum and the fit that can be obtained by assuming thermal equilibrium at a temperature of 1100 K (Miller *et al.*, 1990). The excitation processes have been discussed by Kim *et al.* (1992).

There is a significant production of He^+ ions in the high ionospheres of the outer planets. The ions recombine radiatively as in reaction (6) but slowly. Radiative association (37) and radiative charge transfer (Jura and Dalgarno, 1971; Zygelman and Dalgarno, 1990)

$$He^+ + H \longrightarrow He + H^+ + h\nu \tag{46}$$

neutralize the helium ions but the reaction (39) with vibrationally excited molecular hydrogen may be a more efficient He^+ removal process.

In models of the Jovian ionosphere it has been assumed that the rate coefficient of the reaction of He^+ with H_2 is equal to the upper limit 2×10^{-13} cm^3 s^{-1} obtained in room temperature measurements (Böringer and

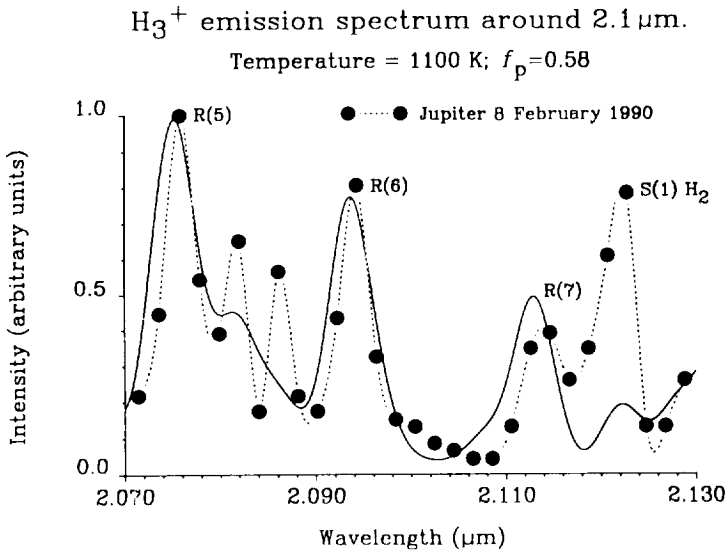

Figure 1.8 The points are the observational data on the infrared emission spectrum of Jupiter. The solid curve is the thermal emission spectrum at 1100 K predicted for H_3^+. (From Miller *et al.*, 1990)

Arnold, 1986) and that, in addition to the end products in reaction (39), channels leading to H_2^+ and HeH^+ also occur (McElroy, 1973a; Johnsen *et al.*, 1980; Atreya, 1986). If reaction (39) is adopted instead, the predicted He^+ concentrations are larger, by as much as two or three orders of magnitudes.

At altitudes near the homopause, the abundance of H^+ and He^+ are greatly modified by the presence of hydrocarbon molecules in the atmosphere.

1.3 PLASMAS WITH AN ADMIXTURE OF HEAVY ELEMENTS

The introduction of even a small fraction of heavy elements into a hydrogen–helium plasma drastically modifies its chemical composition, ionization balance and thermal structure. In interstellar clouds, carbon, oxygen and nitrogen make up at most one part in a thousand by number of the material, yet the millimeter and radiofrequency spectrum is dominated by molecules into which one or more heavy elements has been incorporated. In the atmospheres of the outer planets below the altitudes of the homopause, the increased relative abundances of heavy atoms leads to a diverse array of complex molecular species. Methyl acetylene has been detected on Jupiter and possibly on Saturn.

1.3.1 ASTROPHYSICAL ENVIRONMENTS

Other than the early Universe, astrophysical plasmas contain an important component of heavy elements and their chemistry involves an elaborate set of ion–molecule reactions.

1.3.1.1 Diffuse and translucent interstellar clouds

An interstellar cloud is a collection of material in interstellar space in which the constituent particles move with the same mean velocity. Diffuse and translucent molecular clouds are identified by their absorption of the light from individual stars. Absorptions by the diatomic molecules CH, CN, CH^+, OH, CO, H_2, C_2 and NH have been observed in the visible, ultraviolet and infrared. The diatomic molecule CS has been found through its emission in the millimeter region. The absence of polyatomic systems is ascribed to the destructive effects of the interstellar radiation field. The temperatures of diffuse clouds, at least of their central cores, is low, of the order of 30 K. Because the clouds are cold, the chemistry is driven by ionization. Translucent clouds are more extensive versions of diffuse clouds through which optical and infrared radiation can still penetrate.

Ionization is created by interstellar ultraviolet photons, which produce C^+, S^+, Si^+ and ionized metals, and by cosmic rays which ionize everything. The

carbon chemistry initiated by ultraviolet ionization starts with the radiative association

$$C^+ + H_2 \longrightarrow CH_2^+ + h\nu \tag{47}$$

followed by dissociative recombination

$$CH_2^+ + e \longrightarrow CH + H \tag{48}$$

to produce CH. The CH_2^+ ion may react with H_2 to form CH_3^+ in the abstraction reaction

$$CH_2^+ + H_2 \longrightarrow CH_3^+ + H \tag{49}$$

The dissociative recombination

$$CH_3^+ + e \longrightarrow CH + H_2 \tag{50a}$$

$$\longrightarrow CH_2 + H \tag{50b}$$

leads to CH and CH_2. In dense clouds in which the fractional electron density is small, radiative association

$$CH_3^+ + H_2 \longrightarrow CH_5^+ + h\nu \tag{51}$$

may occur before dissociative recombination.

The CH_2, made in reaction (50b), will undergo photodissociation

$$CH_2 + h\nu \longrightarrow CH + H \tag{52}$$

to again produce CH.

In diffuse clouds, CH is removed by photodissociation

$$CH + h\nu \longrightarrow C + H \tag{53}$$

and by photoionization

$$CH + h\nu \longrightarrow CH^+ + e \tag{54}$$

It is also converted to CO and CN by the neutral exchange reactions

$$CH + O \longrightarrow CO + H \tag{55}$$

$$CH + N \longrightarrow CN + H \tag{56}$$

The bringing together of two carbon atoms to form C_2 can be accomplished by the sequence

$$C^+ + CH \longrightarrow C_2^+ + H \tag{57}$$

$$C_2^+ + H_2 \longrightarrow C_2H^+ + H \tag{58}$$

$$C_2H^+ + e \longrightarrow C_2 + H \tag{59}$$

$$C_2^+ + C \longrightarrow C_2 + C^+ \tag{60}$$

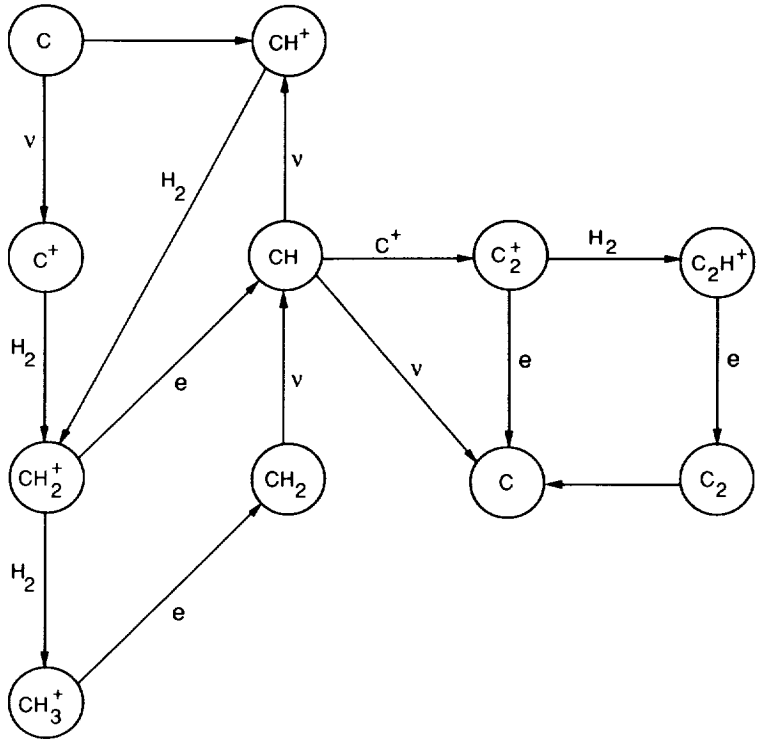

Figure 1.9 The carbon chemistry in interstellar clouds

The carbon chemistry is summarized in Figure 1.9.

Branching reactions with oxygen and nitrogen, (55), (56) and

$$C_2 + O \longrightarrow CO + C \tag{61}$$

$$C_2 + N \longrightarrow CN + C \tag{62}$$

produce CO and CN.

The sequence

$$CH_3^+ + O \longrightarrow HCO^+ + H_2 \tag{63}$$

$$HCO^+ + e \longrightarrow H + CO \tag{64}$$

is also a source of CO. A similar sequence with N leads to CN. The CN molecules can be converted to CO by

$$CN + O \longrightarrow CO + N \tag{65}$$

Carbon monoxide is the end product of numerous sequences, because of its

large dissociation energy. It is lost by photodissociation

$$CO + h\nu \longrightarrow C + O \tag{66}$$

and by the reaction with He^+

$$He^+ + CO \longrightarrow He + C^+ + O \tag{67}$$

Because the reaction of He^+ with H_2 is slow at low temperatures, reaction (67) is an efficient destruction mechanism in cold clouds. In warmer regions, reaction (39) removes the helium ions.

This system of reactions rests upon the radiative association of C^+ with H_2. Models of interstellar clouds (Black and Dalgarno, 1977; Black *et al.*, 1978; van Dishoeck and Black, 1986, 1989; Viala, 1986; Viala *et al.*, 1988) require a rate coefficient of about 5×10^{-16} cm^3 s^{-1} for the process. An experimental upper limit of 1×10^{-15} cm^3 s^{-1} has been obtained (Luine and Dunn, 1989; Gerlich and Hornung, 1992).

Cosmic ray ionization is needed in diffuse clouds to produce O^+ and N^+. The O^+ ions are produced mostly by charge transfer of H^+

$$H^+ + O \longrightarrow H + O^+ \tag{68}$$

They react with H_2 in a series of abstraction reactions

$$O^+ + H_2 \longrightarrow OH^+ + H \tag{69}$$

$$OH^+ + H_2 \longrightarrow H_2O^+ + H \tag{70}$$

$$H_2O^+ + H_2 \longrightarrow H_3O^+ + H \tag{71}$$

terminating in H_3O^+. Then dissociative recombination

$$H_3O^+ + e \longrightarrow H_2O + H \tag{72a}$$

$$\longrightarrow OH + H_2 \tag{72b}$$

leads to H_2O and OH. The branching ratios for reaction (72b) have been measured recently (Adams, 1992) in what is a major advance for the interstellar chemistry of dense clouds. The branching ratio is less critical in diffuse cloud chemistry because any H_2O formed is rapidly photodissociated

$$H_2O + h\nu \longrightarrow OH + H \tag{73}$$

to yield OH. The sequence is illustrated in Figure 1.10.

The formation of OH provides other pathways for production of CO

$$C^+ + OH \longrightarrow CO + H^+ \tag{74}$$

and

$$C^+ + OH \longrightarrow CO^+ + H \tag{75}$$

$$CO^+ + H_2 \longrightarrow HCO^+ + H \tag{76}$$

$$HCO^+ + e \longrightarrow H + CO \tag{77}$$

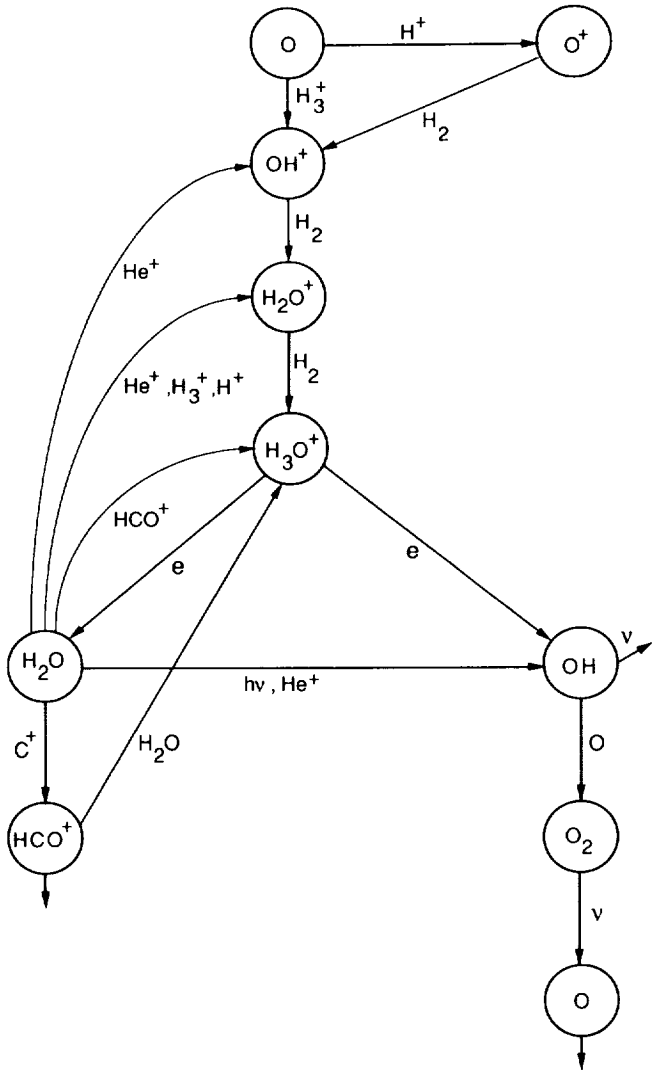

Figure 1.10 The oxygen chemistry in interstellar clouds

Cosmic ray ionization is particularly effective in producing OH because it does so through the ionization of the major constituents H and H_2 to produce H^+ and H_2^+. The H_2^+ ions are quickly converted to H_3^+ by reaction (42)

$$H_2^+ + H_2 \longrightarrow H_3^+ + H \tag{78}$$

and H^+ and H_3^+ then react with O atoms. The analogous reactions do not occur with N atoms and the nitrogen ion–molecular chemistry is initiated by the direct cosmic ray ionization of N to produce N^+. The reaction

$$N^+ + H_2 \longrightarrow NH^+ + H \tag{79}$$

is slightly endothermic (Gerlich and Hornung, 1992) and in cold clouds must compete with

$$N^+ + CO \longrightarrow NO + C^+ \tag{80}$$

$$\longrightarrow N + CO^+ \tag{81}$$

In warmer diffuse clouds, reaction (79) proceeds and is followed by an abstraction sequence leading to NH_3. Photodissociation of NH_3 and NH_2 leads to NH. Photodissociation of NH itself

$$NH + h\nu \longrightarrow N + H \tag{82}$$

is fast (Kirby and Goldfield, 1991) and it is difficult to reproduce the observed abundance of NH by gas phase chemistry (Crutcher and Watson, 1976; Meyer and Roth, 1991). Formation of NH_3, NH_2 and NH on the surfaces of grains and their release into the gas phase provides a possible resolution of the discrepancies (Wagenblast *et al.*, 1993).

The detection of CS in a diffuse cloud (Drdla *et al.*, 1989) is significant in providing information on the sulfur chemistry. The ionization structure of molecular clouds and perhaps the sizes of collapsing regions of gas are sensitive to the chemistry of sulfur (Hartquist *et al.*, 1993). Like carbon, sulfur is ionized by the interstellar radiation field

$$S + h\nu \longrightarrow S^+ + e \tag{83}$$

Charge transfer from C^+

$$C^+ + S \longrightarrow C + S^+ \tag{84}$$

is an additional source of S^+. Like C^+, S^+ does not react with hydrogen but it can undergo radiative association

$$S^+ + H_2 \longrightarrow H_2S^+ + h\nu \tag{85}$$

The rate coefficient of reaction (85) is uncertain. A value of $10^{-17}(T/300)^{-0.2}$ $cm^3\,s^{-1}$ (Millar and Herbst, 1990) is usually adopted. Because the process is slow, ionization due to S^+ persists deeply into interstellar clouds. The slowness of reaction (85) permits the efficient formation of CS through (Drdla *et al.*, 1989)

$$S^+ + CH \longrightarrow CS^+ + H \tag{86}$$

$$S^+ + C_2 \longrightarrow CS^+ + C \tag{87}$$

$$CS^+ + H_2 \longrightarrow HCS^+ + H \tag{88}$$

$$HCS^+ + e \longrightarrow H + CS \tag{89}$$

Photodissociation of CS is the main destruction channel. The exothermic reaction

$$CS + O \longrightarrow CO + S \tag{90}$$

has an activation energy of 760 K (Millar *et al.*, 1991) and is slow in diffuse clouds. It is effective in warm gas. Other reactions that can destroy CS tend to enter sequences that lead back to it.

The chemical models that have been constructed of diffuse clouds, and indeed of translucent and dense clouds, are based on sets of reactions and rate coefficients listed by Anicich and Huntress (1986), Millar *et al.* (1991) and Anicich (1993). For reactions for which no measurements exist it is assumed that reactions of ions with homonuclear molecules occur at the Langevin rate of about 10^{-9} cm^3 s^{-1}, independent of temperature. For reactions of ions with heteronuclear molecules, one or another of several theoretical models (Clary, 1990; Dubernet *et al.*, 1992; Wickham *et al.*, 1992) is adopted. In agreement with experiments (Adams *et al.*, 1985; Marquette *et al.*, 1985; Clary, 1990), the theoretical models indicate a rate coefficient increasing with decreasing temperature. The theoretical models also demonstrate that the rate coefficients are sensitive to the rotational level of the molecule. In astronomical environments, the rotational populations are often far from thermal equilibrium. Reaction rate coefficients may also be affected by the fine-structure populations in the case of ions such as N^+ (Marquette *et al.* , 1988) and C^+ and Si^+ (Graff, 1989).

The models have met with mixed success (Brown and Rice, 1986; Millar *et al.*, 1987; Suzuki *et al.*, 1988; Herbst and Leung, 1989, 1990) despite the flexibility offered by the uncertainties in the values of the reaction rate coefficients at the ambient cloud temperatures. Perhaps large molecules participate in the chemistry. There are observational evidence and theoretical arguments (Léger and Puget, 1984; Allamandola *et al.*, 1985; Lepp *et al.*, 1988) to support the view that a substantial component of polycyclic aromatic hydrocarbons and fullerenes is present in the diffuse interstellar medium. In diffuse clouds the large molecules will be singly and doubly ionized (d'Hendecourt and Léger, 1987; Lepp and Dalgarno, 1988a; Millar, 1991), at least in the boundary region, and interesting chemistry may occur (Lepp and Dalgarno, 1988b; Millar, 1991).

Translucent clouds are intermediate in extent between diffuse and dense clouds (van Dishoeck and Black, 1980; Lepp and Dalgarno, 1988b; van Dishoeck, 1990). Similar to translucent clouds is a class of high-latitude clouds, seen through CO millimeter emission (van Dishoeck and Black, 1980). In some translucent and high-latitude clouds, the polyatomic molecules H_2CO and C_3H_2 have been detected in addition to the diatomic molecules observed in diffuse clouds. Formaldehyde can be made from (Dalgarno *et al.*, 1973b)

$$CH_3 + O \longrightarrow H_2CO + H \tag{91}$$

and perhaps

$$CH_5^+ + O \longrightarrow H_3CO^+ + H_2 \quad (92)$$

$$H_3CO^+ + e \longrightarrow H_2CO + H \quad (93)$$

but not in the abundances that are found. Similarly cyclopropenylidene can be made by a sequence of reactions involving C^+, but again not in the observed abundances. Large molecules may play a role. The vulnerability of H_2CO and C_3H_2 to photodissociation means that an efficient production mechanism is needed.

None of the models is successful in reproducing the abundances of CH^+, which is readily destroyed by dissociative recombination

$$CH^+ + e \longrightarrow C + H \quad (94)$$

photodissociation

$$CH^+ + h\nu \longrightarrow C + H^+ \quad (95)$$

and reactions with H and H_2

$$CH^+ + H \longrightarrow C^+ + H_2 \quad (96)$$

$$CH^+ + H_2 \longrightarrow CH_2^+ + H \quad (97)$$

A major additional source of CH^+ is needed. It seems necessary to invoke

$$C^+ + H_2 \longrightarrow CH^+ + H \quad (98)$$

Reaction (98) is endothermic by 0.4 eV so it will proceed rapidly only if the ambient gas is warm or the H_2 vibrational levels are anomalously excited or the C^+ ion is accelerated (Duley *et al.*, 1992). It must also occur in a gas with a high H/H_2 ratio to avoid the overproduction of CH that would otherwise result. Shocked gas appears to be excluded by the absence of a velocity difference between CH^+ and CH or CO.

However the CH^+ is produced, it may be an important source of CO and CN through reactions following

$$CH^+ + O \longrightarrow CO^+ + H \quad (99)$$

$$CH^+ + N \longrightarrow CN^+ + H \quad (100)$$

Because the models underestimate CH^+, they may also underestimate CO and CN.

Many diffuse molecular clouds may be the boundary regions of more extensive clouds. When subjected to intense radiation fields they are called photon-dominated regions or photodissociation regions (PDRs). They occur in the nuclei of external galaxies and starburst galaxies (Stacey *et al.*, 1991) and in the Milky Way, the Orion Molecular Cloud being a dramatic example (Stacey

et al., 1993). The chemistry is driven by photoionization and limited by photodissociation (Tielens and Hollenbach, 1985a, 1985b; Sternberg and Dalgarno, 1989). The irradiated edge of the PDR may be heated to temperatures above 1000 K and the chemistry is modified. Photodissociation can be more efficient than dissociative recombination in removing molecular ions.

1.3.1.2 Dense molecular clouds

Dense molecular clouds are the birthplaces of stars. Emission from molecules formed within them cools the clouds and brings regions of them to the point of gravitational collapse. The cooling radiation is detected and provides a diagnostic probe of star formation. Table 1.1 (Dalgarno, 1993b) is a collection of molecular species that have been detected in interstellar clouds. Although ion–molecule chemistry in itself does not explain the observed abundances, ion–molecule reactions play a major part in determining the chemical composition of dense clouds.

The ion–molecule chemistry begins with the production of H_2^+ by cosmic rays followed by reaction (42). Proton transfer reactions such as (69) followed by abstraction sequences (68) to (70) lead to polyatomic molecular ions which undergo dissociative recombination to form neutral molecules. Figure 1.10 illustrates the reaction sequence.

Mechanisms for building the complex hydrocarbons of Table 1.1 are illustrated in Figure 1.11. The radiative association process

$$CH_3^+ + H_2 \longrightarrow CH_5^+ + h\nu \tag{101}$$

is a critical step. There remains a considerable uncertainty in its rate coefficient at the temperatures of dense clouds near 10–20 K (Gerlich and Hornung, 1992).

Insertion reactions such as

$$C^+ + CH_4 \longrightarrow C_2H_3^+ + H \tag{102}$$

followed by

$$C_2H_3^+ + e \longrightarrow C_2H_2 + H \tag{103}$$

makes acetylene, which reacts again with C^+

$$C^+ + C_2H_2 \longrightarrow C_3H^+ + H \tag{104}$$

to continue the build-up of carbon atoms. Condensation reactions

$$CH_3^+ + CH_4 \longrightarrow C_2H_5^+ + H_2 \tag{105}$$

also help to form complex organic molecules.

Rate coefficients for radiative association are generally uncertain. Yet the processes are an essential component of the formation of the complex organic

Table 1.1 Interstellar molecules

H_2	Hydrogen	CH	Methylidyne
CH^+	Methylidyne ion	OH	Hydroxyl
C_2	Carbon	CN	Cyanogen
CO	Carbon monoxide	NO	Nitric oxide
CS	Carbon monosulfide	SiO	Silicon monoxide
SO	Sulfur monoxide	NS	Nitrogen sulfide
SiS	Silicon sulfide	PN	Phosphorous nitride
HCl	Hydrogen chloride	SiN	Silicon nitride
H_2O	Water	C_2H	Ethynyl
HCN	Hydrogen cyanide	HNC	Hydrogen isocyanide
HCO	Formyl	HCO^+	Formyl ion
N_2H^+	Protonated nitrogen	H_2S	Hydrogen sulfide
HNO	Nitroxyl	OCS	Carbonyl sulfide
SO_2	Sulfur dioxide	HCS^+	Thioformyl ion
C_2O	Carbon suboxide	C_2S	Dicarbon sulfide
H_2CO	Formaldehyde	H_2CS	Thioformaldehyde
NH_3	Ammonia	HCNS	Isothiocyanic acid
HNCO	Isocyanic acid	$HOCO^+$	Protonated carbon dioxide
C_3H	Propynylidyne	C_3N	Cyanoethynyl
C_3S	Tricarbon sulfide	C_3O	Tricarbon monoxide
C_2H_2	Acetylene	H_3O^+	Hydronium ion
$HCNH^+$	Protonated hydrogen cyanide	C_3H_2	Cyclopropenylidene
CH_4	Methane	H_2CCC	Propadienylidene
HCOOH	Formic acid	CH_2CO	Ketene
HC_3N	Cyanoacetylene	HNCCC	
HCCNC	Ethynyl isocyanide	C_4H	Butadinyl
NH_2CH	Cyanamide	CH_2CN	Cyanomethyl radical
CH_2NH	Methanimine	CH_3CN	Methyl cyanide
H_2CCCC	Butatrienylidene	CH_3SH	Methyl mercaptan
C_5H	Pentynylidyne	HCC_2HO	Propynal
CH_3OH	Methyl alcohol	CH_3C_2H	Methyl acetylene
NH_2CHO	Formamide	HC_5N	Cyanodiacetylene
CH_2CHCN	Vinyl cyanide	CH_3NH_2	Methylamine
C_6H	Hexatrinyl	$HCOOCH_3$	Methyl formate
CH_3CHO	Acetaldehyde	CH_3C_4H	Methyl diacetylene
CH_3C_3N	Methyl cyanoacetylene	CH_3CH_2CN	Ethyl cyanide
$(CH_3)_2O$	Dimethyl ether	CH_3CH_2OH	Ethyl alcohol
HC_7N	Cyanohexatriyne	HC_9N	Cyano-octatetrayne
$HC_{11}N$	Cyanodecapentayne		

molecules found in dense clouds. Methyl alcohol may be a result of

$$CH_3^+ + H_2O \longrightarrow CH_3^+ \cdot H_2O + h\nu \tag{106}$$

$$CH_3^+ \cdot H_2O + e \longrightarrow CH_3OH + H \tag{107}$$

and ethyl alcohol a result of

$$H_3O^+ + C_2H_4 \longrightarrow H_3O^+ \cdot C_2H_4 + h\nu \tag{108}$$

$$H_3O^+ \cdot C_2H_4 + e \longrightarrow CH_3CH_2OH + H \tag{109}$$

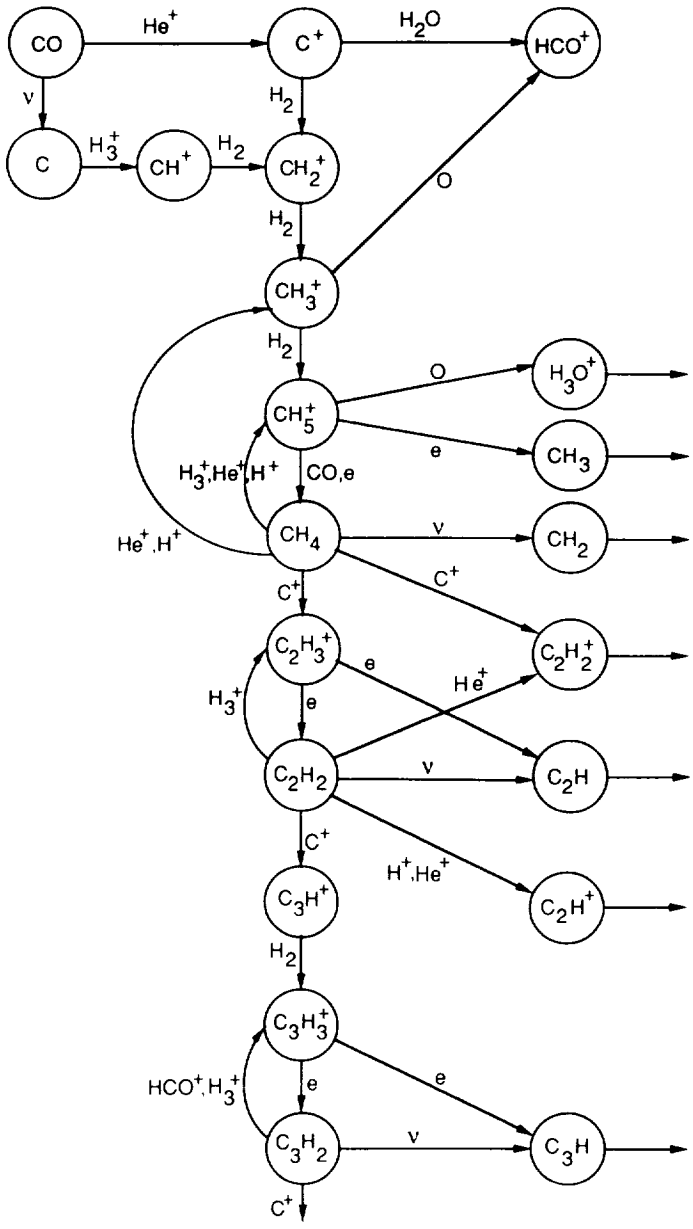

Figure 1.11 Mechanisms for the production of hydrocarbons in dense interstellar clouds

The hydrocarbons and their extensions illustrated in Figure 1.11 undergo branching reactions and incorporate other species. Reactions with N lead to the polyacetylenes. The reactions with O and with S are mostly unknown. The high relative abundances of C_2S and C_3S (Saito *et al.*, 1987; Yamamoto *et al.*, 1987) suggest that sulfur insertion reactions

$$S + C_3H_3^+ \longrightarrow HC_3S^+ + H_2 \qquad (110)$$

are rapid (Smith *et al.*, 1988; Suzuki *et al.*, 1988). The reactions with oxygen may be destructive (Bettens and Brown, 1992). They are often neglected.

The neutral molecules are destroyed by reactions with He^+. Acetylene, which is an important molecule in the hydrocarbon chain of Figure 1.11, is lost by

$$He^+ + C_2H_2 \longrightarrow He + H_2 + C_2^+ \qquad (111a)$$

$$\longrightarrow He + C_2H_2^+ \qquad (111b)$$

$$\longrightarrow He + C_2H^+ + H \qquad (111c)$$

$$\longrightarrow He + CH^+ + CH \qquad (111d)$$

reaction (111b) being the major channel. Methane is also destroyed by He^+ in the reactions

$$He^+ + CH_4 \longrightarrow He + CH_4^+ \qquad (112a)$$

$$\longrightarrow He + CH_3^+ + H \qquad (112b)$$

$$\longrightarrow He + CH_2^+ + H_2 \qquad (114c)$$

$$\longrightarrow He + CH^+ + H_2 + H \qquad (112d)$$

$$\longrightarrow He + H^+ + CH_3 \qquad (112e)$$

reaction (112b) being the major channel (Anicich, 1993). These reactions occur also in the ionospheres of the outer planets to which we now turn.

1.3.2 OUTER PLANETS

As shown in Figure 1.7(a), at an altitude below 350 km on Jupiter, a sharp layer of hydrocarbon ionization appears due to photons with wavelengths longer than the ionization thresholds of H, H_2 and He. The ionization potential of methane is 12.5 eV. Most larger hydrocarbons have still lower potentials. CH_3 and C_2H_5 can be ionized by the strong solar Lyman alpha line at 121.6 nm, corresponding to an energy of 10.2 eV. Photons are absorbed at the centers of the Lyman and Werner bands of H_2 but penetrate down in the wings, causing direct ionization of hydrocarbon molecules down to about 300 km (Kim and Fox, 1992).

Any He^+ ions are quickly removed by reactions such as (111) and (112). Of the H^+ ions that have diffused down, some can form H_3^+ in the three-body reaction (43) but most react rapidly with CH_4 (Dheandhanoo *et al.*, 1984)

$$H^+ + CH_4 \longrightarrow CH_3^+ + H_2 \tag{113a}$$

$$\longrightarrow CH_4^+ + H \tag{113b}$$

and with C_2H_6 (Mackay *et al.*, 1981).

On Saturn, the electron densities may be reduced to the measured values by postulating an influx of water (Chen, 1983; Shimizu, 1983; Connerny and Waite, 1984; Majeed and McConnell, 1991). Protons can then be removed by

$$H^+ + H_2O \longrightarrow H + H_2O^+ \tag{114}$$

The H_2O^+ dissociatively recombines

$$H_2O^+ + e \longrightarrow OH + H \tag{115}$$

or reacts with H_2 as in reaction (70), producing H_3O^+.

The H_2O is also photodissociated

$$H_2O + h\nu \longrightarrow OH + H \tag{116}$$

and H^+ can charge transfer to OH

$$H^+ + OH \longrightarrow H + OH^+ \tag{117}$$

Then reaction (70) and dissociative recombination

$$OH^+ + e \longrightarrow O + H \tag{118}$$

occur.

A detailed model of the ionosphere on Saturn (Majeed and McConnell, 1991) suggests that the presence of vibrationally excited H_2 or the injection of H_2O from the rings at a flux exceeding $10^7\ cm^{-2}\ s^{-1}$ can reproduce the peak electron density, provided an upward drift along the field lines is imposed on the ions. In Figures 1.12 and 1.13, we present for the two theoretical models comparisons of the predicted ion and electron density profiles with the measurements recorded by the Voyager 2 spacecraft on the exit portion of the Saturn flyby. Little difference is found between the two models and the model topside scale heights are too large by a factor of three. In regions where transport is unimportant the scale height is inversely proportional to mass and directly proportional to temperature. Because it is unlikely that the ionosphere is colder by a factor of three or that the major ion is H_3^+ and not H^+, it appears it is not chemistry but dynamical effects due to strong winds or electric fields that control the ionization structure.

In the region of the ionosphere near and below the Jovian homopause, direct photoionization of hydrocarbons and, to a lesser extent, charge transfer from

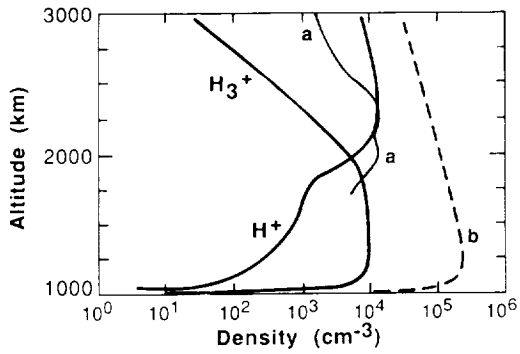

Figure 1.12 Computed profiles for H^+ and H_3^+ and total electron densities in the Saturn ionosphere compared to Voyager 2 egress profile (curve a). The curves labeled H_3^+ and H^+ were computed with an effective rate coefficient for loss of H^+ by reaction with vibrationally excited H_2 (reaction 44) of 1.38×10^{-14} cm^3 s^{-1}, while curve b was computed without this reaction. A vertical drift along field lines of 15 ms^{-1} was imposed. (Adapted from Majeed and McConnell, 1991)

H^+ and He^+ to neutral hydrocarbon molecules produce a layer of hydrocarbon ions. Figure 1.14 shows that the major source of hydrocarbon ions with a single carbon atom below the homopause is photoionization of CH_4 and CH_3, and the major loss processes near 320 km are reactions with methane and acetylene, such as (105) and

$$CH_5^+ + C_2H_2 \longrightarrow C_2H_3^+ + CH_4 \qquad (119)$$

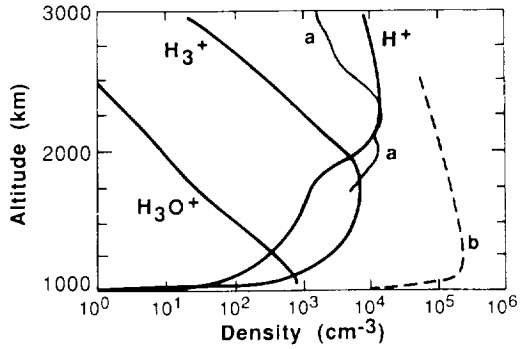

Figure 1.13 Computed profiles for H^+ and H_3^+ and total electron densities in the Saturn ionosphere compared to Voyager 2 egress profile (curve a). The curves labeled H_3^+ and H^+ were computed with an influx of water from the rings of 2.2×10^7 cm^{-2} s^{-1}, while curve b was computed without such a flux. A vertical drift along field lines of 15 ms^{-1} was imposed. (Adapted from Majeed and McConnell, 1991)

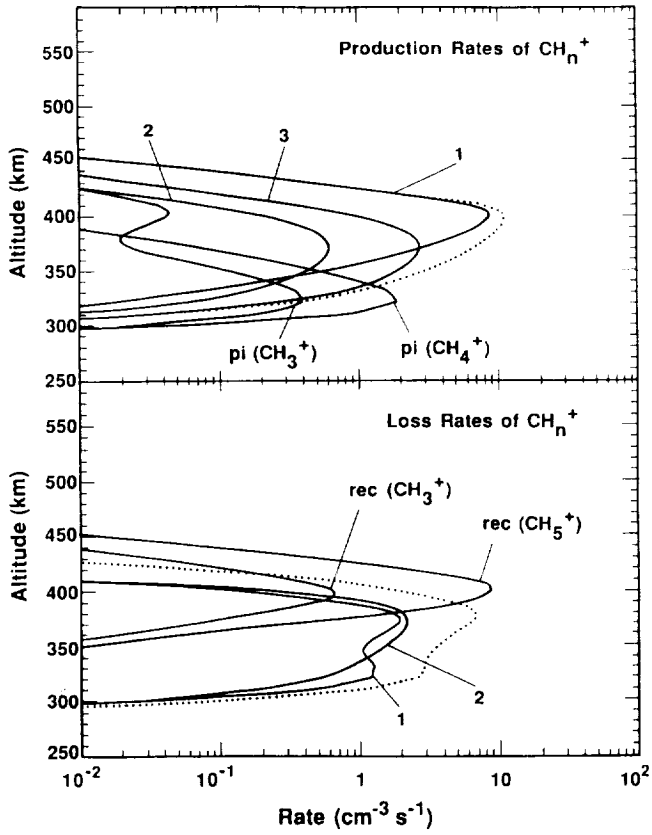

Figure 1.14 Sources (a) and sinks (b) of C_1 hydrocarbon ions in the Jovian ionosphere. (a) The labels pi(CH_4^+) and pi(CH_3^+) refer to the photoionization of CH_4 and CH_3 leading to CH_4^+ and CH_3^+, respectively. The labels 1, 2 and 3 are the production rates due to the reactions $H_3^+ + CH_4 \longrightarrow CH_5^+ + H_2$, $H^+ + CH_4 \longrightarrow CH_4^+ + H$ and $H^+ + CH_4 \longrightarrow CH_3^+ + H_2$, respectively. (b) The labels rec(CH_3^+) and rec(CH_5^+) refer to dissociative recombination of CH_3^+ and CH_5^+, respectively. The labels 1 and 2 refer to the reactions $CH_5^+ + C_2H_2 \longrightarrow C_2H_3^+ + CH_4$ and $CH_3^+ + CH_4 \longrightarrow C_2H_5^+ + H_2$. The dotted curve is the total rate of reactions that convert C_1 into C_2 hydrocarbon ions. (Adapted from Kim, 1991)

The largest sources of hydrocarbon ions with two carbon atoms near 320 km are photoionization of C_2H_2, C_2H_4 and C_2H_6 and the most rapid loss processes are

$$C_2H_5^+ + C_2H_2 \longrightarrow C_3H_3^+ + CH_4 \quad (120)$$

$$C_2H_5^+ + C_2H_2 \longrightarrow C_4H_5^+ + H_2 \quad (121)$$

and to a lesser extent reactions with CH_4 such as

$$C_2H_5^+ + CH_4 \longrightarrow C_3H_7^+ + H_2 \quad (122)$$

Above about 380 km, most of the hydrocarbon ions are destroyed in dissociative recombination but near 320 km almost all the hydrocarbon ions produced react to form C_3 and C_4 hydrocarbon ions. Rate coefficients for possible reactions of large hydrocarbon ions are not well known, but it is likely that the large ions will also react, especially with acetylene, to produce higher hydrocarbon ions which will ultimately be destroyed by dissociative recombination.

The major ions in the ionospheres of the outer planets and the reactions that connect them are shown in Figure 1.15. In one model of the Jovian E region (Kim and Fox, 1992), reactions of hydrocarbons with one or two carbon atoms were included explicitly. Higher hydrocarbons were taken into account as two groups of ions called $C_3H_n^+$ and $C_4H_n^+$, which were assumed to be lost by dissociative recombination with rate coefficients of 3.5×10^{-7} $(300/Te)^{0.5}$ $cm^3\ s^{-1}$. Figure 1.16 shows computed altitude profiles of electron densities and the major ions H^+, H_3^+, He^+ and H_2^+, and the two groups of hydrocarbon ions for a latitude of 22.5° and a local time of noon. The peak density of hydrocarbon ions is greater than $10^4\ cm^{-3}$ near 320 km.

Although the solar flux at Uranus is 400 times less than at Earth, electron density profiles measured by the radio occultation experiment on Voyager 2 show a number of layers peaking below about 2000 km (Lindal *et al.*, 1987). An influx of H_2O or CH_4 from the rings could reduce the electron densities in the equatorial regions (Strobel *et al.*, 1991) in much the same way as predicted for Saturn (Connerny and Waite, 1984). Because Uranus does not have as strong an internal heat source as do Jupiter and Saturn, the tropopause is very cold, about 50 K. Consequently, the hydrocarbon densities at higher altitudes are much smaller (Strobel *et al.*, 1991) and the hydrocarbon ion layer predicted for Jupiter and Saturn is probably absent.

Electron density profiles determined from the Pioneer 10 and 11 radio occultation measurement of the Jovian ionosphere showed a number of layers below the main ionospheric peak (Fjeldbo *et al.*, 1974, 1976). The lower layers may be composed of metallic ions (Atreya *et al.*, 1974; Atreya and Donahue, 1976), similar to those found in the terrestrial ionospheric E region (Atreya *et al.*, 1974), and which result from photoionization and charge exchange reactions of the major ions with metal atoms that are produced by ablation of meteorites (Hunten *et al.*, 1980; Hunten, 1981). The major meteoritic ions are Fe^+, Mg^+ and Si^+ (Swider, 1992). The flux of meteors into the Jovian ionosphere may be enhanced over the terrestrial value by gravitational focusing (Grebowsky, 1981). For plausible meteoroid fluxes at Jupiter in contrast to the terrestrial case, photoionization is not important compared to charge exchange as a source of Fe^+ ions and the peak metallic ion production rates are similar to those of H_2^+, H^+, He^+ and CH_3^+. The peak densities were estimated to be in the

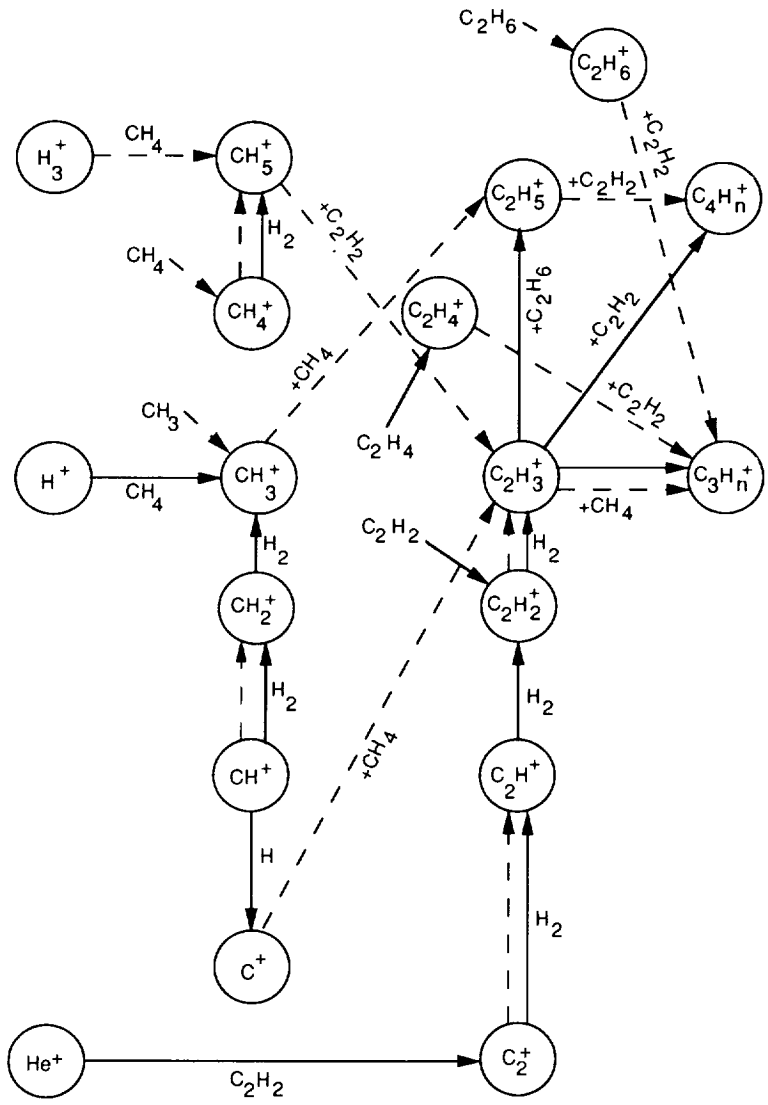

Figure 1.15 Chemical network among ions in the Jovian ionosphere. The major production processes for the species shown are indicated by solid arrows and the major loss processes are shown by dashed arrows. (Adapted from Kim, 1991)

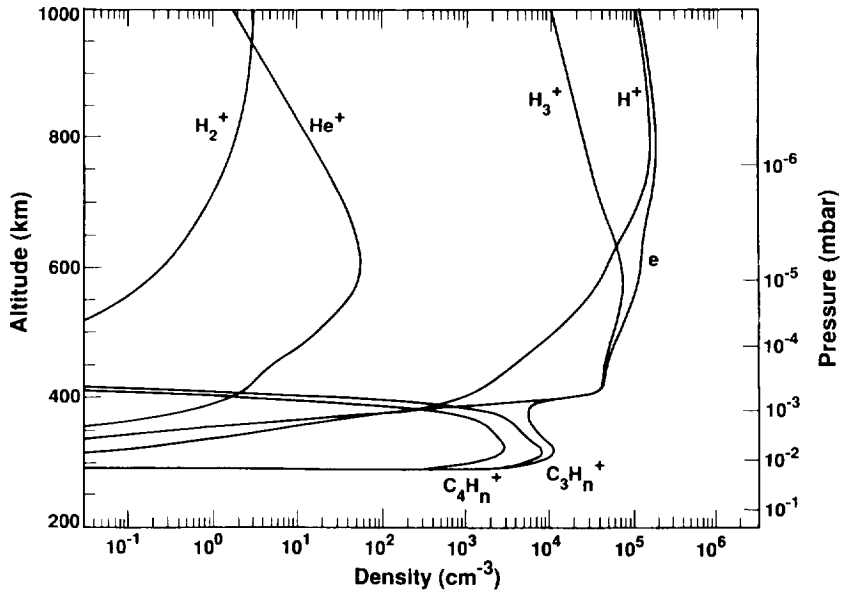

Figure 1.16 Computed ion density profiles for H^+, H_3^+, He^+ and H_2^+, and two groups of hydrocarbon ions: $C_3H_n^+$ and $C_4H_n^+$ for a local time of noon and a latitude of 22.5°. (Adapted from Kim, 1991)

10^3–10^6 cm^{-3} range, with similar contributions from other metal ions, such as Mg^+. The observed layers, which have thicknesses of about 100 km, can be reproduced by postulating fluxes of Na^+ and S^+ ions from the Galilean satellites and high wind shears (Chen, 1981). The models described here, however, considered only radiative recombination as a loss mechanism for metal ions. As in the terrestrial ionosphere, the ions may form clusters which are destroyed by dissociative recombination.

1.4 HEAVY ELEMENT PLASMAS

By heavy element plasma we mean plasmas in which hydrogen and helium play a lesser role, though they may still have a significant impact on the behavior of the plasma. The ionospheres of the terrestrial planets and the satellites Titan and Triton are examples, as is the mantle of the Supernova 1987a.

1.4.1 SUPERNOVA 1987a

The detection of carbon monoxide in the ejecta of Supernova 1987a about 100 days after the explosion of a blue supergiant star in the Large Magellanic Cloud

testifies to the durability of molecular systems in environments that are apparently inimical to their formation and hostile to their survival.

The ejecta are subjected to γ-rays and fast positrons produced in the radioactive decay of ^{56}Ni to ^{56}Co to ^{56}Fe. At later times, the longer-lived isotopes ^{57}Co and ^{44}Ti become the main sources of continuing energy deposition into the ejecta. The γ-rays undergo Compton scattering with free and bound electrons and are degraded into X-rays. The X-rays are preferentially absorbed by heavy elements and by Auger ionization produce multiply charged positive ions. The positive ions capture electrons in radiative

$$X^{m+} + e \longrightarrow X^{(m-1)+} + h\nu \tag{123}$$

and dielectronic

$$X^{m+} + e \longrightarrow X^{(m+1)+*} \tag{124a}$$

$$\longrightarrow X^{(m-1)+} + h\nu \tag{124b}$$

recombination.

Once some neutral material has been produced, charge transfer processes such as

$$X^{m+} + H \longrightarrow X^{(m-1)+} + H^+ \tag{125}$$

$$X^{m+} + He \longrightarrow X^{(m-1)+} + He^+ \tag{126}$$

quickly reduce the ionization stages and the plasma becomes a mixture of electrons, singly charged ions and neutral atoms. A tentative identification of an emission feature at 22.92 μm to Fe^{2+} has been made (Moseley *et al.*, 1989). The presence of Fe^{2+} would not be expected because of the rapidity of the charge transfer recombination processes (Dalgarno, 1990)

$$Fe^{2+} + He \longrightarrow Fe^+ + He^+ \tag{127}$$

$$Fe^{2+} + O \longrightarrow Fe^+ + O^+ \tag{128}$$

The distribution of the ionization after the charge transfer of multiply charged ions has occurred depends on the abundances of the elements and the rate coefficients for the charge transfer of singly charged ions in collision with neutral atoms. The values are uncertain. Of particularly importance are the reactions of He^+ ions. Calculations of the potential energy curves of the HeO^+ (Augustin *et al.*, 1973) indicate that the most probable mechanism for the charge transfer

$$He^+ + O \longrightarrow He + O^+ \tag{129}$$

is spin-orbit and rotational coupling of $^2\Pi$ and $^2\Sigma$ molecular states. A rate coefficient of the order of 10^{-13} cm^3 s^{-1} is possible. It cannot be much greater because of the observation that He^+ ions exist in abundance in the topside ionosphere.

A value of 3.3×10^{-9} cm^3 s^{-1} has been recommended for

$$He^+ + Si \longrightarrow He + Si^+ \tag{130}$$

but it appears to be an arbitrary estimate (Prasad and Huntress, 1980).

Explicit calculations of the potential energy curves and coupling matrix elements of HeC^+ have been carried out. The charge transfer

$$He^+ + C \longrightarrow He + C^+ \tag{131}$$

appears to be driven by a rotational coupling between the $D^2\Sigma^-$ and $B^2\Pi$ states, leading to a rate coefficient at 3000 K of 1×10^{-13} cm^3 s^{-1} (Kimura *et al.*, 1993).

In contrast to the reactions of He^+, charge transfer of ions of complex atoms are likely to be fast because of the accessibility of favorably located potential energy curves. If so, the ionization will flow from elements of high ionization potential like oxygen to elements of low ionization potential like the metals Fe, Ni and Co in reactions such as

$$O^+ + C \longrightarrow O + C^+ \tag{132}$$

$$C^+ + Fe \longrightarrow C + Fe^+ \tag{133}$$

Estimates of the rate coefficients of charge transfer reactions between heavy ions and heavy atoms have been made (Péquignot and Aldrovani, 1986).

The detailed distribution of the neutral atom and ion abundances depend on the specific charge transfer rate coefficients, the element abundances, the ultraviolet photon flux and the energetic electron flux, but the spectra are qualitatively consistent with a scenario dominated by exothermic charge transfer processes.

At early times the formation of molecules is due to three-body processes such as

$$He + C + O \longrightarrow He + CO \tag{134}$$

but the gas is hot and the molecular species are removed by thermal dissociation processes such as

$$He + CO \longrightarrow He + C + O \tag{135}$$

$$e + CO \longrightarrow e + C + O \tag{136}$$

Once the gas has cooled below about 5000 K, CO can survive and emission from vibrationally excited carbon monoxide was detected at 110 days (Oliva *et al.*, 1987; Rank *et al.*, 1988; Spyromlio *et al.*, 1988). The 1–0 fundamental emission of SiO was also detected (Roche *et al.*, 1991; Wooden *et al.*, 1993). The diminishing intensity of the CO emission with the disappearance of emission from high vibrational levels could be attributed to the decreasing temperature.

Several mechanisms have been suggested that led to the formation of CO. At the time when CO was first detected, the particle density was about 10^{11} cm^{-3}, too small for three-body collision to be effective. The initiating reactions had to be two-body collisions in which the formation of a composite system is stabilized by the emission of a photon. Radiative association (Petuchowski *et al.*, 1989; Lepp *et al.*, 1990)

$$C^+ + O \longrightarrow CO^+ + h\nu \tag{137}$$

followed by charge transfer

$$CO^+ + O \longrightarrow CO + O^+ \tag{138}$$

is a possibility. The radiative association is slow with a rate coefficient of about 10^{-18} cm^3 s^{-1} (Dalgarno *et al.*, 1990) and much of the CO^+ that is produced is lost by dissociative recombination

$$CO^+ + e \longrightarrow C + O \tag{139}$$

with a rate coefficient of $1 \times 10^{-7}(300/T)^{0.48}$ cm^3 s^{-1} (Mitchell and Hus, 1987). More efficient because the carbon is mostly neutral is the direct association

$$C + O \longrightarrow CO + h\nu \tag{140}$$

which has a larger rate coefficient of about 10^{-17} cm^3 s^{-1} (Dalgarno *et al.*, 1990).

A potentially significant source is provided by sequences initiated by the formation of negative ions (Lepp *et al.*, 1990). Thus O^- is formed by radiative attachment

$$O + e \longrightarrow O^- + h\nu \tag{141}$$

with a rate coefficient of 10^{-15} cm^3 s^{-1}. Then associative detachment

$$C + O^- \longrightarrow CO + e \tag{142}$$

leads to carbon monoxide. The efficiency of the sequence is impacted by the destruction of O^- by mutual neutralization

$$He^+ + O^- \longrightarrow He + O \tag{143}$$

and photodetachment

$$O^- + h\nu \longrightarrow O + e \tag{144}$$

Less direct sequences can make some contribution. The radiative association

$$O + O \longrightarrow O_2 + h\nu \tag{145}$$

followed by

$$C + O_2 \longrightarrow CO + O \tag{146}$$

is an example. Still less direct but potentially significant in the core if the light elements are mixed back and surely important in the envelope is the sequence of reactions (37), (16) and (26) to form H_2 followed by

$$C + H_2 \longrightarrow CH + H \tag{147}$$

and reaction (55) or

$$O + H_2 \longrightarrow OH + H \tag{148}$$

and

$$OH + C \longrightarrow CO + H \tag{149}$$

The radicals CH and OH can also be formed by radiative association.

Satisfactory agreement with observations can be obtained, but it is necessary to limit the degree of microscopic mixing of helium with the carbon and oxygen (Liu *et al.*, 1992).

The molecule SiO is also detected in the supernova ejecta (Roche *et al.*, 1991; Wooden *et al.*, 1993). It is made mostly by

$$Si + O \longrightarrow SiO + h\nu \tag{150}$$

with some contribution from

$$Si + O_2 \longrightarrow SiO + O \tag{151}$$

It is destroyed by

$$C^+ + SiO \longrightarrow Si^+ + CO \tag{152}$$

The rate coefficient of reaction (150) is unknown. A value of order 10^{-18} $cm^3\ s^{-1}$ is sufficient to reproduce the derived abundances provided there is no fine-scale mixing of helium (Liu and Dalgarno, 1994).

1.4.2 TERRESTRIAL PLANETS

1.4.2.1 Dayside ionospheres

The atmospheres of Mars and Venus are composed mostly of CO_2 with small amounts of N_2: 3.5% for Venus (von Zahn and Moroz, 1985) and about 2.7% for Mars (Owen *et al.*, 1977). The atmosphere of Mars also contains argon with an abundance comparable to that of the Earth, about 1.6%. In the thermospheres of both planets, photodissociation of CO_2 and N_2 results in the formation of small amounts of the photolysis products CO, O and N, along with photochemically produced O_2 and NO. The compositions of the lower thermospheres of Venus and Mars are compared in Table 1.2 (Fox, 1992a). The major difference between the thermospheres of the two planets is the smaller

Table 1.2 Mixing ratios of minor constituents in the atmospheres of Venus and Mars (from Fox, 1992b)

Species	Mars (120 km)	Venus (135 km)
O	0.6(−2)–1.2(−2)	7.3(−2)
CO	4.2(−3)	7.0(−2)
N_2	2.5(−2)	7.4(−2)
NO	7(−5)	3(−5)
O_2	12.2(−3)	3(−3)
Ar	1.5(−2)	6.3(−5)
N	2.1(−4)	1.6(−3)
C	2.5(−5)	4(−4)
He		1(−6)–12(−6)

mixing ratios of O and CO on Mars. Figures 1.17 and 1.18 show model thermospheres of Mars and Venus, constructed from data from the Viking and Pioneer Venus orbiter mass spectrometers (Nier and McElroy, 1976; Hedin *et al.*, 1983). Above the homopauses, which are located near 120–125 km and 135–140 km on the Martian and Venusian daysides, respectively, the lighter constituents become more important, and atomic oxygen eventually becomes the dominant constituent. The Viking mass spectrometers show a transition

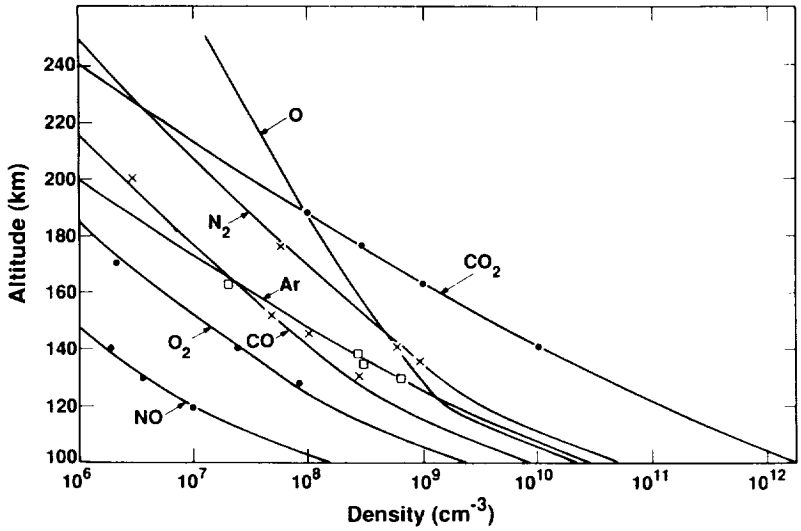

Figure 1.17 Altitude profiles of the major neutral species in the Martian atmosphere. The points are from the Viking 1 mass spectrometer data (Nier and McElroy, 1976). (Adapted from Fox and Dalgarno, 1979)

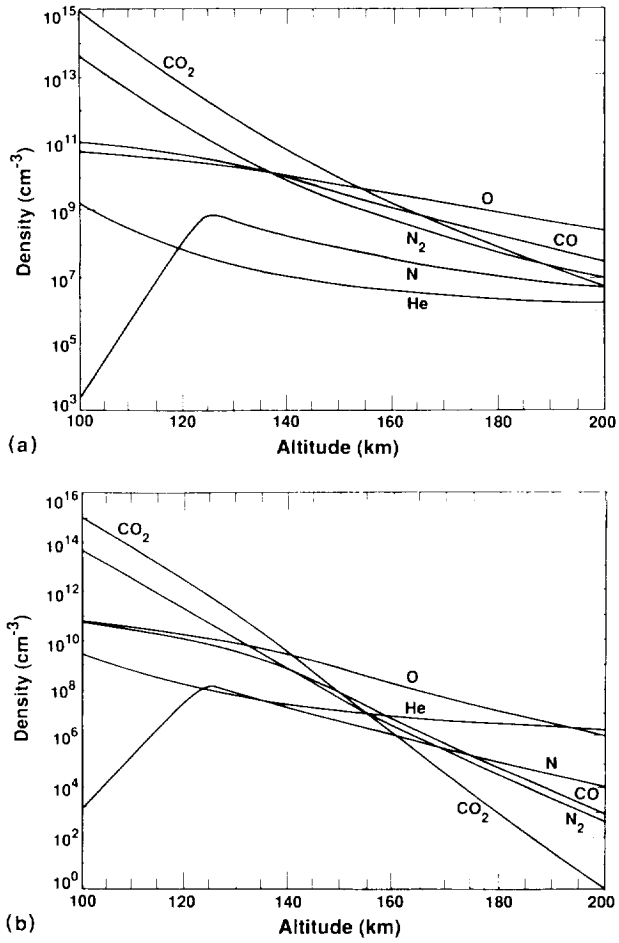

Figure 1.18 Altitude profiles of the major neutral species in the Venus thermosphere for the equator at (a) noon and (b) midnight from a model based on Pioneer Venus neutral mass spectrometer data. (Adapted from Hedin *et al.*, 1983)

altitude of about 195 km on Mars (Nier and McElroy, 1976, 1977); models derived from Pioneer Venus data place the transition altitude near 155 and 140 km on the dayside and nightside of Venus, respectively (Hedin *et al.*, 1983).

Early investigations of the ionosphere of Mars predicted that the ion composition would be simpler than that of the Earth. The model of McElroy (1973b) predicted that, below 250 km, only O_2^+ and CO_2^+ would be important; the computed densities of N^+, NO^+, CO^+ and O^+ were smaller at their maxima by one to three orders of magnitude. Only the major ion densities could be

derived from data recorded by the retarding potential analyzers on the Viking entry probes. Figure 1.19 shows the profiles derived from Viking 1 data (Hanson *et al.*, 1977). Among other instruments, the Pioneer Venus orbiter carried an ion mass spectrometer to Venus in 1978. Data were taken inside the ionosphere for more than 600 orbits at the beginning of the mission, and again for several orbits in the re-entry phase in 1992. An example of the ion density profiles obtained on the dayside is shown in Figure 1.20 (Keating *et al.*, 1985). The ion composition is complex. The increased knowledge of ion chemistry on Venus obtained from the Pioneer Venus measurements and subsequent modeling allowed the ion densities on Mars to be modeled with greater confidence (Nagy *et al.*, 1980; Fox, 1982a, 1982b, 1985, 1989, 1992b). Except where noted, the following discussion refers to the low solar activity model shown in Figure 1.21 for Mars and the high solar activity model shown in Figure 1.22 for Venus.

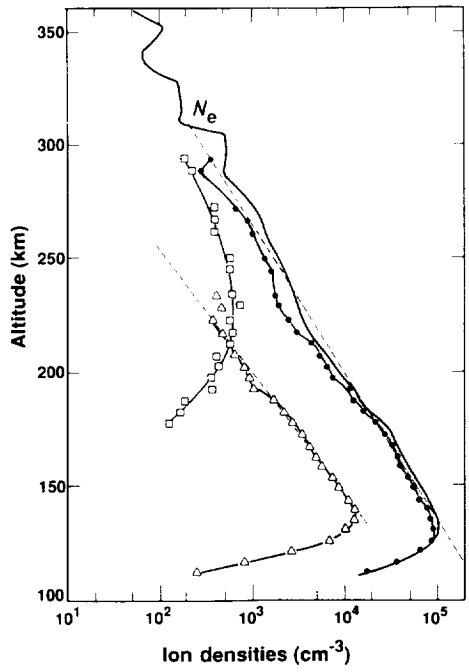

Figure 1.19 Altitude profiles of the ion densities derived from the Viking 1 retarding potential analyzer. The filled circles are O_2^+, the open triangles are CO_2^+ and the open squares are O^+. The heavy solid curve labeled N_e is the sum of the individual ion densities. The dashed lines through the O_2^+ and CO_2^+ data are linear fits to the topside data, and exhibit scale heights of 29 and 23 km, respectively. (Adapted from Hanson *et al.*, 1977)

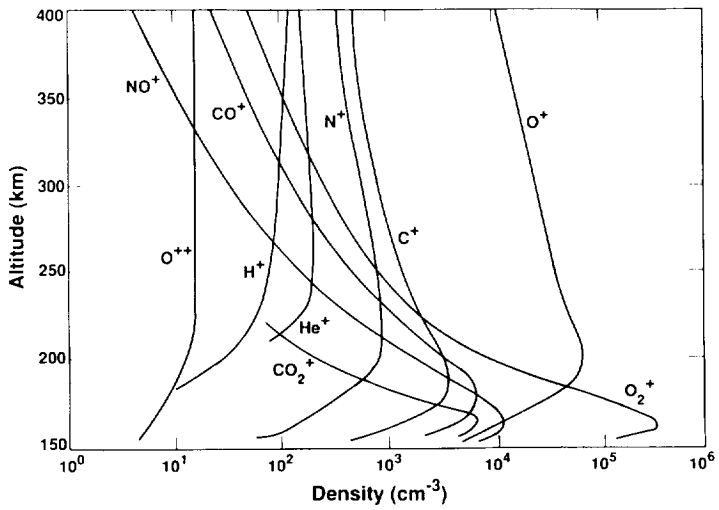

Figure 1.20 Ion density profiles for species measured with the Pioneer Venus orbiter ion mass spectrometer. The original data have been smoothed. (Adapted from Bauer *et al.*, 1985)

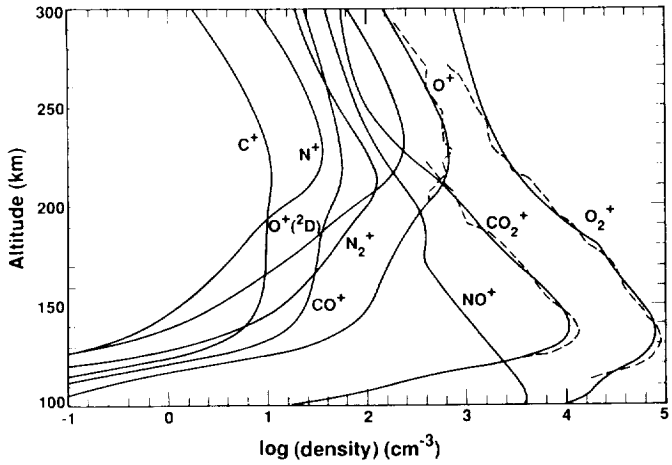

Figure 1.21 Computed altitude profiles of the ions in the ionosphere of Mars for a low solar activity model based on Viking 1 data. The neutral densities employed are those shown in Figure 1.17 and the solar zenith angle is 45°. The dashed curves are the ion densities inferred from the Viking retarding potential analyzer data. (Hanson *et al.*, 1977)

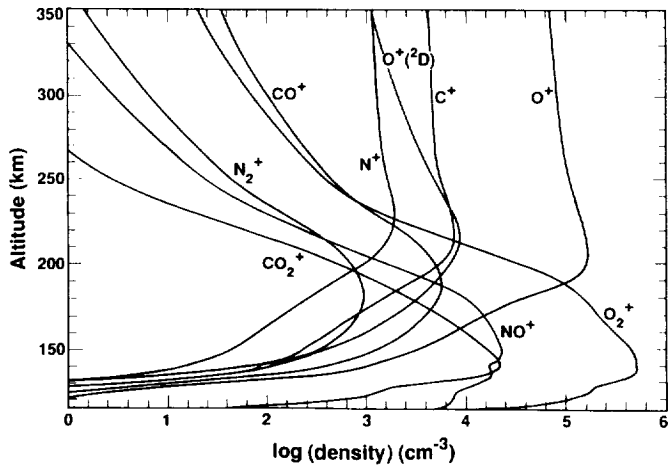

Figure 1.22 Computed altitude profiles of ions in the Venus ionosphere for high solar activity and 45 °. The neutral model employed was that of Hedin *et al.* (1983) for $F_{10.7} = 200$

These models were based on the model thermospheres shown in Figures 1.17 and 1.18.

On both planets, CO_2^+ is produced mostly by photoionization and photoelectron impact ionization of CO_2:

$$CO_2 + (h\nu, e) \longrightarrow CO_2^+ + (e,2e) \tag{153}$$

with a peak production rate near 130 km for Mars and 140 km for Venus. On Venus, the reaction

$$CO^+ + CO_2 \longrightarrow CO_2^+ + CO \tag{154}$$

exceeds direct production of CO_2 above about 165 km, but on Mars, where the CO mixing ratio is smaller, direct production of CO_2^+ exceeds production by all chemical reactions up to about 205 km, and reaction (154) provides only about 10% of the total source at 200 km. It is less important there than charge transfer from N_2^+

$$N_2^+ + CO_2 \longrightarrow CO_2^+ + N_2 \tag{155}$$

Reaction (155) is of minor importance in the Venus ionosphere, providing only 6% of the source from the ion peak to 175 km. At higher altitudes, charge transfer from $O^+(^2D)$ and $O^+(^2P)$

$$O^+(^2D,^2P) + CO_2 \longrightarrow O + CO_2^+ \tag{156}$$

is the most important source of CO_2^+. Reaction of $O^+(^2D)$ and $O^+(^2P)$ with

CO_2 can also proceed by

$$O^+(^2D,^2P) + CO_2 \longrightarrow O_2^+ + CO \tag{157}$$

The rate coefficient for reactions (156) and (157) has been measured (Viggiano *et al.*, 1990) to have a value of 1.06×10^{-9} cm^3 s^{-1}, with the reaction proceeding via charge transfer (channel 156) 94% of the time. On Mars, the smaller densities of O^+ resulting from the smaller mixing ratio of O renders reactions (156) less important; at 200 km, they are comparable to reaction (155).

In the presence of a small amount of O, CO_2^+ is transformed by the reaction

$$CO_2^+ + O \longrightarrow O_2^+ + CO \tag{158}$$

but charge transfer may also take place (Fehsenfeld *et al.*, 1970)

$$CO_2^+ + O \longrightarrow CO_2 + O^+ \tag{159}$$

Reaction with O is the most important loss process for CO_2^+ over most of the photochemical equilibrium regions, which for CO_2^+ is below approximately 235 km on Venus and 210 km on Mars. At higher altitudes, in addition to chemical production and loss, transport by diffusion becomes important in determining the density profiles. Dissociative recombination

$$CO_2^+ + e \longrightarrow CO + O \tag{160}$$

is the most effective chemical loss process for CO_2^+ above about 225 km on Venus. On Mars, although the O mixing ratio is smaller, the total electron densities are less by more than an order of magnitude over most of the topside ionosphere, and dissociative recombination exceeds reactions with neutral species only about 375 km.

O^+ can be produced both by photodissociative ionization of CO_2 and CO

$$CO_2 + h\nu \longrightarrow CO + O^+ + e \tag{161}$$

$$CO + h\nu \longrightarrow C + O^+ + e \tag{162}$$

and by direct photoionization of O

$$O + h\nu \longrightarrow O^+ + e \tag{163}$$

On Mars, reaction (159) is more important than direct ionization as a source of O^+ below about 180 km. Because of the larger abundance of O in the atmosphere of Venus, direct production and reaction (159) are comparable near 145 km, but at higher altitudes direct production dominates. In addition, the reaction

$$CO^+ + O \longrightarrow O^+ + CO \tag{164}$$

also occurring in the supernova mantle, exceeds reaction (159) as a source of O^+ above 170 km on Venus. Production of O^+ is followed nearly always by

$$O^+ + CO_2 \longrightarrow O_2^+ + CO \tag{165}$$

Reactions (158) and (165) are comparable sources of O_2^+ near the ion peaks of both Venus and Mars. At high altitudes, above 190 and 150 km for Mars and Venus, respectively, reaction (165) becomes more important. Loss is mainly by dissociative recombination

$$O_2^+ + e \longrightarrow O + O \tag{166}$$

at all altitudes in the photochemical equilibrium region.

O_2^+ may react with both N and NO to produce NO^+

$$O_2^+ + N \longrightarrow NO^+ + O \tag{167}$$

$$O_2^+ + NO \longrightarrow NO^+ + O_2 \tag{168}$$

Reaction (167) is the largest source of NO^+ below about 180 km on Mars and 195 km on Venus. Above those altitudes the reaction

$$N_2^+ + O \longrightarrow NO^+ + N \tag{169}$$

is more important. Since NO has the lowest ionization potential of any major or minor species in the thermospheres of the terrestrial planets, its loss is almost completely by dissociative recombination

$$NO^+ + e \longrightarrow N + O \tag{170}$$

N_2 has the very high ionization potential of 15.58 eV, so it can be produced chemically in only a few reactions, including

$$Ar^+ + N_2 \longrightarrow N_2^+ + Ar \tag{171}$$

$$He^+ + N_2 \longrightarrow N_2^+ + He \tag{172}$$

and

$$O^+(^2D) + N_2 \longrightarrow N_2^+ + O \tag{173}$$

Reaction (171) is insignificant as a source of N_2^+ for Mars, although the reverse reaction, charge transfer from vibrationally excited N_2 is the major source of Ar^+ at high altitudes. The mixing ratio of Ar on Venus is much smaller than that on Mars (see Table 1.2). The densities He and He^+ have been measured by the mass spectrometers on the Pioneer Venus orbiter. It appears that the source of N_2^+ from reaction (172) is insignificant on the dayside, but it plays a larger role in the predawn sector on the nightside of Venus, where the densities of light ions maximize. The mixing ratio of He on Mars is unknown and the contribution of this reaction is uncertain.

The rate coefficient for reaction (173) has been measured to be close to the gas kinetic value, about 8×10^{-10} cm^3 s^{-1} (Johnsen and Biondi, 1980; Rowe *et al.*, 1980). Reaction (173) is a potentially important source of N_2^+, especially at high altitudes where O^+ is produced mainly by photoionization and electron-impact ionization of O. Photoionization of O by unattenuated sunlight

produces 37% $O^+(^2D)$ and 21% $O^+(^2P)$. Reaction (173) is significant, but not dominant at high altitudes on Mars; it is the source of 35% of the N_2^+ at 200 km. On Venus, where the O mixing ratio is higher, charge transfer from $O^+(^2D)$ is the source of 10% of the N_2^+ at the ion peak and the most important source above about 175 km. Recently, that conclusion has become more secure since the rate coefficients for reactions (156) and (157) have been measured. They are the dominant loss processes for $O^+(^2D)$ over most of the ionosphere of Mars and below 165 km on Venus. Above that altitude reaction with CO

$$O^+(^2D) + CO \longrightarrow CO^+ + O \tag{174}$$

becomes more important. At high altitudes on both planets, radiation and quenching of $O^+(^2P)$ are significant sources of $O^+(^2D)$. Some uncertainty still exists in the $O^+(^2D)$ budget because the rate coefficients for $O^+(^2D)$ and $O^+(^2P)$ in reactions (156) and (157) have not been measured separately and because the rate coefficient for quenching of $O^+(^2D)$ by O

$$O^+(^2D) + O \longrightarrow O^+(^4S) + O \tag{175}$$

has not been measured. A value of 1×10^{-11} cm^3 s^{-1} was derived from one analysis of Atmosphere Explorer data (Orsini *et al.*, 1977), but another (Oppenheimer *et al.*, 1976) suggested a larger value of 1×10^{-10} cm^3 s^{-1}. This reaction is of little importance for the Martian ionosphere, where the densities of O are small, but is significant on Venus. At 205 km, reaction (175) comprises either 8 or 45% the $O^+(^2D)$ loss, for the smaller and larger rate coefficient, respectively.

The analog of reaction (173) for $O^+(^2P)$

$$O^+(^2P) + N_2 \longrightarrow N_2^+ + O \tag{176}$$

is also potentially important, but the rate coefficient has not been measured at thermal energies. The measured rate coefficient for a mixture of $O^+(^2D)$ and $O^+(^2P)$ with N_2 is 1.35×10^{-10} cm^3 s^{-1} (Glosik *et al.*, 1978). Cross sections for the reactions of $O^+(^4S)$, $O^+(^2D)$ and $O^+(^2P)$ with N_2 have been measured for relative energies from 5 to 20 eV (Lavollee and Henri, 1989), with the result that the ratio of the cross sections for reactions (176) and (173) is about 0.6. The importance of reaction (176) as a source of N_2^+, however, cannot be accurately ascertained until the rate coefficients for the reactions of $O^+(^2P)$ alone with CO_2 and with O have been determined. Measurements of the rate coefficients for reactions (175) and (176) would greatly improve our understanding of the N_2^+ densities in the ionospheres of the Earth and Venus.

N_2^+ is destroyed mainly by charge transfer to CO_2 (reaction 155) in the Martian ionosphere, but reaction with O (reaction 169) is also significant at high altitudes, providing more than 20% of the total sink above 200 km. The chemistry of N_2^+ is more complicated on Venus. At low altitudes reaction (155) is the dominant sink for N_2^+, but above about 170 km, reaction (169) becomes

more important. Reaction with CO

$$N_2^+ + CO \longrightarrow CO^+ + N_2 \quad (177)$$

is a minor loss process for N_2^+ on Venus. Dissociative recombination

$$N_2^+ + e \longrightarrow N + N \quad (178)$$

is insignificant as an N_2^+ sink in the ionosphere of Mars, for the same reasons previously given for dissociative recombination of CO_2^+, but is comparable to reaction (169) above 200 km on Venus.

The ionization potential of CO is about 14 eV. On Venus, the production of CO^+ is dominated by direct photoionization and electron-impact ionization of CO, but the reaction

$$C^+ + CO_2 \longrightarrow CO^+ + CO \quad (179)$$

also contributes significantly, making up about 25% of the total source at the ion peak and somewhat less at higher altitudes. The major source above about 175 km is charge transfer from $O^+(^2D)$ to CO:

$$O^+(^2D) + CO \longrightarrow CO^+ + O \quad (180)$$

On Mars, where the mixing ratios of O and CO are smaller, reaction (179) provides a larger fraction, about 40% of the production of CO^+ at the ion peak, and reaction (180) is negligible as a source of CO^+.

The contribution of the reaction of atomic carbon with O_2^+

$$C + O_2^+ \longrightarrow CO^+ + O \quad (181)$$

is a potentially important source of CO^+ in the ionosphere of Venus, especially in the region of the ion peak, but the rate coefficient is unknown and the possible products include C^+ as well as CO^+. Using the estimated rate coefficient of 5×10^{-11} cm^3 s^{-1} (Prasad and Huntress, 1980), we find that reaction (181) produces 5% of the CO^+ at 145 km. If the reaction actually proceeds at near gas kinetic rates, about 1×10^{-9} cm^3 s^{-1}, the source would be much larger.

Loss of CO^+ is by reaction with CO_2

$$CO^+ + CO_2 \longrightarrow CO_2^+ + CO \quad (182)$$

at the ion peaks of both Mars and Venus, but charge transfer to O becomes more important above about 175 km on Venus. On Mars, reaction (164) is a minor sink, providing more than 20% of the total loss only above 200 km. Dissociative recombination (Mitchell, 1990)

$$CO^+ + e \longrightarrow C + O \quad (183)$$

is not a significant loss process at any altitude in the Martian ionosphere, but is the dominant loss process for CO^+ above about 250 km on Venus.

Density profiles of C^+ were measured *in situ* by the ion mass spectrometer

on the Pioneer Venus orbiter (Taylor *et al.*, 1980), but no measurements have been carried out in the Mars ionosphere. C^+ is produced in dissociative photoionization of CO_2 and CO and in direct photoionization and electron-impact ionization of atomic carbon. The atomic carbon densities on Venus and Mars have not been measured *in situ*, but the ultraviolet emission lines of C were observed by the Mariner and Pioneer Venus spacecraft (Barth *et al.*, 1971; Barth *et al.*, 1972; Paxton, 1985) and in ultraviolet spectra of Venus taken from a rocket (Rottman and Moos, 1973). The major source of C in the Venus thermosphere and at high altitudes in the Martian thermosphere is photodissociation of CO

$$CO + h\nu \longrightarrow C + O \tag{184}$$

but photodissociation of CO_2

$$CO_2 + h\nu \longrightarrow C + O + O \tag{185}$$

also contributes, especially near the ion peak on Mars (Krasnopolsky, 1982, 1983; Fox, 1982b).

The major source of C^+ is direct ionization at all altitudes on Mars. On Venus the reaction

$$O_2^+ + C \longrightarrow O_2 + C^+ \tag{186}$$

provides 25% of the total source near the ion peak and is comparable to direct production near 175 km if the rate coefficient is near the estimated value of 5×10^{-11} cm^3 s^{-1} (Prasad and Huntress, 1980). Photoionization of atomic carbon is the most important production mechanism for C^+ above about 200 km (Fox, 1982b). There is also a potential source due to the reaction (Paxton, 1983)

$$O^+ + C \longrightarrow C^+ + O \tag{187}$$

The process may also be an important source of C^+ in the supernova, but the rate coefficient is unknown. The reaction will dominate the production of C^+ at high altitudes on Venus if the rate coefficient is greater than 1×10^{-10} cm^3 s^{-1}, but will be insignificant if the rate coefficient is less than 1×10^{-11} cm^3 s^{-1}. The C^+ budgets on Venus and Mars cannot be completely understood until the rate coefficients for reactions (186) and (187) have been measured.

Density profiles of N^+ with peak values sometimes exceeding 10^3 cm^{-3} have been measured in the Venus ionosphere (Taylor *et al.*, 1980). The major sources below about 200 km are dissociative ionization of N_2

$$N_2 + (h\nu, e) \longrightarrow N^+ + N + (e, 2e) \tag{188}$$

and photoionization and electron-impact ionization of N

$$N + (h\nu, e) \longrightarrow N^+ + (e, 2e) \tag{189}$$

Chemical production of N^+ in the reactions

$$O_2^+ + N(^2D) \longrightarrow N^+ + O_2 \quad (190)$$

$$O^+(^2D) + N \longrightarrow N^+ + O \quad (191)$$

and

$$O^+(^2P) + N_2 \longrightarrow N^+ + NO \quad (192)$$

provides about 14% of the source at the ion peak and exceeds direct production above about 200 km. Reaction (190) is nearly resonant and the rate coefficient can be derived from the measured value of the reverse reaction (Dalgarno, 1970); a value of 9.3×10^{-11} cm^{-3} s^{-1} is implied by the measurements (Smith *et al.*, 1983b; O'Keefe *et al.*, 1986). The rate coefficient for reactions (191) and (192) have not been measured, and values estimated from Atmosphere Explorer Data (Dalgarno, 1979) are used in the model. Measurements of these rate coefficients would be valuable to interpreting the measured N^+ densities for both Venus and Earth, and predicting the densities for Mars.

Loss of N^+ on Venus is dominated at low altitudes by reaction with CO_2, which proceeds at nearly gas kinetic rates by

$$N^+ + CO_2 \longrightarrow N + CO_2^+ \quad (193)$$

and

$$N^+ + CO_2 \longrightarrow NO^+ + CO \quad (194)$$

The branching ratios between reactions (193) and (194) are 75 and 25%, respectively (Smith *et al.*, 1978). At altitudes above 175 km, reaction of N^+ with CO

$$N^+ + CO \longrightarrow CO^+ + N \quad (195a)$$

$$\longrightarrow NO^+ + C \quad (195b)$$

is more important than that with CO_2. Reaction (195b) is also important in dense interstellar cloud chemistry. Reaction with O

$$N^+ + O \longrightarrow N + O^+ \quad (196)$$

is a minor loss mechanism, providing only 5% of the total N^+ sink at 200 km.

The chemistry of N^+ in the Martian ionosphere is much simpler due in part to the lower thermospheric mixing ratios of O and CO. Its production is largely by ionization of N (reaction 188) and dissociative ionization of N_2 (reaction 189). The only significant chemical source is reaction of O_2^+ with $N(^2D)$ (reaction 190). Loss is mainly by reaction with CO_2 (reactions 193 and 194). Reactions (195a) and (195b) are not important, accounting for only 5% of the loss at 200 km.

1.4.2.2 Nightside ionospheres

The nightside ionosphere of Venus was first detected by the radio occultation experiments on the Mariners 5 and 10 spacecraft (Kliore *et al.*, 1967; Fjeldbo *et al.*, 1975) and more recently by the Venera 9 and 10 spacecraft and the Pioneer Venus orbiter (Gringauz *et al.*, 1977; Kliore *et al.*, 1979). *In situ* measurements of the ion densities were carried out by the PV orbiter ion mass spectrometer (OIMS) (Taylor *et al.*, 1980). Although the same constituents were detected by the OIMS on the nightside as on the dayside, the densities of heavy atomic ions, such as O^+, N^+ and C^+, were observed to be about an order of magnitude less, and the molecular ion densities about two orders of magnitude less than dayside values.

The densities of light atomic ions, such as He^+ and H^+, were observed to maximize in the predawn sector. Both the neutral densities, as measured by the neutral mass spectrometer, and the ion densities on the nightside were observed to be highly variable (Niemann *et al.*, 1980).

The nightside ionosphere of Venus is produced by some combination of plasma transport from the dayside (Knudsen *et al.*, 1980; Spenner *et al.*, 1981; Cravens *et al.*, 1983) and precipitation of electrons that have been observed in the umbra (Chen and Nagy, 1978; Gringauz *et al.*, 1979; Breus *et al.*, 1985; Knudsen and Miller, 1985). Probably the former is more important at high solar activity and the latter at a low solar activity (Knudsen, 1988; Kliore *et al.*, 1991). Even at high solar activity, however, the source due to electron precipitation varies (Fox and Taylor, 1990). Fox (1992b) has discussed the chemistry of the nightside ionosphere that is produced by transport of atomic ions from the dayside. In this case, the ion sources are chemical. Ions that are produced from parents with high ionization potentials, such as N_2^+, CO^+ and CO_2^+, are difficult to produce chemically. For example, in the absence of ultraviolet photons or energetic electrons, the only potential sources of N_2^+ are

$$He^+ + N_2 \longrightarrow N_2^+ + He \tag{197}$$

$$O^{2+} + N_2 \longrightarrow N_2^+ + O^+ \tag{198}$$

and

$$O^+(^2D) + N_2 \longrightarrow N_2^+ + O \tag{199}$$

The products of reaction (198) are unknown, but the large exothermicity implies that dissociative channels probably dominate. It is also likely that $O^+(^2D)$ does not survive transport to the nightside; consequently reaction (199) probably is not important. Only reaction (197) is found to be important, especially in the predawn region where the densities of light ions are seen to maximize.

For CO^+ there are more chemical production mechanisms, including reac-

tions, that are analogous to reactions (197) to (199)

$$He^+ + CO_2 \longrightarrow He + CO^+ + O \quad (200)$$

$$O^{2+} + CO \longrightarrow CO^+ + O \quad (201)$$

$$O^+(^2D^+) + CO \longrightarrow CO^+ + O \quad (202)$$

The reaction of He^+ with CO proceeds mostly by dissociative charge transfer (67)

$$He^+ + CO \longrightarrow C^+ + O + He$$

and is therefore not a source of CO^+. The same comments apply to reactions (201) and (202) as to reactions (198) and (199). The most important source of CO^+ near the peak of the nightside ionosphere is the reaction

$$C^+ + CO_2 \longrightarrow CO^+ + CO \quad (203)$$

At high altitudes, the most important source is charge transfer from N^+ to CO in reaction (195a). The fractions of C^+ and N^+ transported to the nightside ionosphere are, however, small compared to O^+. The dearth of chemical production mechanisms for CO^+ and N_2^+ and their large variability in the nightside OIMS data lead to the suggestion (Fox and Taylor, 1990) that the appearance of large densities of mass-28 ions is a signature of auroral precipitation. The sources of CO^+ and N_2^+ for the dayside and nightside ionospheres are compared in Figures 1.23(a) to (d) and 1.24(a) to (c).

The major chemical production mechanisms of CO_2^+ on the nightside of Venus are charge transfer from N^+

$$N^+ + CO_2 \longrightarrow CO_2^+ + N \quad (204)$$

and from the mass-28 ions CO^+ and N_2^+

$$CO^+ + CO_2 \longrightarrow CO + CO_2^+ \quad (205)$$

and

$$N_2^+ + CO_2 \longrightarrow CO_2^+ + N_2 \quad (206)$$

Reaction (205) dominates near the ion peak, but reaction (204) is more important at high altitudes. CO_2^+ has the potential to be enhanced substantially in the presence of electron precipitation. In the plasma-transport dominated ionosphere, O_2^+ is produced mainly by

$$O^+ + CO_2 \longrightarrow O_2^+ + CO \quad (207)$$

In the presence of electron precipitation, the reaction (158) is the major source in the lower ionosphere. The sources of CO_2^+ in the dayside and nightside ionospheres are compared in Figures 1.23(e) and (f) and 1.24(d) and (e).

NO^+ is produced mainly by the reaction

$$O_2^+ + N \longrightarrow NO^+ + O \quad (208)$$

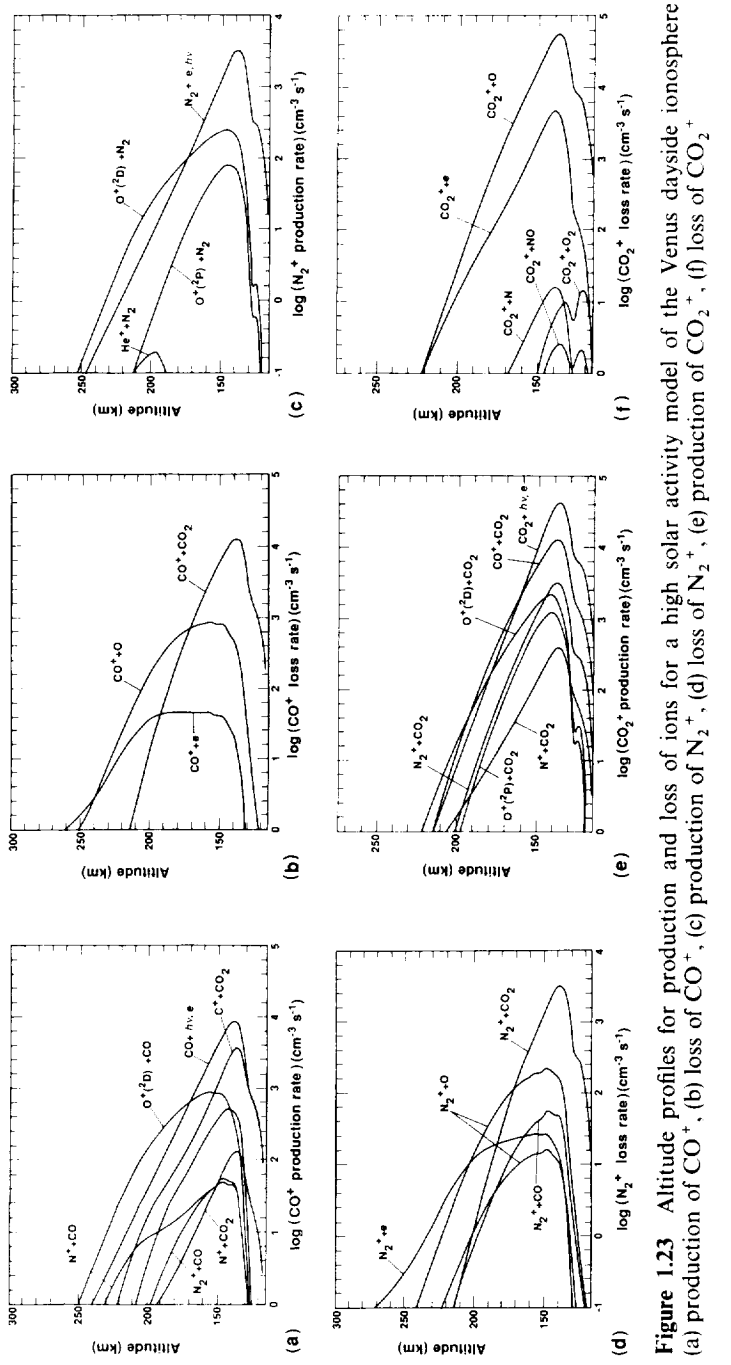

Figure 1.23 Altitude profiles for production and loss of ions for a high solar activity model of the Venus dayside ionosphere: (a) production of CO^+, (b) loss of CO^+, (c) production of N_2^+, (d) loss of N_2^+, (e) production of CO_2^+, (f) loss of CO_2^+

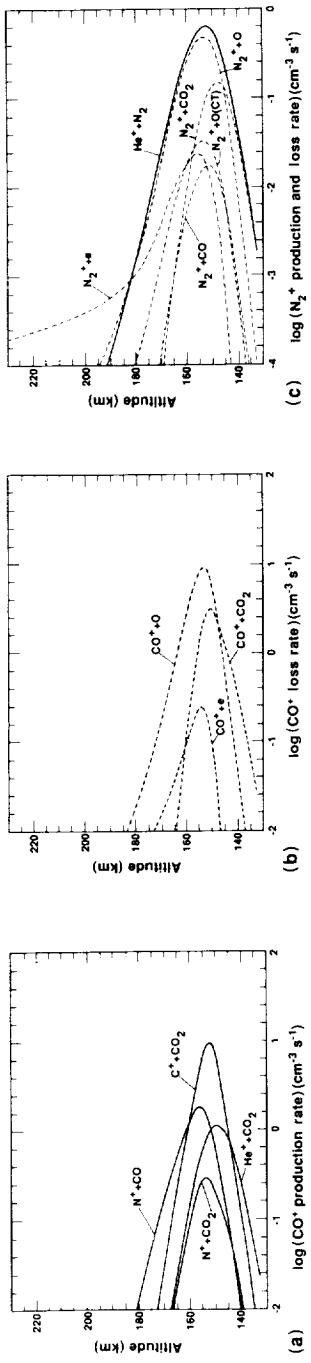

Figure 1.24 Altitude profiles for production and loss of ions for a high solar activity model of the Venus nightside ionosphere. The source of ionization is assumed to be the transport of atomic ions from the dayside. (a) Production of CO^+, (b) loss of CO^+, (c) production and loss of N_2^+, (d) production of CO_2^+, (e) loss of CO_2^+

under low precipitation conditions. Its loss is always by dissociative recombination. Hence its density is given approximately by

$$[NO^+] = k[N][O_2^+]/\alpha[e] \tag{209}$$

where k is the rate coefficient for reaction (208) and α is the dissociative recombination coefficient. Near the ion peak where $[e] \sim [O_2^+]$, the NO^+ density is largely independent of O^+ flux. Computed ion density profiles produced by imposing a downward flux of O^+ of $1 \times 10^8\ cm^{-2}\ s^{-1}$ with smaller fluxes of C^+, N^+ and He^+ near the antisolar point are shown in Figure 1.25.

The nightside ionosphere of Mars has been detected at low solar activity by radio occultation experiments on the Viking and Soviet Mars 4 space probes (Vasil'ev *et al.*, 1975; Zhang *et al.*, 1990). Because the orbit of Mars lies outside that of the Earth, only a small solar zenith angle range on the nightside past the terminators has been investigated. A peak did not always appear, but when it did the peak density averaged about $5 \times 10^3\ cm^{-3}$. The HARP instrument on the Soviet Phobos spacecraft measured large fluxes of electrons in the vicinity of Mars (Verigin *et al.*, 1991). A two-stream code was used to model the ionization rates and perform a photochemical equilibrium calculation of the

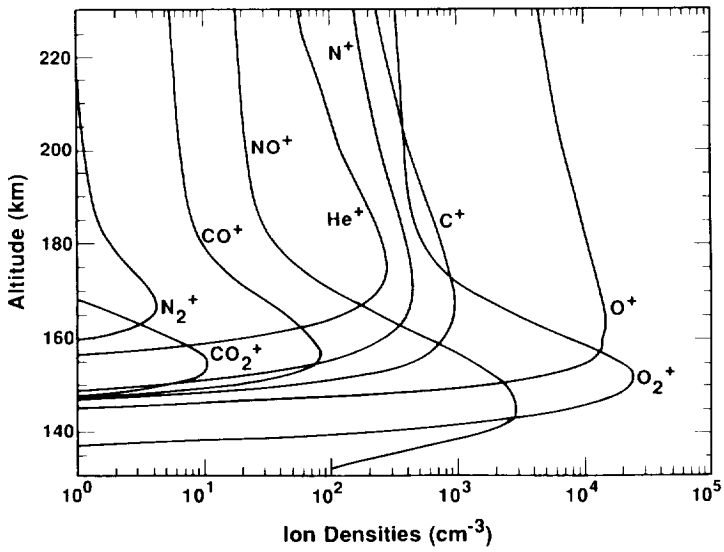

Figure 1.25 Computed altitude profiles of the major ions in the Venus nightside ionosphere resulting from the transport of atomic ions from the dayside. Downward fluxes of O^+, C^+, N^+ and He^+ were imposed at the upper boundary of the model, near 235 km. The neutral model was taken from Hedin *et al.* (1983) and is appropriate to the equator at 2300 h local time

ion and electron density profiles that would result if the observed electrons precipitated into the nightside atmosphere (Haider *et al.*, 1992).

Models of the dayside ionosphere of Mars have shown that the ion density profiles cannot be reproduced without imposing a loss process at the upper boundary of the model (Fox, 1993; Shinagawa and Cravens, 1992). It has been proposed that this loss process is the divergence of the horizontal ion fluxes, by analogy to Venus (Shinagawa and Cravens, 1989, 1992). In order to compute an upper limit to the nightside ion densities, Fox *et al.* (1993) imposed, in the downward direction at the upper boundary of a model of the nightside thermosphere, the upward fluxes O^+, C^+, N^+ and $O_2{}^+$ that were found necessary (Fox, 1993) to reproduce the dayside ion density profiles. Fox *et al.* (1993) also performed a calculation of the ion densities that would result from electron precipitation using a multistream electron transport code. The ionosphere produced by ion transport alone showed a peak density of about $1.3 \times 10^4\ cm^{-3}$ at an altitude of 179 km. When combined with electron precipitation, the peak ion density increased to $1.8–1.9 \times 10^4\ cm^{-3}$. Altitude profiles of the ion densities for plasma transport alone and for precipitation of the electrons detected by the Phobos HARP instrument in the magnetosphere lobes are shown in Figure 1.26(a) and (b).

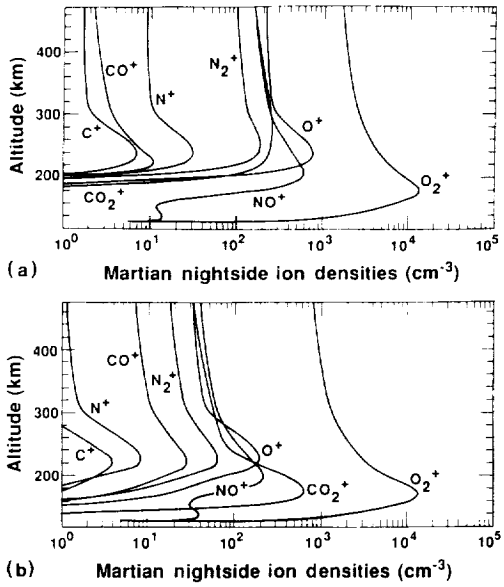

Figure 1.26 Computed nightside ion densities of Mars (a) due to transport of ions from the dayside and (b) precipitation of the electrons detected in the magnetotail lobes by the Phobos HARP instrument (Verigin *et al.*, 1991). (After Fox *et al.*, 1993)

1.4.3 TITAN AND TRITON

The atmosphere of Titan is composed mostly of N_2, with small amounts of methane and higher hydrocarbons, as shown by the model thermosphere in Figure 1.27. In this model, the N_2 and CH_4 density profiles were taken from the Voyager solar occultation measurements (Smith *et al.*, 1982), and those of C_2H_2, C_2H_4 and C_2H_6 were adopted from a photochemical model (Yung *et al.*, 1984). N_2 is the major species below 1700 km and CH_4 is relatively more abundant at higher altitudes. In contrast to the thermosphere of Jupiter, the mixing ratios of the most important hydrocarbons, methane, acetylene, and ethylene do not decrease above the Titan homopause, which is near 925 km. Methane is lighter than N_2, and is therefore more abundant near the altitude of peak ion production (about 1050 km) than in the bulk atmosphere. On Jupiter, the peak photoionization of H_2 is near 600 km, almost 200 km above the homopause. Since methane and other hydrocarbons are heavier than H_2, they are severely depleted in this altitude region and are not involved in the ion chemistry near the peak. On Titan, however, hydrocarbons are important in the ion chemistry above, near and below the peak.

Models of the ionosphere of Titan have been constructed (Ip, 1990a; Fox and Yelle, 1991; Keller *et al.*, 1992). Solar photoionization and photoelectron impact ionization are sufficient to account for the electron density profiles measured by the Voyager radio science experiment (Keller *et al.*, 1992). The

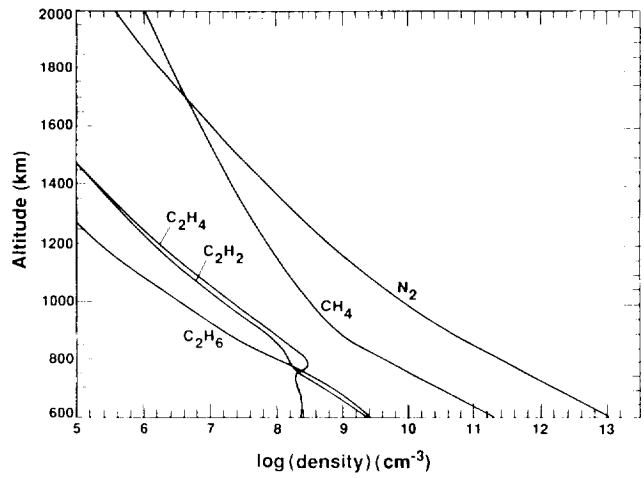

Figure 1.27 Neutral model of the thermosphere of Titan. The densities of N_2 and CH_4 were taken from the solar occultation profiles of Smith *et al.* (1982). The density profiles of ethane, ethylene and acetylene were taken from the photochemical model of Yung *et al.* (1984)

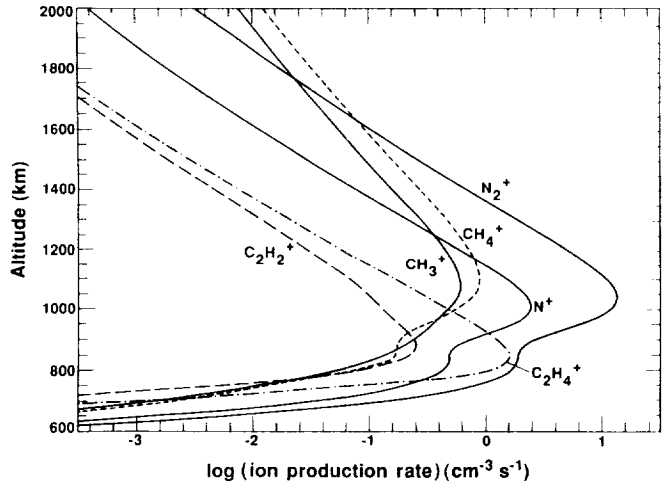

Figure 1.28 Computed production rate profiles of the major ions in the ionosphere of Titan for the neutral thermosphere shown in Figure 1.27. (From Fox and Yelle, 1991)

production rates of six ions due to photoionization and photoelectron impact ionization (Fox and Yelle, 1991) are shown in Figure 1.28. Although N_2^+ is the dominant ion produced below 1700 km, because the ionization potential of N_2 is very large (15.6 eV), N_2^+ is not expected to be the terminal ion. Altitude profiles of the major loss processes for N_2^+ in the ionosphere of Titan are shown in Figure 1.29. N_2^+ is lost in reaction with CH_4, largely by

$$N_2^+ + CH_4 \longrightarrow CH_3^+ + N_2 + H \tag{210}$$

but also by

$$N_2^+ + CH_4 \longrightarrow CH_2^+ + N_2 + H_2 \tag{211}$$

The reaction of N_2^+ with H_2 is also rapid

$$N_2^+ + H_2 \longrightarrow N_2H^+ + H \tag{212}$$

Charge transfer to acetylene

$$N_2^+ + C_2H_2 \longrightarrow C_2H_2^+ + N_2 \tag{213}$$

and to HCN

$$N_2^+ + HCN \longrightarrow HCN^+ + N_2 \tag{214}$$

and dissociative recombination

$$N_2^+ + e \longrightarrow N + N \tag{215}$$

are smaller but significant destruction mechanisms.

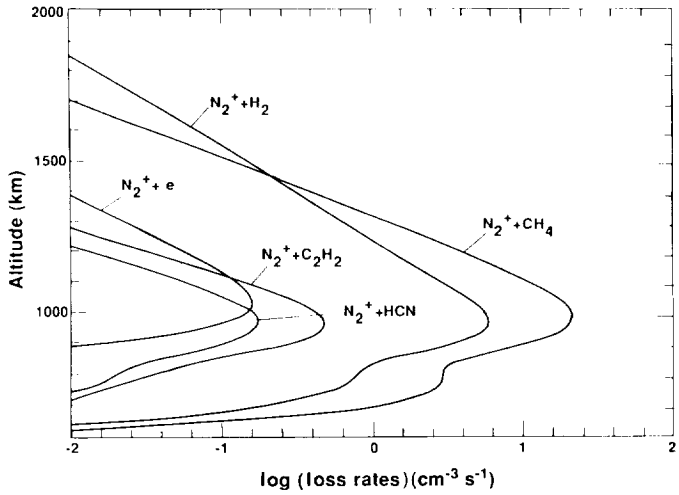

Figure 1.29 Computed loss rate for N_2^+ in the ionosphere of Titan. Ion–molecule reactions are much more important than dissociative recombination, for which the maximum destruction rate is about two orders of magnitude less than reaction with methane

The N_2H^+ produced in reaction (212) above may react with methane to produce CH_5^+

$$N_2H^+ + CH_4 \longrightarrow N_2 + CH_5^+ \tag{216}$$

Figure 1.28 shows that, at high altitudes, CH_4^+ is the most important ion produced; it also reacts at near gas kinetic rates with CH_4 to produce CH_5^+

$$CH_4^+ + CH_4 \longrightarrow CH_5^+ + CH_3 \tag{217}$$

As a result of these reactions, CH_5^+ is the most important ion at high altitudes in the Titan ionosphere (Fox and Yelle, 1991; Keller *et al.*, 1992). It is lost by reaction with acetylene

$$CH_5^+ + C_2H_2 \longrightarrow C_2H_3^+ + CH_4 \tag{218}$$

and with ethylene

$$CH_5^+ + C_2H_4 \longrightarrow C_2H_5^+ + CH_4 \tag{219}$$

and by dissociative recombination

$$CH_5^+ + e \longrightarrow CH_4 + H \tag{220a}$$

$$\longrightarrow CH_3 + 2H \tag{220b}$$

The product channels in reactions (220a) and (220b) have not been determined, but a yield of 1.19 H atoms per dissociative recombination of CH_5^+ has been

measured (Adams *et al.*, 1991) and it has been assumed that reactions (220a) and (220b) proceed by channel (220a) 81% of the time and by channel (220b) 19% of the time (Fox and Yelle, 1991).

Since both *cis*- and *trans*-HCNH have very low ionization potentials of 6.8 and 7.0 eV, respectively (Nesbitt *et al.*, 1991), there are many production mechanisms for $HCNH^+$. The most important pathways leading to the production of $HCNH^+$ are shown in Figure 1.30, and altitude profiles of the most important production and loss mechanisms are presented in Figure 1.31. The most important sources are the proton transfer reactions

$$C_2H_5^+ + HCN \longrightarrow C_2H_4 + HCNH^+ \tag{221}$$

and

$$C_2H_3^+ + HCN \longrightarrow C_2H_2 + HCNH^+ \tag{222}$$

Of somewhat less importance are the reactions

$$N^+ + CH_4 \longrightarrow HCNH^+ + CH_2 \tag{223}$$

and

$$HCN^+ + CH_4 \longrightarrow HCNH^+ + CH_3 \tag{224}$$

Dissociative recombination is the only significant loss mechanism over the entire ionosphere. There are four exothermic product channels for this reaction:

$$HCNH^+ + e \longrightarrow HCN + H \tag{225a}$$

$$\longrightarrow HNC + H \tag{225b}$$

$$\longrightarrow CH_2 + N \tag{225c}$$

$$\longrightarrow H_2 + CN \tag{225d}$$

Measurements (Adams *et al.*, 1991) indicate that 0.63 H atoms are produced per recombination. This implies that the sum of the branching ratios for channels (225a) and (225b) is 63% and the sum of the branching ratios for channels (225c) and (225d) is 37%. One model (Fox and Yelle, 1991) was constructed with the arbitrary assumption that production of HCN, the more stable isomer, is the dominant channel of the first two and that the third channel is more important than the fourth, whereas another (Keller *et al.*, 1992) assumed that all the reactions proceed via channel (225a).

CH_3^+ is produced by dissociative ionization of methane and by photoionization of CH_3 by the strong solar Lyman alpha line. It reacts rapidly with methane to produce $C_2H_5^+$

$$CH_3^+ + CH_4 \longrightarrow C_2H_5^+ + H_2 \tag{226}$$

$C_2H_5^+$ is also produced in proton transfer reactions to ethylene, the most

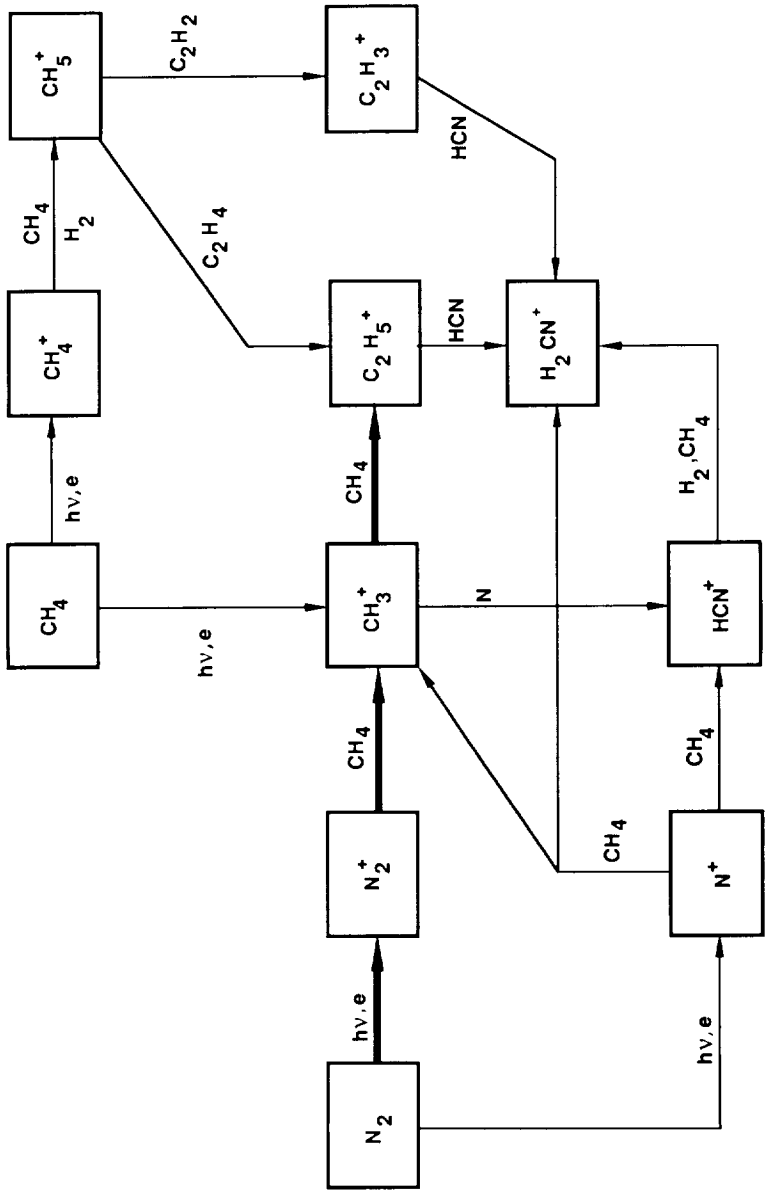

Figure 1.30 Ion–neutral reaction pathways leading to the formation of H_2CN^+. (Adapted from Keller *et al.*, 1992)

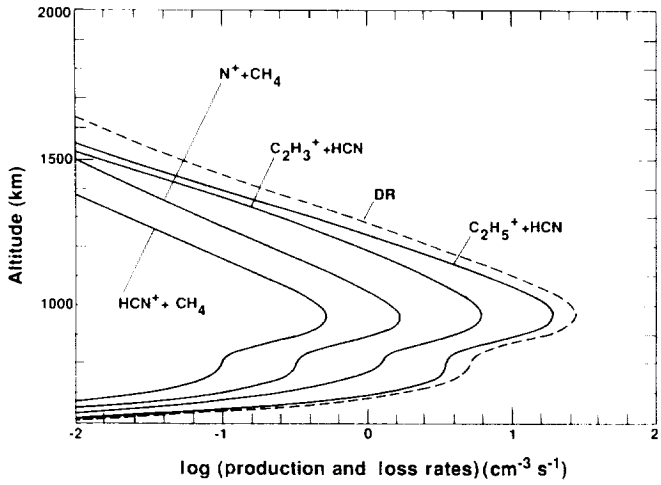

Figure 1.31 Altitude profiles for the major production and loss mechanisms for $HCNH^+$. The solid curves are production mechanisms and the dashed curve is for the only loss process, dissociative recombination

important of which are

$$CH_5^+ + C_2H_4 \longrightarrow C_2H_5^+ + CH_4 \tag{227}$$

and

$$C_2H_3^+ + C_2H_4 \longrightarrow C_2H_5^+ + C_2H_2. \tag{228}$$

$C_2H_5^+$ is destroyed mainly in reactions with HCN (reaction 222) with acetylene

$$C_2H_5^+ + C_2H_2 \longrightarrow C_2H_3^+ + C_2H_4 \tag{229}$$

and in dissociative recombination

$$C_2H_5^+ + e \longrightarrow C_2H_4 + H \tag{230a}$$

$$\longrightarrow CH_3 + CH_2 \tag{230b}$$

Here, again, the actual distribution of the products in dissociative recombination is uncertain. In one model (Fox and Yelle, 1991), the two channels shown above are assumed to be of equal importance and in another (Keller *et al.*, 1992), the reactions are assumed to produce $C_2H_2 + H_2$(or 2H) + H.

Altitude profiles of the eight most important ions predicted for the Titan ionosphere at high solar activity are shown in Figure 1.32 (Fox and Yelle, 1991). The most abundant ions are H_2CN^+ below about 1200 km and CH_5^+ above about 1200 km. The peak electron density is about 6×10^3 cm^{-3}. Upper limits

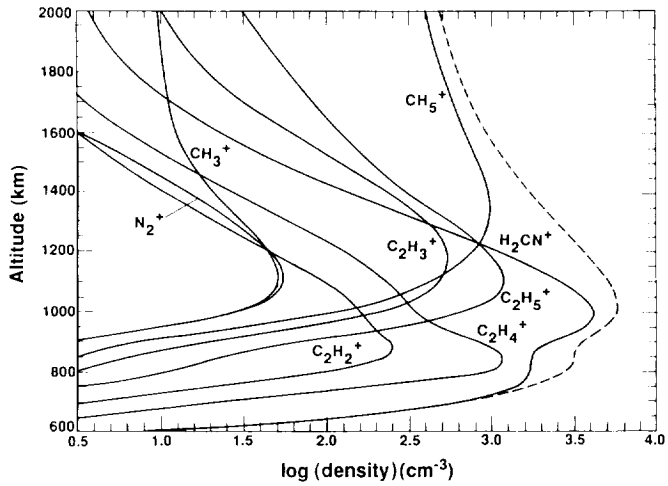

Figure 1.32 Computed density profiles of the major ions in the ionosphere of Titan. The solid curves are ion densities and the dashed curve is the total electron density profile. (From Fox and Yelle, 1991)

to the electron density at the morning and evening terminators of 5×10^3 and 3×10^3 cm^{-3}, respectively, were obtained by the Voyager 1 radio occultation experiment (Lindal *et al.*, 1983). The model shown in Figure 1.32 is for a solar zenith angle of 60° and is consistent with the Voyager upper limits.

The atmosphere of Triton is similar to that of Titan in that the major constituent is N_2. In N_2 atmospheres, usually the minor constituents control the absorption of radiation. For Earth the absorbing species is O_2 and for Titan, CH_4. Triton, however, unlike Titan or Earth, appears to have an extreme dearth of minor constituents. A model of the Triton atmosphere is shown in Figure 1.33 (Krasnopolsky *et al.*, 1993). The surface pressure is only about 14 μbar (Gurrola *et al.*, 1991), and methane in the troposphere is in equilibrium with a surface methane frost at about 38 K. The tropopause temperature is only about 2 K colder than the surface and occurs in the altitude range 8–12 km. The base of the thermosphere is near the tropopause, and temperatures increase monotonically above the tropopause to an exospheric temperature of about 100 K. The methane profiles derived from Voyager stellar occultation data (Herbert and Sandel, 1991) indicate that the methane density decreases more rapidly than the N_2 density from a surface value near 5×10^{11} cm^{-3} to about 10^6 cm^{-3} at 80 km. The higher hydrocarbons, acetylene, ethylene and ethane, condense out between 60 and 90 km. H_2 and H are produced by Lyman alpha photolysis of methane; they diffuse upward toward the exobase near 800–900 km, where they may escape thermally.

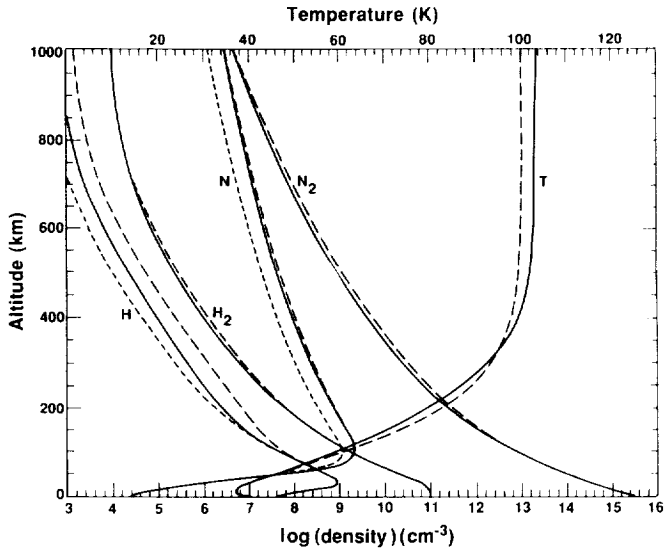

Figure 1.33 Model of the Triton atmosphere based on Voyager Ultraviolet Spectrometer measurements. The CO mixing ratio is assumed to be 10^{-3}. The N_2, N and temperatures profiles are from solar occultation measurements, and the H and H_2 densities are from calculations. The short dashed curves are for solar ionization only, while the solid and long-dashed curves are for different assumptions about the interaction of magnetospheric electrons with Triton's thermosphere. The solid curves are the recommended profiles. (Adapted from Krasnopolsky *et al.*, 1993)

On Triton, the principal ions produced are N_2^+ and N^+. On Titan, N^+ is lost primarily by the reaction with CH_4, via reaction (223) or by

$$N^+ + CH_4 \longrightarrow CH_3^+ + NH \tag{231a}$$

$$\longrightarrow HCH^+ + H_2 + H \tag{231b}$$

$$\longrightarrow CH_4^+ + N \tag{231c}$$

Most of the reactions proceed by channel (223) or (231a) (Anicich *et al.*, 1977). The reaction with C_2H_4 is a minor loss process, as is the reaction

$$N^+ + H_2 \longrightarrow NH^+ + H \tag{232}$$

Radiative recombination

$$N^+ + e \longrightarrow N + h\nu \tag{233}$$

is very slow. On Triton, the CH_4 mixing ratio is too small for reactions (223) and (231) to contribute significantly to the loss of N^+, and reaction (232) with

H_2 is more important. N_2^+ is also destroyed by reaction with H_2:

$$N_2^+ + H_2 \longrightarrow N_2H^+ + H \tag{234}$$

with H

$$N_2^+ + H \longrightarrow N_2 + H^+ \tag{235}$$

and in dissociative recombination (215). Because the N^+ loss rates are very small, N^+ has been predicted to be the major ion near the ionospheric peak of Triton in several models (Ip, 1990b; Majeed *et al.*, 1990; Yung and Lyons, 1990).

It appears that, unlike Titan, solar photoionization and photoelectron impact ionization are not sufficient to produce the electron density profiles inferred from the Voyager radio science experiments, and ionization by energetic electrons from Neptune's magnetosphere has been suggested as the missing source (Tyler *et al.*, 1989). The ingress and egress profiles exhibit maximum electron densities near 350 km of 2.3×10^4 and $4.6 \times 10^4\ cm^{-3}$, respectively. The model shown in Figure 1.34 was constructed by varying the ionization rate to fit the Voyager radio science ingress profile; a column ionization rate (in addition to the solar source) of 3×10^8 (Majeed *et al.*, 1990) or 4×10^8 $cm^{-2}\ s^{-1}$ was inferred (Strobel and Summers, 1993). In order to fit the topside scale height of the electron density profile, it was necessary to impose a loss

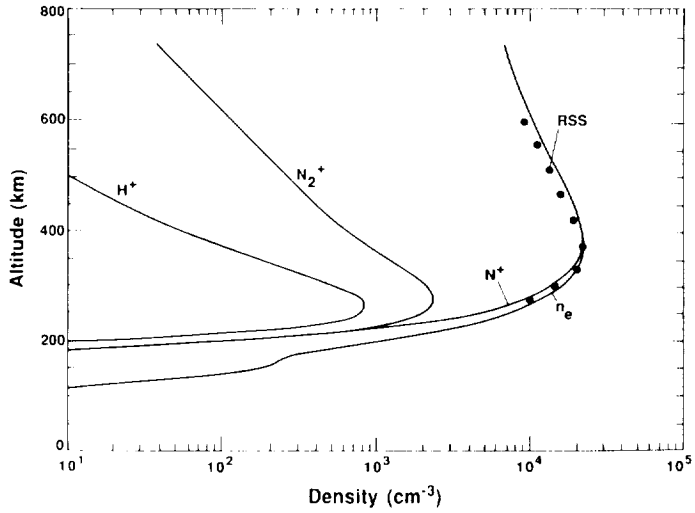

Figure 1.34 Model ionosphere of Triton constructed assuming an ionization rate due to magnetospheric electrons of $3 \times 10\ cm^{-2}\ s^{-1}$, in addition to the solar source. The curve labeled RSS is the electron density profile obtained from the Voyager radio occultation experiment (Herbert and Sandel, 1991). (From Majeed *et al.*, 1990)

process at the top of the ionosphere of 4.3×10^7 N^+ ions $cm^{-2}\,s^{-1}$ (Yung and Lyons, 1990). Cluster ions of the form $N_2^+(N_2)_n$ and $N^+(N_2)_n$, which are strongly favored energetically, should readily form at the low temperatures of the Triton ionosphere. Such clusters may make up most of the ions below about 200 km (Delitsky *et al.*, 1990). However, the chemistry of trace species such as H_2, CH_4 and CO modify the conclusion, which may be valid only in the troposphere (Strobel and Summers, 1993).

The Triton ionosphere could be maintained by solar radiation alone if the major ion was C^+, produced by photoionization of C and by charge transfer from N_2^+ (Lyons *et al.*, 1990)

$$N_2^+ + C \longrightarrow C^+ + N_2 \tag{236}$$

The rate coefficient for reaction (236) has not been measured; a near gas kinetic value is likely. The atomic carbon in the model may originate ultimately from photolysis of methane below 100 km, and be destroyed by photoionization, by ion–molecule reactions, such as reaction (236), and by upward diffusion and Jeans (thermal) escape near the exobase. The major loss process for C^+ is reaction with methane

$$C^+ + CH_4 \longrightarrow C_2H_3^+ + H \tag{237a}$$

$$\longrightarrow C_2H_2^+ + H_2 \tag{237b}$$

The computed C^+ profile exhibited a peak density of $3 \times 10^4\,cm^{-3}$ near 250 km. The addition of the reaction

$$C + N_2 + N_2 \longrightarrow CNN + N_2 \tag{238}$$

to the model reduced the computed atomic carbon densities, and thus the C^+ densities also, by an order of magnitude (Strobel and Summers, 1993).

1.4.4 THE EARTH

The division of the terrestrial atmosphere into regions is based on the structure in the altitude profile of the electron density, which is produced by partially overlapping layers of ions. These layers arise from altitude variations both in the composition of the thermosphere and in the relative importance of different ionization sources. Figure 1.35 shows a schematic diagram of the major terrestrial ionospheric regions and their most important ionization sources (Bauer, 1986). In the lower layers, below about 300 km, the ionosphere is essentially in photochemical equilibrium, and transport processes do not affect substantially the ion and electron density profiles. Molecular ions are the dominant constituents of the D, E and F_1 regions. The rate of plasma transport by ambipolar diffusion increases with decreasing density and, at sufficiently

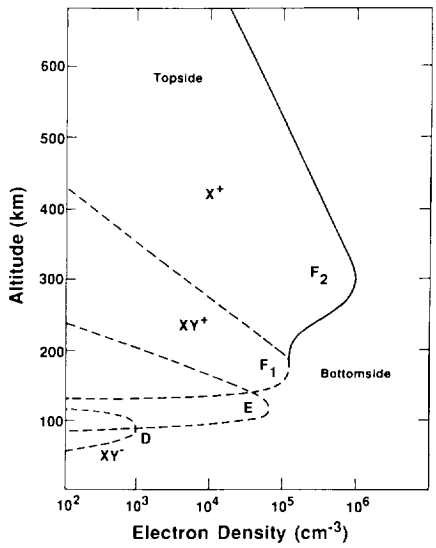

Figure 1.35 Schematic diagram of the regions of the terrestrial ionosphere and their principal ionization sources. (After Bauer, 1973)

high altitudes, the major loss process for atomic ions is diffusion. This results in the formation of a peak in the topmost layer of the ionosphere, the F_2 region. Here the major ion is O^+, and the peak electron density can exceed 10^6 cm^{-3}. A model of the F_1 and F_2 regions of the ionosphere at low solar activity from 100 to 450 km is shown in Figure 1.36. Most of the discussion of sources and

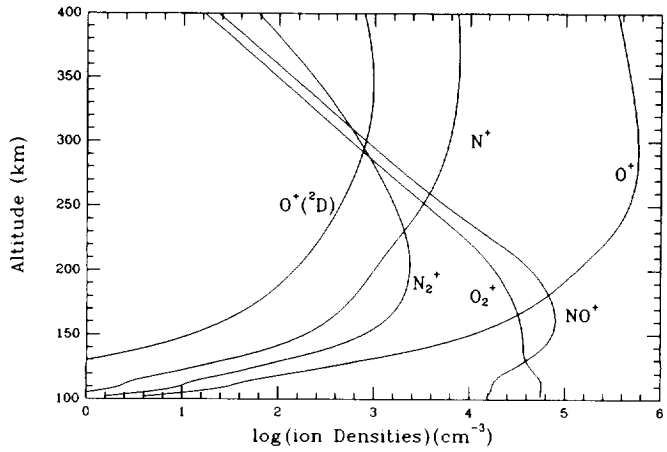

Figure 1.36 Altitude profiles of the densities of the ions in the terrestrial F_1 and F_2 regions for a low solar activity model of the terrestrial ionosphere

sinks that follows is based on this model. At higher solar activity, the neutral temperatures are larger, resulting in a more extended thermosphere and ionosphere than that shown in Figure 1.36. Also, data from ground-based experiments and spacecraft show considerable spatial and temporal variability in the ion and electron density profiles.

NO^+ is the most abundant ion in the F_1 region of the ionosphere. Altitude profiles of its sources and sinks are shown in Figure 1.37. The reactions

$$N_2^+ + O \longrightarrow NO^+ + N \tag{239}$$

and

$$O^+ + N_2 \longrightarrow NO^+ + N \tag{240}$$

produce more than 90% of the NO^+ above 200 km (Breig *et al.*, 1984). In the low solar activity model shown in Figure 1.36, reaction (239) is the most important production mechanism below about 275 km, and at higher altitudes, reaction (240) dominates. Below about 150 km, a number of reactions become significant, including charge transfer from O_2^+ to NO (reaction 168), the reaction

$$N^+ + O_2 \longrightarrow NO^+ + O \tag{241}$$

and the reaction of O_2^+ with N (reaction 208), which is the major source of NO^+ at low altitudes on Mars and Venus. Near 100 km, the reaction

$$O_2^+ + N_2 \longrightarrow NO^+ + NO \tag{242}$$

may also become important if the rate coefficient is near the upper limit of 1×10^{-15} cm^3 s^{-1} reported by Ferguson *et al.* (1965). As in the ionospheres

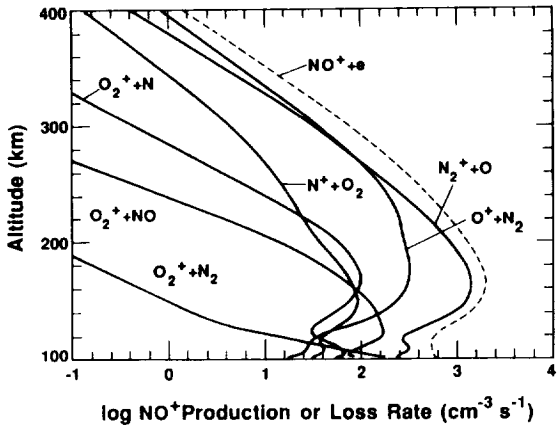

Figure 1.37 Altitude profiles of the production (solid curves) and loss (dashed curve) of NO^+ or a low solar activity model of the terrestrial dayside ionosphere

of Venus and Mars, loss of NO^+ is predominantly by dissociative recombination at all altitudes.

The primary sources and sinks of O_2^+ for a low solar activity model are shown in Figure 1.38. O_2^+ is produced mainly by photoionization and photoelectron impact ionization of O_2 below about 150 km. At higher altitudes, the reaction

$$O^+ + O_2 \longrightarrow O_2^+ + O \tag{243}$$

is more important. Reaction (243) is exothermic by 1.55 eV, and O_2^+ vibrational levels up to $v = 7$ are energetically accessible. O_2^+ has been shown to be significantly vibrationally excited at altitudes above about 250 km (Fox, 1986a). Reaction (243) is also the major source of O_2^+ ($v = 1$) in the altitude range of about 170–325 km. The reaction

$$N^+ + O_2 \longrightarrow N(^2D,^4S) + O_2^+ \tag{244}$$

can produce vibrationally excited O_2^+ only when the N atom is produced in the ^4S ground state. Reaction (244) is the most important source of $O_2^+(v = 1)$

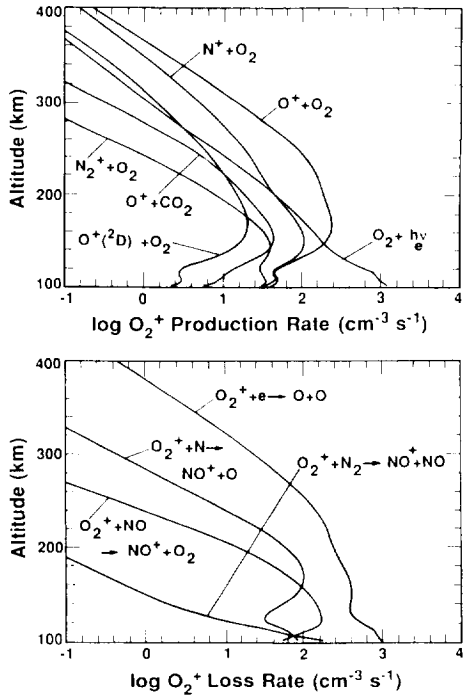

Figure 1.38 Altitude profiles of the (a) sources and (b) sinks of O_2^+ for a low solar activity model of the terrestrial dayside ionosphere

above 325 km and of total O_2^+ above about 450 km. The reaction

$$O^+(^2D) + O_2 \longrightarrow O_2^+ + O \tag{245}$$

has been found to proceed at near gas kinetic rates (Rowe *et al.*, 1980), but is only a minor source of O_2^+ at high altitudes, producing 5% of the O_2^+ at 250 km and about 8% near 350 km. Charge transfer from N_2^+ to O_2

$$N_2^+ + O_2 \longrightarrow O_2^+ + N_2 \tag{246}$$

is significant only at low altitudes. Surprisingly, the reaction of O^+ with CO_2 (reaction 165) is nearly as important as reaction (246) near 150 km, where it constitutes about 8% of the total source of O_2^+.

Loss of O_2^+ is mainly by dissociative recombination (reaction 166) at all altitudes, but the reactions with NO and N (reactions 167 and 168) together contribute about 15% of the total sink near 100 km. Reaction with N_2 (reaction 242) may also be important at low altitudes.

Altitude profiles of the primary sources and sinks of N_2^+ are shown in Figure 1.39. Below about 250 km, most of the N_2^+ is produced by direct photoioniza-

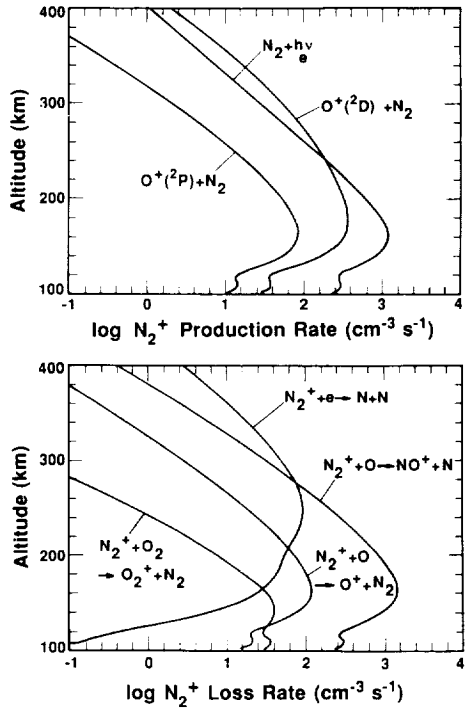

Figure 1.39 Altitude profiles of the primary (a) sources and (b) sinks of N_2^+ for a low solar activity model of the terrestrial dayside ionosphere

tion and photoelectron impact ionization of N_2. Charge transfer from $O^+(^2D)$

$$O^+(^2D) + N_2 \longrightarrow N_2^+ + O \tag{247}$$

becomes more important at higher altitudes. If the rate coefficient measured recently in the 8–20 eV range (Lavollee and Henri, 1989) also applies to thermal energies, the analogous charge transfer reaction from $O^+(^2P)$

$$O^+(^2P) + N_2 \longrightarrow N_2^+ + O \tag{248}$$

provides about 5% of the total production between 150 and 250 km. The sources due to charge transfer from He^+ (reaction 172) and from Ar^+ (reaction 171) are insignificant. The reverse of reaction (171), however, is exothermic for N_2^+ in vibrational levels $v \geq 0$, and has been found to be the most important source of Ar^+ at high altitudes (Fox, 1986a).

Loss of N_2^+ is mostly by reaction with O

$$N_2^+ + O \longrightarrow NO^+ + N \tag{249a}$$

$$\longrightarrow N_2 + O^+ \tag{249b}$$

up to about 280 km. The major product channel is (249a); only about 10% of the reactions proceed via charge transfer (Knutsen *et al.*, 1988). At higher altitudes dissociative recombination (reaction 178) is the dominant loss process. Near 100 km, charge transfer to O_2 (reaction 246) becomes significant, providing about 10% of the total sink of N_2^+.

Analyses based on Atmospheric Explorer (AE) data showed that model N_2^+ densities were larger than the measured values by a factor of about 2 (Breig *et al.*, 1983; Abdou *et al.*, 1984). Suggestions for improving the agreement included increasing the dissociative recombination coefficient for N_2^+ (about 2×10^{-7} $(300/T_e)^{0.39}$ $cm^3\ s^{-1}$) (Zipf, 1980) by a factor of 2–3 and enhancing the rate coefficient for charge transfer to O (reaction 249b). Either end could be at least partially achieved with accepted values for the rate coefficients of ground state N_2^+ if vibrationally excited ions reacted much faster than ground state ions. Fox and Dalgarno (1985) modeled the vibrational distribution of N_2^+ and showed, however, that enhanced loss of vibrationally excited N_2^+ could reduce the densities of N_2^+ by a maximum of about 30%. Recently a slightly larger dissociative recombination coefficient for ground state N_2^+ of about 2.6×10^{-7} $cm^3\ s^{-1}$ at 300 K was measured (Canosa *et al.*, 1991) but a large *ab initio* calculation gives a smaller value of about 1.6×10^{-7} $cm^3\ s^{-1}$ (Guberman, 1991).

$O^+(^4S)$ is the major ion at the F_2 peak. It is produced largely by photoionization of O above 130 km and photoelectron impact ionization at lower altitudes. Dissociative ionization of O_2 is a minor source over the whole ionosphere. Charge transfer from N_2^+ to O (reaction 249b) is more important at low altitudes, where it produces 20–25% of the total source between 100 and

150 km. The rate of production of $O^+(^4S)$ from quenching of $O^+(^2D)$ by N_2

$$O^+(^2D) + N_2 \longrightarrow O^+(^4S) + N_2 \tag{250}$$

exceeds that of reaction (249b) above 250 km, if the rate coefficient is close to the upper limit of 8×10^{-11} cm^3 s^{-1} reported by Johnsen and Biondi (1980). Smaller but significant sources of O^+ (on the order of a few percent) include

$$N^+ + O_2 \longrightarrow O^+ + NO \tag{251}$$

below about 150 km and

$$N^+ + O \longrightarrow O^+ + N \tag{252}$$

above 200 km. No measurements of the rate coefficient for reaction (252) are available, but analysis of AE data has yielded values of 2×10^{-12} cm^3 s^{-1} (Constantinides *et al.*, 1979) and 5×10^{-13} cm^3 s^{-1} (Torr *et al.*, 1979). Bates (1989) applied the Landau–Zener approximation to the relevant potential curves and computed a value similar to the former. Quenching of $O^+(^2D)$ by electrons

$$O^+(^2D) + e \longrightarrow O^+(^4S) + e \tag{253}$$

produces about one-third of the $O^+(^4S)$ near 350 km, and quenching by O (reaction 175) produces about 5% if the rate coefficient is on the order of 1×10^{-11} cm^3 s^{-1} (Orsini *et al.*, 1977). If reaction (253) is faster, as Oppenheimer, Dalgarno and Brinton (1976) have suggested, the source would increase proportionately.

Loss of $O^+(^4S)$ is mainly by reaction with O_2 (reaction 243) below 140 km. At higher altitudes, reaction with N_2 (reaction 244) is more important. Charge transfer to $N(^2D)$

$$O^+ + N(^2D) \longrightarrow N^+ + O \tag{254}$$

is significant as a loss process for O^+ above about 250 km; it constitutes about a third of the chemical loss at 350 km. Of course, above the O^+ peak, near 300 km, downward transport by diffusion is more important than chemistry in determining the O^+ density profile. Altitude profiles of the major chemical sources and sinks of O^+ are shown in Figure 1.40.

$O^+(^2D)$ and $O^+(^2P)$ are produced mainly by photoionization and electron impact ionization of O at all altitudes. Quenching of $O^+(^2P)$

$$O^+(^2P) + O \longrightarrow O^+(^2D) + O \tag{255}$$

$$O^+(^2P) + e \longrightarrow O^+(^2D) + e \tag{256}$$

and radiation

$$O^+(^2P) \longrightarrow O^+(^2D) + h\nu(7319, 7329\ \text{Å}) \tag{257}$$

are the major loss mechanisms for $O^+(^2P)$ above about 150 km. These processes are also secondary sources of $O^+(^2D)$. Quenching of $O^+(^2P)$ is mostly by O

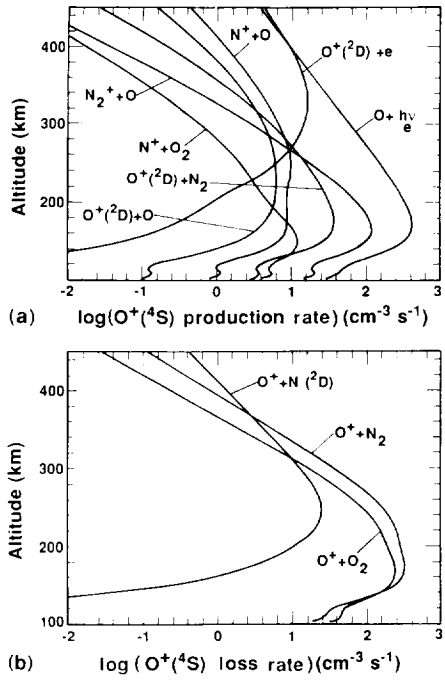

Figure 1.40 Altitude profiles of the major (a) sources and (b) sinks of O^+ for a low solar activity model of the terrestrial dayside ionosphere

below 450 km and by electrons at higher altitudes; loss by radiation exceeds that by quenching above 350 km. The reaction of $O^+(^2P)$ with N_2

$$O^+(^2P) + N_2 \longrightarrow N_2^+ + O \quad (258a)$$

$$\longrightarrow O^+(^2S) + N_2 \quad (258b)$$

$$\longrightarrow NO^+ + O \quad (258c)$$

is the major loss process for $O^+(^2P)$ below about 150 km. If the measured high energy cross sections (Lavolee and Henri, 1989) apply also to thermal energies, the major channel is charge transfer (channel 258a). An AE analysis (Oppenheimer *et al.*, 1976) suggested, however, that at ionospheric temperatures quenching (channel 258b) may be more important. Below 350 km, the major loss process for $O^+(^2D)$ is the reaction with N_2

$$O^+(^2D) + N_2 \longrightarrow N_2^+ + O \quad (259a)$$

$$\longrightarrow O'(^4S) + N_2 \quad (259b)$$

$$\longrightarrow NO^+ + O \quad (259c)$$

This reaction proceeds mainly by charge transfer (channel 259a) (Johnsen and Biondi, 1980). A minor sink for $O^+(^2D)$ is quenching by O (reaction 175). If the rate coefficient for this reaction is less than 1×10^{-11} cm^3 s^{-1}, it contributes a maximum of 3–6% of the total sink from 250–350 km. If the rate coefficient is much larger, reaction (175) could be a significant loss process.

N^+ is a minor ion in the topside ionosphere of the Earth. Its production is mainly through photodissociative and electron-impact dissociative ionization of N_2 below 230 km. Direct ionization of N is more important than dissociative ionization of N_2 below 230 km. Direct ionization of N is more important than dissociative ionization only above about 550 km. Above 230 km, charge transfer of O^+ to $N(^2D)$ (reaction 254) is the dominant source (Constantinides *et al.*, 1979). The rate coefficient for reaction (257) was derived from AE data and values of 1.3×10^{-10} cm^3 s^{-1} were reported by Constantinides *et al.* (1979) and Torr *et al.* (1979), respectively. Bates (1989) computed the similar value of 1.4×10^{-10} cm^3 s^{-1}. Charge transfer from $O^+(^2D)$ to N

$$O^+(^2D) + N \longrightarrow N^+ + O \tag{260}$$

may be significant in the altitude range 250–450 km, but the rate coefficient has not been measured. A value of 7.5×10^{-11} cm^3 s^{-1} was estimated by Torr *et al.* (1974) from analysis of AE data, and Dalgarno (1979) concluded that the data were consistent with an upper limit of 3×10^{-10} cm^3 s^{-1}. If the rate coefficient is 1×10^{-10} cm^3 s^{-1}, reaction (260) contributes about 8% of the total source between 350 and 450 km. Dissociative charge transfer of He^+ to N_2

$$He^+ + N_2 \longrightarrow N^+ + N + He \tag{261}$$

is a minor source at high altitudes, producing about 10% of the N^+ near 500 km (Constantinides *et al.*, 1979). The products of the reaction of O^{2+} with N_2

$$O^{2+} + N_2 \longrightarrow \text{products} \tag{262}$$

are unknown, but even if N^+ is the major product, this reaction provides only about 3% of the total source between 150 and 250 km.

Below about 300–320 km, loss of N^+ is mainly by reaction with O_2. The yields of channels (244), (241) and (251) are 51, 43 and 6%, respectively (Howorka *et al.*, 1980). At high altitudes, downward diffusion is the dominant loss process, but the major chemical loss processes are charge transfer to O (reaction 252) and, to a lesser extent, charge transfer to H

$$N^+ + H \longrightarrow H^+ + N \tag{263}$$

No measurements of the rate coefficients for reaction (263) are available, but a value of 3.6×10^{-12} cm^3 s^{-1} was derived from AE data (Constantinides *et al.*, 1979) and quantal calculations yield 1.2×10^{-12} cm^3 s^{-1} at 1000 K (Butler and Dalgarno, 1979).

Measurements made by the magnetic ion mass spectrometer on the Atmosphere Explorer satellite revealed O^{2+} number densities ranging from about 3 cm^{-3} near 150 km to 30–40 near 400 km (Breig *et al.*, 1977). The sources of O^{2+} include photoionization of O^+, Auger ionization of O by X-rays and double photoionization of outer shell electrons. Although measured cross sections were not available, Victor and Constantinides (1979) derived plausible cross sections for the latter process by analogy to those measured and calculated for noble gases. Using these cross sections they showed that double photoionization of valence electrons is the major source of O^{2+} in the terrestrial ionosphere. The upper and lower limits to the optically thin double photoionization frequency for their derived cross sections were about 2×10^{-9} and 1×10^{-9} s^{-1}, respectively. Recent measurements (Angel and Samson, 1988) have shown that the actual double ionization cross sections are near the lower limit values adopted by Victor and Constantinides. For high solar activity, the optically thin photoionization frequency implied by the measured cross sections is about 1.6×10^{-9} cm^3 s^{-1}.

The major loss process for O^{2+} is reaction with N_2 (reaction 262); at low altitudes reaction with O_2

$$O^{2+} + O_2 \longrightarrow \text{products} \tag{264}$$

is also significant. Reaction (264) has been shown to proceed at near gas kinetic rates, but the products have not been identified (Johnsen and Biondi, 1978; Howorka *et al.*, 1979). Since the second ionization potential of O is about 35 eV, the exothermicities of these reaction are large and therefore, as for reaction (262), dissociative channels probably dominate. The charge transfer reaction of O^{2+} with O

$$O^{2+} + O \longrightarrow O^+ + O^+ \tag{265}$$

may be the major loss process at altitudes greater than 350–400 km, but the rate coefficient has not been measured in the laboratory. Victor and Constantinides (1979) derived a crude upper limit of 1×10^{-10} cm^3 s^{-1} from their analysis. Also using AE data, Breig, Torr and Kayser (1982) derived a value of 6.6×10^{-11} cm^3 s^{-1} for a low solar activity optically thin double photoionization frequency of 2.6×10^{-9} cm^3 s^{-1}. Analysis Pioneer Venus data yielded a rate coefficient for reaction (265) of 1.5×10^{-10} cm^3 s^{-1} (Fox and Victor, 1981). These models were constructed before experimental values for the double photoionization cross sections were available, and should be reconsidered. A measurement of the rate coefficient for reaction (265) would be desirable.

At the high pressures and low temperatures of the terrestrial D region, the terminal ions O_2^+ and NO^+ react to form clusters with N_2, O_2 and CO_2, in reactions such as (Ferguson *et al.*, 1979)

$$NO^+ + N_2 + M \longrightarrow NO^+.N_2 + M \tag{266}$$

Then exchange reactions occur, in which the clusters that form are replaced with more stable clusters

$$NO^+.N_2 + H_2O \longrightarrow NO^+(H_2O) + N_2 \quad (267)$$

Addition of another water molecule

$$NO^+(H_2O) + H_2O + M \longrightarrow NO^+(H_2O)_2 + M \quad (268)$$

is followed by a reaction in which a hydrated proton forms

$$NO^+(H_2O)_2 + H_2O \longrightarrow H^+(H_2O)_2 + HNO_3 \quad (269)$$

Proton hydrates $H^+(H_2O)_n$, with n up to four, have been observed by rocket-borne mass spectrometers (Kopp and Hermann, 1984).

Ablation of meteorites deposits metal atoms such as Fe, Al, Ni, Ca and Na at altitudes from 80 to 100 km (Zhinden *et al.*, 1975). Although the fraction of Na in meteors is only 0.6% (Mason, 1971), sodium was the first metal atom identified in the mesosphere through its intense emission in the nightglow at 589 nm (Chamberlain, 1961). The sodium layer is located between 86 and 100 km, with a peak near 93 km of about 3×10^3 cm^{-3} (Plane, 1991). The total column density is about 5×10^9 cm^{-2}, but the variability is large, about a factor of 10. Metal atoms have low ionization potentials: that for Na is about 5.1 eV. Metal ions can be formed by photoionization and charge transfer from O_2^+ and NO^+

$$O_2^+ + Na \longrightarrow Na^+ + O_2 \quad (270)$$

Na^+ may then combine with N_2, forming clusters

$$Na^+ + N_2 + M \longrightarrow Na^+.N_2 + M \quad (271)$$

which are replaced with more stable clusters such as $Na^+.CO_2$ and $Na^+.H_2O$, in reactions that are analogous to those of O_2^+ and NO^+ in the D region (Richter and Sechrist, 1979; Thomas *et al.*, 1983). These clusters are eventually destroyed by dissociative recombination

$$Na^+.X + e \longrightarrow Na + X \quad (272)$$

1.5 SUMMARY

In this review we have attempted to summarize the ionic reactions that control the distribution of ionization in astrophysical and atmospheric environments. Despite the large number of reactions that we have described, we may well have omitted some that are significant and we have probably included many that are not. It is clear the ion chemistries of the different environments have elements in common, yet with distinctive differences. Many significant reactions

have yet to be studied in laboratory or theoretical studies. Their investigation is particularly challenging because of the need often to measure the influence of rotational and vibrational populations and to determine the identity and state of excitation of the end products of reactions over a wide range of temperatures. Important progress has been made, but much remains to be done.

ACKNOWLEDGMENTS

This work has been supported in part by NASA grants NAGW-2958, NAGW-2238, NAG2-523 and NAGW-2483 to the Research Foundation of the State University of New York at Stony Brook and NAGW-1404 to the Smithsonian Astrophysical Observatory and in part by the National Science Foundation, Division of Atmospheric Sciences Grant ATM 90-19188 to Harvard University. The authors are particularly grateful to Mr J. Singarella for his expert preparation of the figures.

REFERENCES

Abdou, W. A., D. G. Torr, P. G. Richards, M. R. Torr, and E. L. Breig (1984) *J. Geophys. Res.*, **89**, 9069.

Ackermann, J., and H. Hogreve (1991) *Chem. Phys.*, **157**, 75.

Adams, N. G. (1992) *Adv. Gas Phase Ion Chem.*, **1**, 271.

Adams, N. G., D. Smith, and D. C. Clary (1985) *ApJ*, **296**, L131.

Adams, N. G., Herd, C. R., M. Geoghegan, D. Smith, A. Canosa, J. C. Gomet, B. R. Rowe, J. L. Queffelec, and M. Morale (1991) *J. Chem. Phys.*, **94**, 4582.

Allamandola, L. J., A. G. G. M. Tielens, and J. R. Barker (1985) *ApJ*, **290**, L25.

Angel, G., and J. R. Samson (1988) *Phys. Rev. A*, **38**, 5578.

Anicich, V. G. (1993) *Astrophys. J. Suppl.*, **84**, 215.

Anicich, V. G., and W. T. Huntress (1986) *ApJS*, **62**, 553.

Anicich, V. G., J. B. Laudenslager, W. T. Huntress, and J. H. Futrell (1977) *J. Chem. Phys.*, **67**, 4340.

Atreya, S. K. (1986) *Atmospheres and Ionospheres of the Outer Planets and Their Satellites*, Springer-Verlag, Berlin.

Atreya, S. K., and T. M. Donahue (1976) In *Jupiter*, T. Gehrels (ed.), University of Arizona Press, Tucson.

Atreya, S. K., T. M. Donahue, and M. B. McElroy (1974) *Science*, **184**, 154.

Atreya, S. K., T. M. Donahue, and M. C. Festou (1981) *Astrophys. J.*, **247**, L43.

Augustin, S. D., W. H. Miller, P. K. Pearson, and H. F. Schaefer (1973) *J. Chem. Phys.*, **58**, 2845.

Barth, C. A., C. W. Hord, J. B. Pearce, K. K. Kelly, G. P. Anderson, and A. I. Stewart (1971) *J. Geophys. Res.*, **76**, 2213.

Barth, C. A., C. W. Hord, A. I. Stewart, and A. L. Lane (1972) *Science*, **175**, 309.

Bates, D. R. (1989) *Planet. Space Sci.*, **37**, 363.

Bates, D. R. (1992) *J. Phys. B*, **25**, 5479.

Bates, D. R., and A. Dalgarno (1962) In *Atomic and Molecular Processes*, Academic Press, New York, p. 245.

Bates, D. R., M. F. Guest, and R. A. Kendall (1993) *Planet Spa. Sci.*

Bauer, S. J. (1973) *Physics of Planetary Ionospheres*, Springer-Verlag, New York.

Bauer, S. J., L. M. Brace, H. A. Taylor, T. K. Breus, A. J. Kliore, W. C. Knudsen, A. F. Nagy, C. T. Russell and N. A. Savich (1985) *Adv. Space Res.*, **5** (11), 233.

Bettens, R. P. A., and R. D. Brown (1992) *MNRAS*, **258**, 347.

Black, J. H. (1978) *Astrophys. J.*, **222**, 125.

Black, J. H., and A. Dalgarno (1977) *Astrophys. J. Suppl.*, **44**, 303.

Black, J. H., and E. F. van Dishoeck (1987) *Astrophys. J.*, **322**, 412.

Black, J. H., T. W. Hartquist, and A. Dalgarno (1978) *Astrphys. J.*, **224**, 448.

Blitz, L. (1990) In *The Evolution of the Interstellar Medium*, L. Blitz (ed.), Astronautical Society, Pacific.

Böringer, H., and F. Arnold (1986) *J. Chem. Phys.*, **84**, 1459.

Breig, E. L., M. R. Torr, D. G. Torr, W. B. Hanson, J. H. Hoffman, J. C. G. Walker, and A. O. Nier (1977) *J. Geophys. Res.*, **82**, 1008.

Breig, E. L., M. R. Torr, and D. C. Kayser (1982) *J. Geophys. Res.*, **87**, 7653.

Breig, E. L., W. B. Hanson, J. H. Hoffman, and W. A. Abdou (1983) *J. Geophys. Res.*, **88**, 7190.

Breig, E. L., W. B. Hanson, and J. H. Hoffman (1984) *J. Geophys. Res.*, **89**, 2359.

Breus, T. K., K. I. Gringauz, and M. I. Verigin (1985) *Adv. Space Res.*, **5**, 145.

Brown, R. D., and E. H. M. Rice (1986) *MNRAS*, **223**, 405 and 409.

Butler, S. E., and A. Dalgarno (1979) *Astrophys. J.*, **234**, 765.

Canosa, A., J. C. Gomet, B. R. Rowe, and J. L. Queffelec (1991) *J. Chem. Phys.*, **94**, 7159.

Canosa, A., J. C. Gomet, B. R. Rowe, J. B. A. Mitchell, and J. L. Queffelec (1992) *J. Chem. Phys.*, **97**, 1028.

Cecchi-Pestillini, C., and A. Dalgarno (1993) *Astrophys. J.*, **413**, 611.

Chamberlain, W. J. (1961) *Physics of the Aurora and Airglow*, Academic Press, New York.

Chandler, M. O., and J. H. Waite (1986) *Geophys. Res. Lett.*, **13**, 6.

Chen, R. H. (1981) *J. Geophys. Res.* **86**, 7792.

Chen, R. S. (1983) *Moon and Planets*, **28**, 37.

Chen, R. H., and A. F. Nagy (1978) *J. Geophys. Res.*, **83**, 1133.

Chupka, W. A., M. E. Russell, and K. Refaev (1968) *J. Chem. Phys.*, **48**, 1518.

Clary, D. C. (1990) *Ann. Rev. Phys. Chem.*, **41**, 61.

Connerny, J. E. P., and J. H. Waite (1984) *Nature*, **312**, 136.

Constantinides, E. R., J. H. Black, A. Dalgarno, and J. H. Hoffman (1979) *Geophys. Res. Lett.*, **7**, 569.

Cravens, T. E. (1987) *J. Geophys. Res.*, **92**, 11083.

Cravens, T. E., S. L. Crawford, A. F. Nagy, and T. I. Gombosi (1983) *J. Geophys. Res.*, **88**, 5595.

Crosas, M., and J. C. Weisheit (1993) *MNRAS*, **262**, 359.

Crutcher, R. M., and W. D. Watson (1976) *Astrophys. J.*, **209**, 778.

Dalgarno, A. (1970) *Ann. Geophys.*, **26**, 601.

Dalgarno, A. (1979) *AE Reaction Rate Data*, Report AFGL-79-0067.

Dalgarno, A. (1990) In *Molecular Processes in Space*, T. Watanabe, I. Shimamura, M. Shumizu, and Y. Itakawa (eds.), Plenum, New York, p. 1.

Dalgarno, A. (1993a) in *Dissociative Recombination: Theory, Experiment and Applications*, B. R. Rowe, J. B. A. Mitchell and A. Canosa (eds.) Plenum Press, New York.

Dalgarno, A. (1993b) *Trans. Faraday Soc.*, **89**, 2111.

Dalgarno, A., J. H. Black, and J. C. Weisheit (1973a) *Astrophys. Lett.*, **14**, 77.

Dalgarno, A., M. Oppenheimer, and J. H. Black (1973b) *Nature*, **245**, 100.

Dalgarno, A., M. L. Du, and J. H. You (1990) *Astrophys. J.*, **49**, 675.

Delitsky, M. L., R. P. Turco, and M. Z. Jacobson (1990) *Geophys. Res. Lett.*, **17**, 1725.

Dheandhanoo, S., R. Johnsen, and M. A. Biondi (1984) *Planet. Space Sci.*, **32**, 1301.

d'Hendecourt, L. B., and A. Lger (1987) *Astron. Astrophys.*, **180**, 29.

Drdla, K., G. R. Knapp, and E. F. van Dishoeck (1989) *Astrophys. J.*, **345**, 815.

Drossart, P., J.-P. Maillard, J. Caldwell, S. J. Kim, J. K. G. Watson, W. A. Majewski, J. Tennyson, J. H. Waite, and R. Wagener (1989) *Nature*, **340**, 539.

Drossart, P., J.-P., Maillard, J. Caldwell, and J. Rosenquist (1993) *Astrophys. J.*, **402**, 125.

Dubernet, M. L., M. Gargaud, and R. McCarroll (1992) *Astron. Astrophys.*, **259**, 373.

Duley, W. W., T. W. Hartquist, A. Sternberg, R. Wagenblast, and D. A. Williams (1992) *MNRAS*, **255**, 243.

Federman, S. R., and L. Frommhold (1982) *Phys. Rev. A*, **25**, 2012.

Fehsenfeld, F. C., D. B. Dunkin, and E. E. Ferguson (1970) *Planet. Space Sci.*, **18**, 1267.

Ferguson, E. E. (1986) *Chem. Phys. Lett.*, **130**, 218.

Ferguson, E. E., F. C. Fehsenfeld, P. D. Goldan, A. L. Schmeltekopf, and H. I. Schiff (1965) *Planet. Space Sci.*, **13**, 823.

Ferguson, E. E., F. C. Fehsenfeld, and D. L. Anderson (1979) in *Gas Phase Ion Chemistry*, M. T. Bowers (ed.), Academic Press, New York, Vol. 1.

Festou, M. C., and S. K. Atreya (1982) *Geophys. Res. Lett.*, **9**, 1147.

Fjeldbo, G., A. Kliore, B. Seidel, D. Sweetnam, and D. Cain (1974) *Astron. Astrophys.*, **39**, 91.

Fjeldbo, G., B. Seidel, D. Sweetnam, and T. Howard (1975) *J. Atmos. Sci.*, **32**, 1232.

Fjeldbo, G., A. Kliore, B. Seidel, D. Sweetnam, and P. Woiceshyn (1976) In *Jupiter*, T. Gehrels (ed.), University of Arizona Press, Tucson.

Fox, J. L. (1982a) *Icarus*, **51**, 248.

Fox, J. L. (1982b) *J. Geophys. Res.*, **87**, 9211. Erratum in (1985) *J. Geophys. Res.*, **90**, 11106.

Fox, J. L. (1986a) *Planet. Space Sci.*, **34**, 1241.

Fox, J. L. (1986b) *J. Geophys. Res.*, **91**, 1731.

Fox, J. L. (1989) In *Dissociative Recombination: Theory, Experiment and Applications*, J. B. A. Mitchell and S. L. Guberman (eds.), World Scientific, Singapore.

Fox, J. L. (1992a) In *Venus and Mars: Atmospheres, Ionospheres and Solar Wind Interactions*, Geophysical Monograph 66. AGU, Washington.

Fox, J. L. (1992b) *Planet. Space Sci.*, **40**, 1663.

Fox, J. L. (1993) *J. Geophys. Res.*, **98**, 3297.

Fox, J. L., and A. Dalgarno (1979) *J. Geophys. Res.*, **84**, 7315.

Fox, J. L., and A. Dalgarno (1985) *J. Geophys. Res.*, **90**, 7557.

Fox, J. L., and H. A. Taylor, Jr. (1990) *Geophys. Res. Lett.*, **17**, 1625.

Fox, J. L., and G. A. Victor (1981) *J. Geophys. Res.*, **86**, 2438.

Fox, J. L., and R. V. Yelle (1991) Abstract volume for 23rd Annual Meeting of the Division for Planetary Sciences of the American Astronomical Society, p. 69.

Fox, J. L., J. F. Brannon, and H. S. Porter (1993) *Geophys. Res. Lett.*, **20**, 1391.

Gaur, V. P., B. M. Tripathi, G. C. Joshi, and M. C. Pande (1988) *Astrophys. Spa. Sci.*, **147**, 107.

Geballe, T. R., M.-F. Jagod, and T. Oka (1993) *Astrophys. J.*, **408**, L109.

Gerlich, D., and S. Hornung (1992) Chem. Rev., **92**, 1509.

Glassgold, A. E., G. A. Mamon, and P. J. Huggins (1991) *ApJ*, **373**, 254.

Glass-Maujean, M. (1989) *Phys. Rev. Lett.*, **62**, 144.

Glosik, J., A. B. Rakshit, N. D. Twiddy, N. G. Adams, and D. Smith (1978) *J. Phys. B*, **11**, 3365.

Graff, M. M. (1989) *Astrophys. J.*, **339**, 239.

Grebowsky, J. (1981) *J. Geophys. Res.*, **86**, 1537.

Gringauz, K. I., M. I. Verigin, T. K. Breus, and T. Gombosi (1977) *Sov. Phys. Dokl.*, **22**, 53.

Gringauz, K. I., M. I. Verigin, T. K. Breus, and T. Gombosi (1979) *J. Geophys. Res.*, **84**, 2123.

Guberman, S. L. (1991) *Geophys. Res. Lett.*, **18**, 1051.

Gurrola, E. M., E. A. Marouf, V. R. Eshleman, and G. L. Tyler (1991) *Bull. Am. Astr. Soc.*, **23**, 1207.

Haider, S. A., J. Kim, A. F. Nagy, C. N. Keller, M. I. Verigin, K. I. Gringauz, N. M. Shutte, K. Szego, and P. Kiraly (1992) *J. Geophys. Res.*, **97**, 10621.

Hanson, W. B., S. Sanatani, and D. R. Zuccaro (1977) *J. Geophys. Res.*, **82**, 4351.

Hartquist, T. W., J. M. C. Rawlings, D. A. Williams, and A. Dalgarno (1993) *Quart. J. Roy. Astron. Soc.*, **34**, 213.

Hedin, A. E., H. B. Niemann, W. T. Kasprzak, and A. Seiff (1983) *J. Geophys. Res.*, **88**, 73; Erratum in *J. Geophys. Res.*, **88**, 6352.

Herbert, F., and B. R. Sandel (1991) *J. Geophys. Res.*, **96**, 19241.

Herbst, E., and C. M. Leung (1989) *Astrophys. J. Suppl.*, **69**, 271.

Herbst, E., and C. M. Leung (1990) *Astron. Astrophys.*, **233**, 177.

Hollenbach, D., and C. F. McKee (1989) *Astrophys. J.*, **342**, 306.

Howorka, F., A. A. Viggiano, D. L. Albritton, E. E. Ferguson, and F. C. Fehsenfeld (1979) *J. Geophys. Res.*, **84**, 5941.

Howorka, F., I. Dotan, F. C. Fehsenfeld, and D. L. Albritton (1980) *J. Chem. Phys.*, **73**, 758.

Hunten, D. M. (1981) *Geophys. Res. Lett.*, **8**, 369.

Hunten, D. M., R. P. Turco, and O. B. Toon (1980) *J. Atmos. Sci.*, **37**, 1342.

Ip, W.-H. (1990a) *Astrophys. J.*, **363**, 354.

Ip, W. H. (1990b) *Geophys. Res. Lett.*, **17**, 1713.

Johnsen, R., and M. A. Biondi (1978) *Geophys. Res. Lett.*, **5**, 847.

Johnsen, R., and M. A. Biondi (1980) *Geophys. Res. Lett.*, **7**, 401.

Johnsen, R., A. Chen, and M. A. Biondi (1980) *J. Chem. Phys.*, **72**, 3085.

Jones, M. E., S. E. Barton, G. B. Ellison, and E. E. Ferguson (1986) *Chem. Phys. Lett.*, **130**, 218.

Jura, M. A., and A. Dalgarno (1971) *Astron. Astrophys.*, **14**, 243.

Kallman, T., S. Lepp, and P. Giovannoni (1987) *Astrophys. J.*, **321**, 907.

Karpas, Z., V. Anicich, and W. T. Huntress (1979) *J. Chem. Phys.* **70**, 2877.

Keating, G. M., J. L. Bertaux, S. W. Bougher, T. E. Cravens, R. E. Dickinson, A. E. Hedin, V. A. Krasnopol'sky, A. F. Nagy, J. Y. Nicholson, L. J. Paxton, and U. von Zahn (1985) *Adv. Space Res.*, **5** (Venus International Reference Atmosphere), 117–171.

Keller, C. N., T. E. Cravens, and L. Gan (1992) *J. Geophys. Res.*, **97**, 12117.

Kim, Y. H. (1991) *The Ionosphere of Jupiter*, PhD Thesis, State University of New York at Stony Brook.

Kim, Y. H., and J. L. Fox (1992) *Geophys. Res. Lett.*, **97**, 6093.

Kim, S., P. Drossart, J. Caldwell, and J.-P. Maillard (1990) *Icarus*, **84**, 54.

Kim, Y. H., J. L. Fox, and H. S. Porter (1992) *J. Geophys. Res.*, **97**, 6093.

Kimura, M., A. Dalgarno, L. Chantranupong, Y. Li, G. Hirsch, and R. J. Buenker (1993) *Astrophys. J.*, **417**, 812.

Kirby, K. P., and E. Goldfield (1991) *J. Chem. Phys.*, **94**, 1271.

Kliore, A. J., G. S. Levy, D. L. Cain, G. Fjeldbo, and S. I. Rasool (1967) *Science*, **158**, 1683.

Kliore, A. J., I. R. Patel, A. F. Nagy, T. E. Cravens, and T. I. Gombosi (1979) *Science*, **205**, 99.

Kliore, A. J., J. G. Luhmann, and M. H. G. Zhang (1991) *J. Geophys. Res.*, **96**, 11065.

Knudsen, W. C. (1988) *J. Geophys. Res.*, **93**, 8756.

Knudsen, W. C., and K. L. Miller (1985) *J. Geophys. Res.*, **90**, 2695.

Knudsen, W. C., K. Spenner, K. L. Miller, and V. Novak (1980) *J. Geophys. Res.*, **85**, 7803.

Knutsen, K., V. Bierbaum, and S. Leone (1988) *Planet. Space Sci.*, **36**, 307.

Kopp, E., and U. Hermann (1984) *Ann. Geophysicae*, **2**, 83.

Krasnopolsky, V. A. (1982) *Kossm. Issled.*, **20**, 595.

Krasnopolsky, V. A. (1983) *Cosm. Res.* (Engl. Transl.), **20**, 430.

Krasnopolsky, V. A., B. R. Sandel, F. Herbert, and R. J. Vervack (1993) *J. Geophys. Res.*, **98**, 3065.

Larsson, M., H. Danared, J. R. Mowat, P. Sigray, G. Sundstrm, L. Bostrm, A. Filevich, A. Kllberg, S. Mannervik, K. G. Rensfelt, and S. Datz (1993) *Phys. Rev. Lett.*, **70**, 430.

Latter, W. B. (1989) Thesis, University of Arizona.

Latter, W. B., and J. H. Black (1991) *Astrophys. J.*, **372**, 161.

Lavollee, M., and G. Henri (1989) *J. Phys. B*, **22**, 2019.

Leger, A., and J. L. Puget (1984) *Astron. Astrophys.*, **137**, L5.

Lepp, S., and A. Dalgarno (1987) In *Astrochemistry*, M. S. Vardya and S. P. Tarafdar (eds.), Reidel, Dordrecht, p. 109.

Lepp, S., and A. Dalgarno (1988a) *Astrophys. J.*, **335**, 169.

Lepp, S., and A. Dalgarno (1988b) *Astrophys. J.*, **345**, 353.

Lepp, S., A. Dalgarno, E. F. van Dishoeck, and J. M. Black (1988) *Astrophys. J.*, **329**, 418.

Lepp, S., A. Dalgarno, and R. McCray (1990) *Astrophys. J.*, **358**, 262.

Lindal, G. F., G. E. Wood, H. B. Hotz, D. M. Sweetnam, V. R. Eshleman, and G. L. Tyler (1983) *Icarus*, **53**, 348.

Lindal, G. F., J. R. Lyons, D. M. Sweetnam, V. R. Eshleman, D. P. Hinson, and G. L. Tyler (1987) *J. Geophys. Res.*, **92**, 14987.

Liu, W., and A. Dalgarno (1994) *Astrophys. J.*, in press.

Liu, W., S. Lepp, and A. Dalgarno (1992) *Astrophys. J.*, **396**, 679.

Luine, J., and G. H. Dunn (1989) *Astrophys. J.*, **299**, L67.

Lyons, J. R., Y. L. Yung, and M. Allen (1992) *Science*, **256**, 204.
McConnell, J. C., J. B. Holberg, G. R. Smith, B. R. Sandel, D. E. Shemansky, and A. L. Broadfoot (1982) *Planet. Space Sci.*, **30**, 151.
McElroy, M. B. (1973a) *Space Sci. Rev.*, **14**, 460.
McElroy, M. B. (1973b) *Adv. Atom. Mol. Phys.*, **9**, 323.
Mackay, G. I., H. I. Schiff, and D. K. Bohme (1981) *Can. J. Chem.*, **59**, 1771.
Maillard, J.-P., P. Drossart, J. K. G. Watson, S. J. Kim, and J. Caldwell (1990) *Astrophys. J.*, 363, L39.
Majeed, T., and J. C. McConnell (1991) *Planet. Space Sci.*, **39**, 1715.
Majeed, T., J. C. McConnell, D. F. Strobel, and M. E. Summers (1990) *Geophys. Res. Lett.*, **17**, 1721.
Majeed, T., J. C. McConnell, and R. V. Yelle (1991) *Planet. Space Sci.*, **39**, 1591.
Marquette, J. B., B. R. Rowe, G. Dupeyrat, G. Poissant, and C. Rebrion (1985) *Chem. Phys. Lett.*, **122**, 431.
Marquette, J., C. Rebrion, and B. Rowe (1988) *J. Chem. Phys.*, **89**, 2041.
Mason, B. (1971) *Handbook of Elemental Abundances in Meteorites*, Gordon and Breach, New York.
Meikle, W. P. S., D. A. Allen, J. Spyromilio, and G. F. Varani (1989) *MNRAS*, **238**, 193.
Meyer, D. M., and K. C. Roth (1991) *Astrophys. J.*, **376**, L49.
Millar, T. J. (1991) *MNRAS*, **259**, 35P.
Millar, T. J., and E. Herbst (1990) *Astron. Astrophys.*, **231**, 466.
Millar, T. J., C. M. Leung, and E. Herbst (1987) *Astron. Astrophys.*, **183**, 109.
Millar, T. J., J. M. C. Rawlings, A. Bennett, P. D. Brown, and S. B. Charnley (1991) *Astron. Astrophys. Suppl.*, **87**, 585.
Miller, T. M., J. T. Moseley, D. W. Martin, and E. W. McDaniel (1968) *Phys. Rev.*, **173**, 115.
Miller, S., R. D. Joseph, and J. Tennyson (1990) *Astrophys. J.*, **360**, L55.
Miller, S., J. Tennyson, S. Lepp, and A. Dalgarno (1992) *Nature*, **355**, 420.
Mitchell, J. B. A. (1990) *Phys. Rep.*, **186**, 215.
Mitchell, J. B. A., and H. Hus (1987) *J. Phys. B*, **18**, 54, 547.
Moorhead, J. M., R. P. Lowe, J.-P. Maillard, W. H. Wehlau, and P. F. Bernath (1988) *Astrophys. J.*, **326**, 899.
Mosely, S. H., E. Dwek, W. Glaccum, J. R. Graham, R. F. Loewenstein, and R. F. Silverberg (1989) *Astrophys. J.*, **347**, 1119.
Nagy, A. F., T. E. Cravens, S. G. Smith, H. A. Taylor, and H. C. Brinton (1980) *J. Geophys. Res.*, **85**, 7795.
Natta, A., C. Giovanardi, F. Palla, and N. J. Evans (1988) *Astrophys. J.*, **327**, 817.
Nesbitt, F. L., G. Marston, L. J. Stief, M. A. Wickramaaratchi, W. Tao, and R. B. Klemm (1991) *J. Phys. Chem.*, **95**, 7613.
Neufeld, D. A., and A. Dalgarno (1989) *Astrophys. J.*, **340**, 867.
Niemann, H. B., W. T. Kasprzak, A. E. Hedin, D. M. Hunten, and N. W. Spencer (1980) *J. Geophys. Res.*, **85**, 7817.
Nier, A. O., and M. B. McElroy (1976) *Science*, **194**, 1298.
Nier, A. O., and M. B. McElroy (1977) *J. Geophys. Res.*, **82** 4341.
Oka, T., and T. R. Geballe (1990) *Astrophys. J.*, **351**, L53.
O'Keefe, A., G. Mauclaire, D. Parent, and M. T. Bowers (1986) *J. Chem. Phys.*, **84**, 215.

Oliva, E., A. F. M. Moorwood, and I. J. Danziger (1987) *Messenger*, **50**, 18.

Oppenheimer, M., A. Dalgarno, and H. C. Brinton (1976) *J. Geophys. Res.*, **81** 3762.

Orsini, N., D. G. Torr, M. R. Torr, H. C. Brinton, L. H. Brace, A. O. Nier, and J. C. G. Walker (1977) *J. Geophys. Res.*, **82**, 4829.

Owen, T., K. Biemann, D. R. Rushneck, J. E. Biller, D. W. Howarth, and A. L. Lafleur (1977) *J. Geophys. Res.*, **82**, 4635.

Paxton, L. J. (1983) *Atomic Carbon in the Venus Thermosphere: Observations and Theory*, PhD Thesis, University of Colorado.

Paxton, L. J. (1985) *J. Geophys. Res.*, **90**, 5089.

Péquignot, D., and S. M. V. Aldrovani (1986) *Astron. Astrophys.*, **161**, 169.

Petuchowski, S. J., E. Dwek, J. E. Allen, and J. A. Nuth (1989) *Astrophys. J.*, **342**, 406.

Plane, J. M. C. (1991) *Int. Rev. Phys. Chem.*, **10** 55.

Prasad, S. S., and W. T. Huntress (1980) *Astrophys. J. Suppl.*, **43**, 1.

Rank, D. M., P. A. Pinto, S. E. Woosley, J. D. Bregman, F. C. W. W. Heborn, T. S. Axelrod, and M. Cohen (1988) *Nature*, **331**, 505.

Rawlings, J., D. A. Williams, and J. Canto (1988) *MNRAS*, **230**, 695.

Richter, E. S., and C. F. Sechrist (1979) *J. Atmos. Terr. Phys.*, **41**, 579.

Roberge, W., and A. Dalgarno (1992) *Astrophys. J.*, **255**, 489.

Roche, P. F., D. K. Aitken, and C. H. Smith (1991) *MNRAS*, **252**, 39P.

Rottman, G. J., and H. W. Moos (1973) *Geophys. Res.*, **78**, 8033.

Rowe, B. R., D. W. Fahey, F. C. Fehsenfeld, and D. L. Albritton (1980) *J. Chem. Phys.*, **73**, 194.

Saito, S., K. Kawaguchi, S. Yamonoto, M. Ohishi, H. Suzuki, and N. Kaifu (1987) *Astrophys. J.*, **317**, L115.

Seiff, A., J. T. Schofield, A. J. Kliore, F. W. Taylor, S. S. Limaye, H. E. Revercomb, L. A. Sromovsky, V. V. Kerzhanovich, V. I. Moroz, and M. Ya. Marov (1985) *Adv. Space. Res.*, **5**, 3.

Shimizu, M. (1983) *Moon and Planets*, **22**, 521.

Shinagawa, H., and T. E. Cravens (1989) *J. Geophys. Res.*, **94**, 6506.

Shinagawa, H., and T. E. Cravens (1992) *J. Geophys. Res.*, **97**, 1027.

Smith, D., N. G. Adams, and T. M. Miller (1978) *J. Chem. Phys.*, **69**, 308.

Smith, G. R., D. F. Strobel, A. L. Broadfoot, B. R. Sandel, D. E. Shemansky, and J. B. Holberg (1982) *J. Geophys. Res.*, **87**.

Smith, G. R., D. E. Shemansky, J. B. Holberg, A. L. Broadfoot, and B. R. Sandel (1983a) *J. Geophys. Res.*, **88**, 8667.

Smith, M. A., V. M. Bierbaum, and S. R. Leone (1983b) *Chem. Phys. Lett.*, **94**, 398.

Smith, D., N. G. Adams, K. Giles, and E. Herbst (1988) *Astron. Astrophys.*, **200**, 191.

Spenner, K., W. C. Knudsen, R. C. Whitten, P. F. Michelson, K. L. Miller, and V. Novak (1981) *J. Geophys. Res.*, **86**, 9170.

Spyromlio, J., W. P. S. Meikle, R. C. M. Learner, and D. A. Allen (1988) *Nature*, **334**, 327.

Stacey, G. J., N. Geis, R. Genzel, J. B. Lugten, A. Poglitisch, A. Sternberg, and C. H. Townes (1991) *Astrophys. J.*, **373**, 423.

Stacey, G. J., D. T. Jaffe, N. Geis, R. Genzel, A. I. Harris, A. Poglitsch, J. Stutzki, and C. H. Townes (1993) *Astrophys. J.*, **404**, 219.

Stahler, S. W., F. Palla, and E. E. Salpeter (1986) *Astrophys. J.*, **302**, 590.

Stancil, P. C., J. F. Babb, and A. Dalgarno (1993) *Astrophys. J.*, **414**, 672.

Sternberg, A., and A. Dalgarno (1989) *Astrophys. J.*, **338**, 197.

Strobel, D. F., and M. E. Summers (1993) In *Neptune and Triton*, D. P. Cruikshank and M. S. Matthews (eds.), University of Arizona Press, Tucson.

Strobel, D. F., R. V. Yelle, D. E. Shemansky, and S. K. Atreya (1991) In *Uranus*, J. T. Bergstrahl, E. D. Miner, and M. S. Matthews (eds.), University of Arizona Press, Tucson.

Suzuki, H., M. Ohishi, N. Kaifu, T. Kasuga, S. Ishikawa, and T. Miyaji (1988) *Vista Astron.*, **31**, 459.

Swider, W. (1992) *Planet. Space Sci.*, **40**, 247.

Taylor, H. A., H. C. Brinton, S. J. Bauer, R. E. Hartle, P. A. Cloutier, and R. E. Daniell (1980) *J. Geophys. Res.*, **85**, 7765.

Thomas, L., M. C. Isherwood, and M. R. Bowman (1983) *J. Atmos. Terr. Phys.*, **45**, 587.

Tielens, A. G. G. M., and D. Hollenbach (1985a) *Astrophys. J.*, **291**, 722.

Tielens, A. G. G. M., and D. Hollenbach (1985b) *Astrophys. J.*, **291**, 747.

Torr, D. G., D. W. Rusch, M. R. Torr, J. C. G. Walker, J. H. Hoffman, P. B. Hays, and M. Oppenheimer (1974) *Eos (Trans. Am. Geophys. Union)*, **55**, 1159.

Torr, D. G., M. R. Torr, W. B. Hanson, and J. H. Hoffman (1979) *Geophys. Res. Lett.*, **6**, 573.

Trafton, L., D. F. Lester, and K. L. Thomson (1989) *Astrophys. J.*, **343**, L73.

Trafton, L., T. R. Geballe, S. Miller, J. Tennyson, and G. E. Ballester (1993) *Astrophys. J.*, **405**, 761.

Tyler, G. L., D. N. Sweetnam, J. D. Anderson, S. E. Broutzki, J. K. Campbell, V. R. Eshleman, D. L. Greish, E. M. Gurrola, D. P. Hinson, N. Kawashima, E. R. Kurusinski, G. S. Levy, G. F. Lindal, J. R. Lyons, E. A. Marouf, P. A. Rosen, R. A. Simpson, and G. E. Wood (1989) *Science*, **246**, 1466.

Urbain, X., A. Cornet, F. Brouillard, and A. Giusti-Suzor (1991) *Phys. Rev. Lett.*, **66**, 1685.

van Dishoeck, E. F. (1990) In *The Evolution of the Interstellar Medium*, L. Blitz (ed.), Astronautical Society of the Pacific.

van Dishoeck, E. F., and J. H. Black (1980) In *Rate Coefficients in Astrochemistry*, T. J. Millar, and D. A. Williams (eds.), Kluwer, Dordrecht.

van Dishoeck, E. F., and J. H. Black (1986) *Astrophys. J. Suppl.*, **62**, 109.

van Dishoeck, E. F., and J. H. Black (1989) *Astrophys. J.*, **340**, 273.

Vasil'ev, M. B., A. S. Vyshlov, M. A. Kolosov, N. A. Savich, V. A. Samovol, L. N. Samoznaev, A. I. Sidorenko, Yu. N. Aleksandrov, A. I. Danilenko, V. M. Dubrovin, A. L. Zaitsev, G. M. Petrov, O. N. Rzhiga, D. Ya. Shtern, and L. I. Romanova (1975) *Cosmic Res.*, **13**, 41.

Verigin, M. I., K. I. Gringauz, N. M. Shutte, S. A. Haider, K. Szego, P. Kiraly, A. F. Nagy, and T. I. Gombosi (1991) *J. Geophys. Res.*, **96**, 19037.

Viala, Y. P. (1986) *Astron. Astrophys. Suppl.*, **64**, 391.

Viala, Y. P., E. Roueff, and H. Abgrall (1988) *Astron. Astrophys.*, **190**, 215.

Victor, G. A., and E. R. Constaninides (1979) *Geophys. Res. Lett.*, **6**, 519.

Viggiano, A., R. Morris, and J. Paulson (1990) *J. Chem. Phys.*, **93**, 1483.

von Zahn, U., and V. I. Moroz (1985) *Adv. Space Res.*, **5** (Venus International Reference Atmosphere), 173–95.

Wagenblast, R., D. A. Williams, T. J. Millar, and L. A. M. Nejad (1993) *MNRAS*, **260**, 420.

Waite, J. H., T. E. Cravens, J. U. Kozyra, A. F. Nagy, S. K. Atreya, and R. H. Chen, *J. Geophys. Res.*, **88**, 6143.

Wickham, A. G., T. S. Stoecklin, and D. C. Clary (1992) *J. Chem. Phys.*, **96**, 1053.

Wooden, D. W., D. M. Rank, J. D. Bregman, F. C. W. Beborn, A. G. G. M. Tielens, M. Cohen, P. A. Pinto, and T. S. Axelrod (1993) *Astrophys. J. Suppl.*, **88**, 477.

Yamamoto, S., S. Saito, K. Kawaguchi, N. Kaifu, H. Suzuki, and M. Ohishi (1987) *Astrophys. J.*, **317**, L119.

Yan, M., S. Lepp, and A. Dalgarno (1994) *Astrophys. J. Suppl.*, **88**, 477.

Yousif, F. B., and J. B. A. Mitchell (1989) *Phys. Rev. A*, **40**, 4318.

Yousif, F. B., P. J. T. Van der Donk, M. Orakzai, and J. B. A. Mitchell (1991) *Phys. Rev. A*, **44**, 5653.

Yung, Y. L., and J. R. Lyons (1990) *Geophys. Res. Lett.*, **17**, 1717.

Yung, Y. L., M. Allen, and J. P. Pinto (1984) *Astrophys. J. Suppl.*, **55**, 465.

Zbinden, P. A., M. A. Hidalgo, P. Eberhardt, and J. Geiss (1975) *Planet. Space Sci.*, **23**, 1621.

Zhang, M. H. G., J. G. Luhmann, and A. J. Kliore (1990) *J. Geophys. Res.*, **95**, 17095.

Zipf, E. C. (1980) *Geophys. Res. Lett.*, **7**, 645.

Zygelman, B., and A. Dalgarno (1990) *Astrophys. J.*, **365**, 239.

Note added in proof

Recent models of the ionosphere of Triton (J. Lyons, Y. Yung and M. Allen, 1994, *Icarus*, in press) suggest that the major ion is C^+ produced by photoionization of C and charge transfer. The most important source of C is dissociative recombination of CO^+. The electron density profile measured by *Voyager* can be accounted for entirely by solar radiation.

Although the presence of high mass-28 ion densities in the nightside Venus ionosphere has been suggested as an indication of the presence of strong electron precipitation, recent auroral models indicate that the very high mass-28 ion densities cannot be reproduced. An inspection of the instrument operating voltages, and numerical modeling of the instrument response have suggested that offsets in the PV OIMS voltage settings can cause mass-30 ions to be collected in the mass-28 setting. Thus the extremely high mass-28 ion densities may be an instrumental effect (J. Fox, J. Brannon, J. Grebosky and H. Porter, 1994, *EOS*, submitted).